UNIVERSITÀ DEGLI STUDI DI GENOVA

DIPARTIMENTO DI MEDICINA INTERNA E SPECIALITÀ MEDICHE (DiMI)

Corso di Dottorato: MEDICINA TRASLAZIONALE IN ONCOLOGIA ED EMATOLOGIA (XXXIV CICLO)

Curriculum: GENETICA ONCOLOGICA E PATOLOGIA MOLECOLARE

TESI

A NEXT GENERATION SEQUENCING APPROACH TO GENOMIC LANDSCAPE IN MELANOMA PATIENTS: EVOLUTION OF PATIENT-SPECIFIC RESPONSE TO THERAPY

***Tutor*:** Prof. Paola Ghiorzo

PhD course coordinator: Prof. Edoardo Giannini

CANDITATO

Irene Vanni

DECLARATION

I hereby declare that this dissertation is my own original work and that I have fully acknowledged by name all of those individuals and organizations that have contributed to the research for this dissertation. Due acknowledgement has been made in the text to all other material used. Throughout this dissertation and in all related publications I followed the guidelines of "Good Scientific Practice".

SUMMARY

INTRODUCTION

CHALLENGES IN MELANOMA MOLECULAR CLASSIFICATION AND THERAPY RESPONSE

Melanoma is one of the most aggressive malignancies of the skin. Its incidence is globally growing partly because of the increase of early diagnosis, and contextually, the prevalence is also increasing (**Bray et al., 2018; Schadendorf et al., 2018**). Until 10 years ago, advanced melanoma was associated with poor survival due to the lack of durable responses to conventional chemotherapy and biochemotherapy (**Korn et al., 2008**), with a median Overall Survival (OS) of about 6 months in patients with stage IV melanoma. Since 2011, however, the rules of the treatment of stage IV melanoma have been completely rewritten, with the introduction of targeted therapies with BRAF and MEK inhibitors (BRAF+MEKi) (**Larkin et al., 2014; Long et al., 2014; Robert et al., 2016**), and immunotherapy with the anti CTLA-4 ipilimumab (**Hodi et al., 2010**) and the anti-PD-1 nivolumab (**Robert et al., 2015**) and pembrolizumab (**Schachter et al., 2017**). These new therapeutic approaches improved melanoma prognosis, resulting in a 5-year survival rate of 34–43% (**Hamid et al., 2019; Robert et al., 2019**). However, mainly because of primary and acquired resistance to treatments, the majority of patients will ultimately relapse, and only patients harbouring a *BRAF* mutation, observed in about 50% of cutaneous melanoma, can receive a targeted treatment with BRAF+MEKi (**Spagnolo et al., 2015**). The current state of molecular-target drugs and the current therapeutic scenario for patients with *BRAF* mutated melanoma has been extensively described (**Tanda et al., 2020**). Several preclinical and clinical trials are studying new actionable mechanisms and/or molecules to improve the prognosis of melanoma patients further to tackle multiple resistance mechanisms simultaneously. The advent of massive parallel sequencing, allowing the simultaneous analysis of several genes, led, in the past two decades, to Whole-Exome Sequencing (WES) and Whole-Genome Sequencing (WGS) studies that allow the identification of several potential therapeutic targets. In light of this, numerous clinical and preclinical trials are ongoing, to identify new molecular targets. Since the discovery of the first actionable mutation (*BRAF* V600),

several other genes have been identified as putative drivers of melanomagenesis and/or melanoma progression, and additional candidate drivers are currently being assessed, prompting pharmacogenomics studies on potentially actionable targets (**Priestley et al., 2019**). However, melanoma is one of the tumors with the highest mutation burden, and results from different studies were frequently not overlapping, possibly due to dissimilar sample size and cohort characteristics (**Berger et al., 2012; Hodis et al., 2012; Krauthammer et al., 2012; Snyder et al., 2014; Van Allen et al., 2015**). Although this high mutational burden is one of the reasons behind the success of immunotherapy in this tumor, it makes it hard to clearly identify novel driver genes that could be used for targeted therapies (**Davis et al., 2018**). In 2015, The Cancer Genome Atlas analyzed 333 cutaneous melanoma samples by integrating integrated multi-level genomic analyses, namely WES and low-pass WGS, transcriptome sequencing including miRNA, protein expression, and classified melanoma in four major molecular subtypes: mutant BRAF, mutant RAS, mutant NF1 and triple wild-type (**Cancer Genome Atlas Network, 2015**). However, *NF1* mutations were found albeit at a lower frequency in the BRAFmutant and RASmutant subgroups also, not allowing for appropriately define the subset of mutant NF1 melanomas as a real independent molecular subtype. Therefore, the following three main molecular subtypes were proposed: BRAFmutant, RASmutant, and non-BRAFmutant/non-RASmutant (**Palmieri et al., 2018**). The landscape of mutated non-BRAF skin melanoma, in light of recent data deriving from WES or WGS studies in melanoma cohorts, established 33 candidate driver genes altered with a frequency greater than 1.5% (**Vanni et al., 2020A**). Considering the entire scenario of driver genes alterations (mutations and copy number variations) the paradigm of melanoma pathogenesis has become really complex. Therefore, AIOM (Italian Association of Medical Oncology) and the main Italian scientific societies suggest performing NGS-based multigene screening in patients with advanced melanoma [https://www.aiom.it/wp-content/uploads/2019/10/2019_Racc_An_mut_Melanoma.pdf]. In future, large panels of genes will be increasingly used in clinical practice for molecular classification of most or nearly all human

cancers alongside the simplification of the methodology (including data interpretation) and reduction of the overall costs.

Despite the many advances made in the melanoma therapy and the exciting results achieved, some issues remain unanswered. Among all, one the most important is the identification and overcoming of primary and acquired resistances.

In this context, the liquid biopsy and in particular the analysis of circulating free DNA (cfDNA) from different body fluids spread in the recent years as useful biological tool for non-invasive and quantitative characterization of the whole tumor genome, identification of tumor heterogeneity, identification of drug resistance mechanisms, and clonal evolution during treatment and toward disease progression in melanoma patients (**Kanemaru et al., 2022**).

In summary, the assessment of *BRAF* mutations has become a key diagnostic procedureand a priority in determining the oncologist's choice and course of therapy. In this context, several molecular strategies are available for mutational analysis of the *BRAF* gene, such as Next-Generation Sequencing (NGS) target techniques (**Vanni et al., 2020B**). For the employment of this diagnostic approach, several guidelines and recommendations need to be applied to standardize the implementation of NGS-based panels in the clinical setting by prior technical validation to ensure the detection of somatic variants and high quality of sequencing results. In part II of my dissertation, I discuss a recent collaborative study that we finalized to evaluate the NGS concordance data obtained among two groups using an NGS melanoma panel aiming to adopt it within the Italian Melanoma Intergroup (Published; Vanni et al., 2020. doi. 10.1186/s13000-020-01052-5). However, the increasing interest in the molecular characterization of melanoma, aiming to identify additional molecular markers either targetable by new drugs or useful for predicting response to therapy and prognosis, paves the way to employment of exome/genome level high-throughput sequencing, in real-world settings of melanoma patients, with integration of WES and RNA-seq data, to provide an extensive melanoma genetic layout, as reported in Part I of my dissertation.

ABBREVIATIONS

AF : Allele Frequency

AIOM : Italian Association of Medical Oncology

BOR : Best Overall Response

BRAF+MEKi : BRAF and MEK inhibitors

cfDNA : circulating free DNA

CI : Confidence Interval

CNAs : Copy Number Alterations

CNR: National Research Council

CNVs : Copy Number Variations

CR : Complete Response

ctDNA : circulating tumour DNA

DDR : Damage Response and Repair

DIN : DNA Integrity Number

EMQN : European Molecular Genetics Quality Network

EQA : External Quality Assessment

FFPE : Formalin-Fixed Paraffin-Embedded

gDNA : Genomic DNA

GWAS : Genome-Wide Association Study

HPO : Human Phenotype Ontology

ICB : Immunological Checkpoint Blocking

ICC: Intraclass Correlation Coefficient

IGV : Integrative Genomics viewer

IHC : Immunohistochemistry

indels : small insertions and deletions

Irecist : immune-RECIST

LDH : Lactate Dehydrogenase

LOF : Loss Of Function

LOH : Loss Of Heterozygosity

MLPA : Multiplex Ligation-dependent Probe Amplification

MNVs: Multi Nucleotide Variants

NED : No Evidence of Disease

NGS : Next-Generation Sequencing

NRs : Non-Responders

OS : Overall Survival

PCR : Polymerase Chain Reaction

PD : Progression Disease

PFS : Progression-Free Survival

PNA: Peptide Nucleic Acid

PR : Partial Response

PVs : Pathogenic Variants

RECIST : Response Evaluation Criteria in Solid Tumors

Rs : Responders

SBS : Single-Base Substitution

SD : Stable Disease

SigMa : Signature Multivariate Analysis

SNPs : Single Nucleotide Polymorphisms

SNVs: Single Nucleotide Variants

SS : Sanger Sequencing

TF : Fresh Frozen Tissue

TGCA: The Cancer Genome Atlas

TMB : Tumor Mutational Burden

TT : Target Therapy

VAF: Variant allele frequency

VCF : Variant Call Format

VUS : Variant of Uncertain Significance

WB : Western-Blotting

WES : Whole-genome Sequencing

WGS : Whole-Genome Sequencing

PART I: GENETIC DETERMINANTS OF RESPONSE TO THERAPY IN A REAL-WORLD SETTINGS OF MELANOMA PATIENTS

ABSTRACT

Thirty-six advanced or metastatic melanoma patients, treated in adjuvant or advanced disease setting according to clinical practice guidelines with Target Therapy (TT) (BRAF+MEKi) or immunotherapy with Immunological Checkpoint Blocking (ICB) agents (nivolumab, pembrolizumab alone or in combination with ipilimumab), were recruited into the study. For each patient included in this study, the clinical benefit was assessed according to the setting of treatment.

Thirty-six tumour biopsies, belonging to 19 *BRAF* V600+ and 17 *BRAF* V600- patients, were analyzed by WES and correlated with clinical response in order to characterize molecular mechanisms of response and/or resistance to therapy. For each patient germline DNA was also analyzed by WES and the results were subtracted to somatic WES data obtained from the tumour. Moreover, for 12 melanoma patients (4 *BRAF* V600+ and 8 *BRAF* V600-), matched pre-therapy and post-therapy biopsies underwent WES to reveal potential genetic predictors of intrinsic resistance and/or acquired resistance to therapy. Since a subset of melanoma patients harbour germline pathogenic variants which increase melanoma susceptibility, 166 cancer predisposition genes were also analysed from WES data in our cohort. Finally, cfDNA from 14 patients were sequenced by target NGS in order to characterize the molecular heterogeneity in advanced melanoma patients and dynamic changes in response to the therapy.

Performing a deep molecular profiling by WES in a real-world setting of advanced and/or metastatic melanoma patients, we revealed an average of CNVs and mutations in melanoma driver genes higher in *BRAF* V600+ non-responder than in *BRAF* V600+ responder cohort. No difference was found in the cohort of *BRAF* V600- patients. Conversely, *BRAF* V600- responders showed a a two-fold higher TMB compared to non-responders (30.5 *vs* 15.9). Germline data obtained from our

cohort supported the clinical relevance of performing germline testing secondary to somatic WES. Several determinants of intrinsic or acquired resistance were identified.

Finally, I showed that ctDNA is a feasible source of genetic material for *BRAF*/*KIT* mutations assessment in clinical practice in patients with advanced melanoma, especially when a tissue sample is not available or in patients with rapidly progressive disease. The nearly 70% of concordance between the results obtained from tissue and ctDNA confirms the clinical utility of liquid biopsies in following dynamic changes in response to therapy.

BACKGROUND AND RATIONALE

TT with BRAF+MEKi and ICB agents (anti -CTLA4, -PD-1, -PD-L1) significantly improved metastatic/advanced melanoma therapy yet complete remission is rare and resistance develops in the majority of patients. TT results in a high response rate but short-term responses (**Tanda et al., 2020; Spagnolo et al., 2015**). ICB has a lower response rate, but more durable responses (**Carlino et al., 2021**).

Therefore, *BRAF* mutation testing has become a priority to determine the oncologist's choice and course of therapy, both in the advanced and adjuvant setting. In the absence of a standardized therapeutic algorithm for *BRAF* mutated patients, clinicians can choose whether to start with BRAF plus MEK inhibitors or with immunotherapy, based on the experience of their center, characteristics of the patient (i.e., his compliance with treatment, concomitant pathologies), and characteristics of the disease (i.e., Tumor Mutational Burden (TMB), Lactate Dehydrogenase (LDH) level) (**Tanda et al., 2020**).

Despite a large number of studies addressing the molecular landscape of metastatic melanoma, genetic determinants of resistance are still largely not clarified. In clinical practice, predicting patients showing a durable response *vs* patients relapsing is an urgent clinical need.

Here we performed a comprehensive genomic characterization of selected consecutive metastatic biopsies obtained from a real-world series of melanoma patients treated with either target or immunotherapy according to their *BRAF* mutational status and showing a complete/durable response or a rapid disease progression (with or without clinical benefit), by WES and RNA sequencing. Our aim was to integrate genomic findings on driver melanoma genes, with a special focus on DNA Damage Response and Repair (DDR) and germline predisposition genes to predict response to therapy, characterize primary and acquired resistance and approach longitudinal follow-up of patients by tumour/cfDNA analysis.

An increasing number of studies demonstrated the potential use of cfDNA as a surrogate marker for multiple indications in melanoma cancer, including diagnosis, prognosis, and monitoring. However, its use should be limited to offer additional clinically relevant information, such as clonality and tumor heterogeneity since mutation testing in the liquid biopsy of melanoma patients is not a surrogate of solid biopsy. cfDNA mutation analysis, when available, could help the characterization of molecular heterogeneity in advanced/metastatic melanoma patients representing an efficient non-invasive tool to overcome the problem (**Vanni et al., 2020B**).

AIM

Explore genetic and genomic determinants of response to different current therapies in a real-world setting of melanoma patients in order to discriminate those who could benefit from one treatment over another. Moreover, we aimed to determine the frequency of patients carriers of a germline variant in known melanoma predisposition and DDR genes.

MATERIAL AND METHODS

MELANOMA PATIENT COHORT

On the basis of the availability of a fresh tissue biopsy, thirty-six melanoma patients (19 *BRAF* V600+ and 17 *BRAF* V600- patients) with advanced or metastatic melanoma were consecutively and prospectively recruited at the IRCCS Ospedale Policlinico San Martino and treated in the adjuvant or advanced disease setting according to clinical practice (with ICB agents (PD-1 and/or CTLA-4 inhibitors) and/or TT (BRAF+MEKi in BRAFmutant patients, or KIT inhibitor in KITmutant patients) (**Gershenwald et al., 2017**). Tumour reassessments were performed according to Response Evaluation Criteria in Solid Tumors (RECIST) 1.1 and immune-RECIST (iRECIST) criteria (**Seymour et al., 2017**).

The clinical benefit was assessed for each patient according to the treatment setting.

The clinical benefit from adjuvant treatment was defined as the absence of disease recurrence at the follow-up cut-off. In patients who received first-line treatment for advanced disease with BRAF+MEKi, clinical benefit was defined by Progression-Free Survival (PFS) > 11 months, according to COMBI-d study results (**Robert et al., 2019**). In patients treated with PD-1 inhibitors (monotherapy or in combination with CTLA-4 or BRAF+MEKi) clinical benefit was defined by a Best Overall Response (BOR) of Stable Disease (SD), Partial Response (PR) or Complete Response (CR).

In selected cases, treatment was continued beyond disease progression. The clinical characteristics of the patients are reported in **Supplementary Table 1**.

For each patient included in the study, the somatic DNA of the pre and/or post therapy metastasis was extracted from Fresh Tissue (TF). In the absence of TF from the pre-therapy melanoma, DNA was extracted from six archival Formalin-Fixed Paraffin-Embedded (FFPE) sections. For 8 patients, cell lines were established from the post-therapy metastatic TF. In addition, peripheral blood was taken for germline DNA extraction from all patients.

Tumour tissue samples were selected and revised based on tissue quality and tumour cellularity by the pathology team. The study was approved by the local IRB (046REG2017), and written informed consent was obtained from all the patients.

DNA/cfDNA EXTRACTION

Genomic DNA (gDNA) was extracted from peripheral blood using the Diatech MagCore® HF16Plus (RBC Bioscience, New Taipei City, Taiwan) with the Genomic DNA Large Volume Whole Blood kit. gDNA purity was assessed with both Nanodrop 2000 spectrophotometer (Thermo Fisher Scientific, Carlsbad, CA) to measure the whole absorption spectrum (220–750 nm) and calculate absorbance ratios at 260/280 and 260/230. gDNA yield was evaluated by fluorometric quantitation using Qubit® Fluorometer (Life Technologies Corporation, San Francisco, USA).

Somatic DNA from FFPE was extracted from the tumor sections using the Genomic DNA FFPE One-Step Kit for Diatech MagCore® HF16Plus extractor (RBC Bioscience) according to the manufacturer's instructions.

Somatic DNA from TF was isolated using DNeasy® Blood & Tissue Kit (QIAGEN, Valencia, CA, USA). Quantity and purity of the tumour gDNA were examined by SPECTROstar Nano (BMG Labtech, Offenburg, Germany) to measure the whole absorption spectrum (220–750 nm) and calculate absorbance ratios at both 260/280 and 260/230. Moreover, all somatic samples were quantified by Qubit® 2.0 Fluorometer (Invitrogen, Carlsbad, CA, USA) and Agilent 2200 TapeStation system using the Genomic DNA ScreenTape assay (Agilent Technologies, Santa Clara, CA, USA). gDNA fragmentation status was evaluated by the Agilent 2200 TapeStation system using the Genomic DNA ScreenTape assay (Agilent Technologies) able to produce a DNA Integrity Number (DIN).

cfDNA was isolated from 1–5 mL of plasma using MagMAX™ Cell-Free DNA Isolation Kit according to the manufacturer's instructions (ThermoFisher Scientific) and quantified using the Qubit® dsDNA HS Assay Kit on the Qubit 2.0 fluorometer (ThermoFisher Scientific). The purity and quantity of DNA

size fragments were analyzed by the Agilent High Sensitivity DNA Analysis Kit (Agilent Technologies) using TapeStation 2200 instrument (Agilent Technologies).

WHOLE EXOME SEQUENCING (WES)

gDNA from peripheral blood and somatic DNA from tumour tissue (TF and/or FFPE) were subjected to WES at a coverage of 100X and 300X, respectively.

Nextera Flex for Enrichment solution (Illumina, San Diego, CA) combined with 'SureSelect Human All Exon V7' probes (Agilent Technologies) was used for library preparation and exome enrichment, targeting 50 Mb of human exonic content. All samples were quantified, and quality tested using the Qubit 2.0 Fluorometer (Invitrogen, Carlsbad, CA) and Agilent 2100 Bioanalyzer (Agilent Technologies). Libraries were sequenced on NovaSeq 6000 (Illumina, San Diego, CA) in 150 pair-end mode. Raw data were first processed for both format conversion and de-multiplexing by the Bcl2Fastq 2.0.2 version of the Illumina pipeline (https://support.illumina.com/content/dam/illumina-support/documents/documentation/software_documentation/bcl2fastq/bcl2fastq2-v2-20-software-guide-15051736-03.pdf). Adapter sequences were masked with Cutadapt v1.11 from raw fastq data using the following parameters: --anywhere (on both adapter sequences) --overlap 5 --times 2 --minimum-length 35 --mask-adapter (**Martin M., 2011**). Subsequently, Illumina DRAGEN Germline 3.5.7 and Somatic Pipelines 3.5.7 were used to map reads to GRCh38/hg38 assembly and identify germline and somatic tumor/normal matched pair variants, respectively (https://emea.illumina.com/products/by-type/informatics-products/basespace-sequence-hub/apps/dragen-germline.html; https://emea.illumina.com/products/by-type/informatics-products/basespace-sequence-hub/apps/edico-genome-inc-dragen-somatic-pipeline.html).

Variants were functionally annotated by Annovar (**Wang et al., 2010**). Single Nucleotide Polymorphisms (SNPs) and small insertions and deletions (indels) summary reports contain variant

coordinates, base pair changes, amino acid change annotation, and functional annotation, including the clinical significance of a sequence variation to human health, population frequencies, and a series of scores (SIFT, PolyPhen, LRT, MutationTaster, etc.) as well as Human Phenotype Ontology (HPO) and other information helpful for variant prioritization. TMB of each tumour sample was calculated by using the total number of PASSING filter non-synonymous somatic mutations (SNPs and indels) divided per mega-base of callable somatic regions included in the total genomic target region captured with the exome assay (35 Mb).

CNVkit 0.9.7 was used to detect somatic Copy Number Alterations (CNAs) (**Talevich et al., 2014**). BAM files of the 36 germline melanoma patients were used to generate a reference of per-bin reads count. Similarly, tumour samples were bin-counted using default parameters, and each was compared to the reference normalized 0-centered signal. For each tumour sample, bins were segmented using default parameters (circular binary segmentation). Bins with log2 normalized coverage values below -15 were removed. CNAs call thresholds on log2 parameters were as follows: < -1.1 = 0, < -0.4 = 1, < 0.4 = 2, < 0.8 = 3. Calls with log2 confidence intervals overlapping zero were removed. Loss of heterozygosity (LOH) was performed using ASCAT (**Van Loo et al., 2010**). Bona fide LOH events were defined as region with number of copies of the minor allele equal to zero. Melanoma driver genes, interferon-gamma pathway, DDR genes selected for mutation, CNV and LOH analysis were reported in **Supplementary Figure 1**.

The tumour Single-Base Substitution (SBS) signatures were calculated starting from the Variant Call Format (VCF) file of the somatic tissue samples (subtracted from the germline variants resulting from the germline analysis of the corresponding patient) through three different tools: DeconstructSigs, Signature Multivariate Analysis (SigMa), and SigProfiler v3.2 (**Rosenthal et al., 2013**).

NGS ANALYSIS ON cfDNA

Targeted libraries were amplified using Oncomine™ Pan-Cancer Cell-Free Assay (ThermoFisher Scientific), which detects hotspot mutations, small indels, copy number changes, and gene fusions across 52 genes. In particular, this assay includes 177 amplicons covering 980 key hotspot mutations in 44 known cancer genes (*AKT1*, *ALK*, *APC*, *AR*, *ARAF*, *BRAF*, *CHEK2*, *CTNNB1*, *DDR2*, *EGFR*, *ERBB2*, *ERBB3*, *ESR1*, *FBXW7*, *FGFR1*, *FGFR2*, *FGFR3*, *FGFR4*, *FLT3*, *GNA11*, *GNAQ*, *GNAS*, *HRAS*, *IDH1*, *IDH2*, *KIT*, *KRAS*, *MAP2K1*, *MAP2K2*, *MET*, *MTOR*, *NRAS*, *NTRK1*, *NTRK3*, *PDGFRA*, *PIK3CA*, *PTEN*, *RAF1*, *RET*, *ROS1*, *SF3B1*, *SMAD4*, *SMO*, and *TP53*) and CNAs in 12 genes (*CCND1*, *CCND2*, *CCND3*, *CDK4*, *CDK6*, *EGFR*, *ERBB2*, *FGFR1*, *FGFR2*, *FGFR3*, *MET*, and *MYC*). Furthermore, it allows the identification of de novo variants in the *TP53* gene with frequency> 1%.

The recommended cfDNA input amount for the Oncomine assay is 20 ng. However, as low as 2 ng of cfDNA may be sufficient to evaluate circulating tumour DNA (ctDNA) with this assay (Thermo Fisher Scientific). Patients cfDNAs (range 2–20 ng per reaction) were employed to prepare manually targeted libraries following manufacturer's instructions, quantified with the Agilent High Sensitivity DNA Analysis Kit (Agilent Technologies) using TapeStation 2200 instrument (Agilent Technologies), diluted to 100 pM, and pooled for automated templating with an Ion 540™ kit for the IonChef Instrument. Sequencing was performed with the GeneStudio S5 system and Ion 540™ chips (4 samples/chip).

Sequence data were processed using the Torrent Suite 5.10.1 pipeline software optimized for the Ion Torrent platform to perform raw data analysis, base calling, remove low-quality reads, and make alignments to the human genome (GRCh37/hg19). Variant calling was performed with Ion Reporter Server 5.12 and the software Oncomine™ TagSeq S540 Liquid Biopsy—w2.4—Single Sample detecting and annotating low-frequency variants, including SNPs/InDels (down to 0.1% limit of detection), fusions, and Copy Number Variations (CNVs).

The hotspot calls were reviewed by uploading each VCF file on (IGV) (http://www.broadinstitute.org/igv) (**Robinson et al., 2011**).

BRAF MULTIPLEX LIGATION-DEPENDENT PROBE AMPLIFICATION (MLPA) ANALYSIS

All *BRAF* mutated samples, including in this study that revealed a CNV in *BRAF* gene by WES, were validated by Multiplex Ligation-dependent Probe Amplification (MLPA) analysis using the SALSA MLPA Probemix P298 BRAF-HRAS-KRAS-NRAS (MRC Holland BV, Amsterdam, the Netherlands). This probemix contains 57 probes for the detection of deletions and/or duplications in the RAS genes (*HRAS*, *KRAS*, and *NRAS*) and the *BRAF* gene and includes one probe specific for the *BRAF* p.Val600Glu (c.1799T>A) mutation and two probes for *KRAS* c.34G and c.35G, both located in codon 12. The MLPA assay was performed according to the manufacturer's instructions (MRC Holland BV). The MLPA products were separated by capillary electrophoresis in an automated sequencer (ABI 3130XL Genetic Analyzer, Applied Biosystems). The results were interpreted using the Coffalyser.Net software (MRC Holland BV). Ratios of <0.75, 0.75–1.30, and >1.3 were considered to indicate deletion, normal, and duplication, respectively.

TERT CORE PROMOTER MUTATIONAL STATUS

Mutational status of the *TERT* core promoter was determined in the tumour samples by Polymerase Chain Reaction (PCR) and Sanger Sequencing (SS) between genomic positions 1294925 and 1295198). In detail, we amplified the *TERT* promoter (located on chromosome 5) target region (LRG_343, NG_009265.1, NM_198253.3) using the following forward and reverse primers: TERT_Forward: gTC CTg CCC CTT CAC CTT and TERT_reverse: AgC ACC TCg Cgg TAg Tgg. The specific primer pairs were designed using the Primer3 algorithm (https://primer3plus.com) (**Untergasser et al., 2007**), a primer designing tool. The PCR reactions were performed by amplifying 40 ng of tumour gDNA in a final volume of 15.5 µL containing 200 mol/L dNTPs, 10× Taq buffer, 0.322 µM of each

PCR primer, 1.5 U of Taq Hot Start (Qiagen). The PCR program consists of 10 min at 95 °C and 35 cycles with 30 s at 95 °C, 30 s at 60°C for annealing temperature, and 30 s at 72 °C, followed by 5 min at 72 °C. Purified products were sequenced using the same primers of the PCR amplification with the BigDye Terminator v1.1 cycle sequencing kit (Applied Biosystems) under the following conditions: 1 µl BigDye Terminator v1.1, 2 µl sequencing buffer 5X, 3.2 pmol forward or reverse primer, 1.5 µl PCR purified product and 4 µl sterile water to a final reaction volume of 10.5 µl. Cycle sequencing was performed using an initial denaturation step at 96 °C for 10 s followed by 25 cycles at 96 °C for 10 s, 60 °C for 3 min on GeneAmp® PCR System 9700 (Applied Biosystems). The sequencing products were separated by capillary electrophoresis in an automated sequencer (ABI 3130XL Genetic Analizer, Applied Biosystems) with a 36 cm length capillary and POP-7™ polymer, according to the manufacturer's instructions. Data were analyzed with Sequencing Analysis Software version 5.3.1 (Applied Biosystems). The two most frequently identified variations within the *TERT* promoter gene region at genomic positions 1295228 and 1295250, known as C228T and C250T, respectively, were analyzed. These mutations are located at −124 and −146 bp upstream of the ATG start codon and were considered for analysis.

TOTAL RNA SEQUENCING

RNAs from 20 TF belonging to 16 melanoma patients were extracted by Tissue Lyser plus Maxwell® RSC simplyRNA Tissue Kit (AS1340 Promega, Southampton, UK) in accordance to the manufacturer's protocol (**Supplementary Table 2**). Total RNA concentration and purity were measured via SPECTROstar Nano (BMG Labtech) to measure the whole absorption spectrum (220–750 nm) and calculate absorbance ratios at both 260/280 and 260/230. Moreover, all RNAs were quantified by Qubit® 2.0 Fluorometer (Invitrogen) using Qubit™ RNA High Sensitivity (HS) Assay Kits (ThermoFisher Scientific). RNA libraries were prepared using the Illumina Stranded Total RNA Prep with Ribo-Zero Plus (Illumina Inc., CA). Briefly, after ribosomal and globin RNA depletion, RNA was

fragmented and denatured, and cDNA synthesized. Then the 3' ends were adenylated, and anchors ligated, followed by a PCR amplification step to add the index-adapter sequences. After clean up and final amplification of the dual indexed libraries, the quality of the libraries was assessed by the 2100 Bioanalyzer with a High Sensitivity DNA chip (Agilent Technologies), and libraries concentration was assessed with a High Sensitivity Assay on a Qubit 4 fluorometer (ThermoFisher Scientific). Libraries were then pooled at 1.4nM, and Paired-End sequenced (2x150) on a NovaSeq 6000 Sequencing System instrument (Illumina Inc., CA) with the addition of 1% PhiX. Run metrics were 85.13% PF (clusters Passing Filter) and 91.02 Q30.

Sequencing reads were aligned to the reference genome (GENCODE GRCh38 version 33) using STAR v.2.7.3a in two-pass basic mode preventing multimappings (**Dobin et al., 2013**). Gene fusions for all TFs were identified using STAR-Fusion v. 1.9.0 with options --min_FFPM 0 --FusionInspector validate --examine_coding_effect.

RESULTS

CLINICAL RESPONSE IN A REAL-WORLD COHORT OF PATIENTS WITH ADVANCED/METASTATIC MELANOMA TREATED ACCORDING TO CLINICAL PRACTICE: TUMOUR SAMPLES SELECTION

Thirty-six tumour samples from 19 *BRAF* V600+ and 17 *BRAF* V600- patients (three of which had pathogenetic mutations in the *KIT* gene) were analysed and their mutational profiles/CNV/LOH correlated with clinical response. Overall, 17 patients were considered Responders (R) and 19 Non-Responders (NR); for 13 patients we considered the pre-therapy tumour and for 23 patients the post-therapy tumour.

Eight *BRAF* V600+ tumours were from patients responding to TT (n° 6) or ICI agents (n° 2), while eleven tumours were from patients non-responding to TT (n°7), ICI agents (n°1) and adjuvant TT (n°3). Nine *BRAF* V600- tumours were from non-responders patients to ICI agents (2 in adjuvant

setting) and eight where from patients non-responding (4 in adjuvant setting and 1 treated with Imatinib) (**Table 1**).

Table 1. Real-world cohort of tumour biopsies belonging to 36 melanoma patients.

***BRAF* V600+ Patients**	**Total N=19**	**R**	**NR**
SEX	F	4	6*
	M	4	5
TUMOUR ONSET MEDIAN		55.5y	54.1y
THERAPY	BRAF+MEKi	6	7
	Anti-PD-1	2	1
	Adjuvant with BRAF+MEKi	0	3*
***BRAF* V600- Patients**	**Total N=17**	**R**	**NR**
SEX	F	3	3
	M	6	5
TUMOUR ONSET MEDIAN		69.7y	62.7y
THERAPY	Anti-PD-1	6	3
	Anti-CTLA-4	1	0
	Imatinib	0	1
	Adjuvant with Anti-PD-1	2	3
	Ipilimumab/Adjuvant with Anti-PD-1	0	1

*Abbreviations: F: Female; M: Male; y: years; R: Responder; NR: Non-Responder; *: 1 FFPE biopsy analysed.*

GENETIC LAYOUT ASSOCIATED WITH RESPONSE

BRAF V600 mutations were identified in 52.8% of patients (19/36), *RAS* mutantions in 30.6% (11/36), and non-*BRAF* mutations /non-*NRAS* mutations in 19.4% (7/36), in line with previous literature data (**Palmieri et al., 2018**; **Cancer Genome Atlas Network, 2015**). Among the 6 non-*BRAF* mutations /non-*NRAS* mutations patients, we found 1 patient (#34) with an *NF1* mutation (NM_001042492.3: c.3089C>T, p.Ser1030Leu, Allele Frequency (AF) of 10.3%). Two other patients (#21 and #14) showed

NF1 mutations coexisting with either *BRAF* or *NRAS* mutation. The #21 patient showed one *NF1* mutation (NM_001042492.3: c.6278C>, p.Ser2093Phe, AF of 30%) coexisting with *NRAS* p.Gln61Arg. Finally, the patient #14 revealed two *NF1* mutations (NM_001042492.3: c.5019_5020insAATAAAAAATTTGCCCATGAGTCAAGAAAGGAAGAAAACAGTGGGAATTAGTTG, p.Asn1673_Val1674insAsnLysLysPheAlaHisGluSerArgLysGluGluAsnSerGlyAsnTerLeu, AF of 10.5%; NM_001042492.3: c.2980A>T, p.Asn994Tyr, AF of 7%) coexisting with *BRAF* p.Val600Glu. One patient (#56) revealed *NRAS* mutation in the post therapy lesion and loss of the *BRAF* V600 mutation previously detected in the pre-therapy biopsy; this patient was considered *BRAF* V600 mutant for the adjuvant therapy. Moreover, all *BRAF* V600+ mutations found by WES were further validated by *BRAF* MLPA analysis and/or SS confirming data obtained by our diagnostic routine.

We then looked exons somatic variants with 'PASSING' filters (missense, indel, stop mutations) both in melanoma driver and in the interferon-gamma pathway genes (**Supplementary Figure 2**) in the R *versus* NR cohort (**Roh et al., 2017; Vanni et al., 2020A**).

Interestingly, we found an average of melanoma driver gene mutations in non-responders *BRAF* V600+ 1.7 times higher than in responders *BRAF* V600+ (3.3 and 2.0, respectively). In the cohort of NR *BRAF* V600+ patients, this finding suggests a genetic mechanism allowing tumour to escape from response to TT. In contrast, no differences for both driver melanoma genes and interferon pathway genes were found in the cohort of *BRAF* V600- patients.

WGS studies analysing *TERT* promoter report a frequency of 81.2% in acral and cutaneous melanomas (**Hayward et al., 2017**; **Vanni et al., 2020A**).

TERT promoter sequencing in 30/36 tumour samples showed a 73.3% frequency of activating mutations (C228T and C250T). Interestingly, in the cohort of 16 *BRAF* V600+ samples for which it was possible to carry out the TERT analysis, we observed a 100% *vs* 70% frequency, respectively in the R and NR cohort, as previously reported (**Tan et al., 2020; Thielmann et al., 2022**). Conversely, no difference was revealed in the 14 *BRAF* V600- patients.

TMB analysis showed a similar mutational tumour load between R and NR patients (37.5 *vs* 29.7, respectively), while *BRAF* V600- responders showed a doubled TMB compared to non-responders (30.5 *vs* 15.9) (**Figure 1**). However, a difference in terms of TMB was revealed in the cohort (N°17 patients) of *BRAF* V600- in which the R patients had a TMB higher (30.5 TMB) than NR patients (15.9 TMB) according with the literature data (**Hodi et al., 2021**).

Figure 1. Tumour Mutational Burden (TMB) in our real-world cohort of melanoma patients.

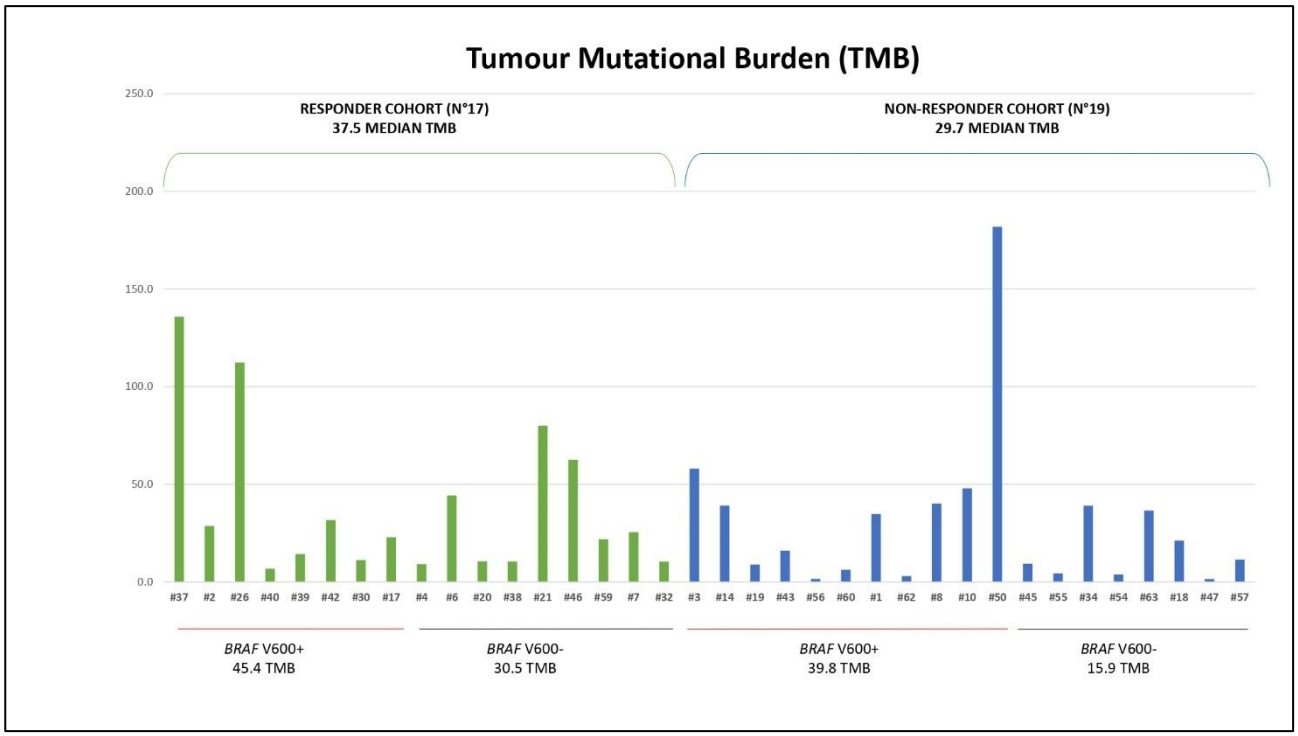

Tumor Mutational Burden (TMB) of each tumor sample belonging to our 36 melanomas patient's cohort (x-axis) and comparison between responders or non-responders. TMB was calculated by using the total number of PASSING filter non-synonymous somatic mutations (SNPs and small indels) divided per mega-base of callable somatic regions included in the total genomic target region captured with the exome assay (35 Mb).

CNV analysis using WES was evaluated in melanoma driver genes reporting an average of CNVs 1.2 times higher in *BRAF* V600+ NR than in *BRAF* V600+ R cohort. No difference was found in the cohort of *BRAF* V600- patients confirming the trend observed for driver genes mutations (**Supplementary Figure 3**). Interestingly, the most frequent melanoma driver genes showing amplification were *HRAS (11p15.5)*, *GNA11 (19p13.3)*, *STK19 (6p21.33)*, *MAP2K2 (*19p13.3), *EZH2* (7q36.1), *TERT* (5p15.33),

and *MTOR (1p36.22)*, whereas the most frequent deleted region was found in the chromosome 10 cytoband 10q23.31 containing *PTEN* gene.

Finally, we evaluated the CNVs presence in the of *HLA-A*, *HLA-B*, *HLA-C*, *TAP2*, *PD-1* (PDCD1), *PD-L1* (CD274) and *PDL2* (PDCD1LG2) genes as possible determinants of response in 17 *BRAF* V600- patients, finding 6 patients (4 of them responding, 66%) with at least one amplification in one of these genes, confirming the literature trend (**Olbryt et al., 2020**; **Liu et al., 2020**; **Gupta et al., 2019**). LOH analysis using ASCAT was evaluated in DDR genes reporting an average of LOH 1.4 times higher in *BRAF* V600+ NR than in *BRAF* V600+ R cohort. Similar trend was observed in the *BRAF* V600- cohort (**Supplementary Table 3**).

Interestingly, the agreement on 36 tumours between the three tools (DeconstructSigs, SigMa, and SigProfiler v3.2) used for mutational signatures was 94.4% (**Supplementary Table 4**). Only two tumour samples (#55 and #43) showed a discordance between DeconstructSigs/SigMa and SigProfiler (Signature_clock-like *vs* SBS7 for #55; Signature_msi *vs* SBS1 for #43). COSMIC mutational signature calculated by SigProfiler v.3.2, showed the SBS3, SBS5, and SBS7 as the three most represented signatures, with no association with R or NR cohort. Moreover, a prevalence of signature SBS5 was found in the NR cohort (26.3% *vs* 17.6%) (**Supplementary Table 4**). The SBS5 is clock-like in that the number of mutations correlates with the individual's age. Rates of acquisition of SBS5 mutations over time differ between different cancer types, but the cause for SBS5 mutations is unknown and likely represents a collective of endogenous background mutational process. In our cohort, we found 5 NR patients that displayed the SBS5 with a median age at tumour onset of 59 not correlating with a higher TMB (60.1). In the R SBS5 cohort the median age of tumour onset was 55, and TMB was 90.2. Overall, the most prevalent SBS signature found in our cohort was SBS7 (16/36; 44.4%), a signature caused by UV-radiation, in line with data previously described for melanoma (**Hayward et al., 2017**).

GENETIC LAYOUT ASSOCIATED WITH INTRINSIC AND ACQUIRED RESISTANCE

Among our cohort of 36 patients, we analysed 12 melanoma patients (4 *BRAF* V600+ and 8 *BRAF* V600-) for which matched pre-therapy and post-therapy biopsies were available, in order to reveal potential genetic predictors of intrinsic resistance and/or acquired resistance to therapy (**Supplementary Figure 4**).

In the matched tumour samples, we found 20 melanoma driver gene mutations in common between the two melanoma lesions (**Table 2**).

Table 2. Melanoma driver gene mutations detected by Whole Exome Sequencing (WES) in common between pre-therapy and post-therapy melanoma lesions.

Patient ID	*BRAF*V 600 status	R	Gene	Ref seq	aa change	codon change	AF %
#1	**+**	**n**	*RAC1**	NM_018890.4	p.Pro29Ser	c.85C>T	4.2 to 13.8
			*GNAQ**	NM_002072.5	p.Thr96Ser	c.286A>T	3.0 to 66.7
#62	**+**	**n**	*ARID2**	NM_152641.4	p.Gln1313*	c.3937C>T	27.1 to 7.0
#20	**-**	**y**	*NRAS**	NM_002524.3	p.Gln61Arg	c.182A>G	6.5 to 42.0
			HRAS	NM_005343.4	p.Pro140Thr	c.418C>A	20.4 to 41.2
#21	**-**	**y**	*NRAS**	NM_002524.3	p.Gln61Arg	c.182A>G	25.0 to 50.0

			NF1*	NM_001042492.3	p.Ser2093Phe	c.6278C>T	30.0 to 45.2
			*PPP6C**	NM_001123355.1	p.Arg301Cys	c.901C>T	56.4 to 96.6
			*CTNNB1**	NM_001098209.2	p.Ser45Pro	c.133T>C	27.8 to 49.3
			*IDH1**	NM_005896.3	p.Arg132Cys	c.394C>T	37.5 to 23.0
#7	**-**	**y**					
			*MAP2K2***	NM_030662.3	p.Leu102_Ile107del	c.304_321delCTGATCCACCTTGAGATC	65.8 to 45.1
			*NRAS**	NM_002524.3	p.Gln61Lys	c.181C>A	69.8 to 74.0
#63	**-**	**n**					
			*FBXW7***	NM_001349798.2	p.Lys652*	c.1954A>T	64.2 to 71.4
			*KIT**	NM_000222.2	p.Leu576Pro	c.1727T>C	88.8 to 86.4
			TP53	NM_000546.5	p.Pro27Ser	c.79C>T	48.8 to 52.2
#18	**-**	**n**					
			*RAC1**	NM_018890.4	p.Pro29Ser	c.85C>T	13.1 to 36.0
			GNAQ	NM_002072.5	p.Gly64Arg	c.190G>A	10.3 to 15.5
			*BRAF**	NM_001374258.1	p.Leu624Phe	c.1870C>T	29.2 to 60.8
#57	**-**	**n**					
			*BRAF**	NM_001374258.1	p.Gly509Ala	c.1526G>C	32.8 to 58.7

*KIT**	NM_000222.2	p.Lys642Glu	c.1924A>G	20.7 to 47.9

*Abbreviations: R: Response; no: no; y: yes; *: Pathogenic Mutations; **: potential pathogenic mutations; AF: Allele Frequency.*

Among them, 13 mutations were reported as pathogenic in the COSMIC v96 database and 2 novel mutations were considered potentially pathogenic because of their predicted impact on protein function (**Table 2**). Among the two novels potentially pathogenic mutations, only one was reported in a NR patient (#63): the p.Lys652* stop mutation in the *FBXW7* gene. This mutation could confer resistance to immunotherapy and its loss has been recently described to confer radiosensitivity to cancer cells through a mechanism that leads to the accumulation of TP53 (**Gstalder et al., 2020; Cui et al., 2020**).

Among the 13 mutations in *BRAF*, *KIT*, *NRAS*, *HRAS*, *GNAQ*, *NF1*, *PPP6C*, *CTNNB1, ARID2* and *IDH1* genes, already reported as pathogenic in the COSMIC database, two (p.Pro29Ser and p.Thr96Ser in the *RAC1* and *GNAQ* gene, respectively) were found in the same *BRAF* V600+ NR patient (#1). *In vitro* studies have shown that melanoma cell lines harbouring the p.Pro29Ser mutation in the *RAC1* gene are resistant to BRAF and MEK inhibitors. Still, its role in conferring this resistance has yet to be elucidated. However, RAC1 inhibitor drugs are not currently available although SRF / MRTF inhibitors in combination with BRAF inhibitors have recently been shown to be useful in the treatment of BRAFmutant and P29S RAC1 mutant melanoma (**Vanni et al., 2020A**). This finding supports an intrinsic resistance mechanism driven by this mutation.

WES frequently reported the p.Thr96Ser somatic mutation in the *GNAQ* gene in patients with Natural killer / T cell lymphoma (NKTCL). Knockout mice experiments demonstrated how Gαq deficiency improved natural killer (NK) cell survival. In that study, Gαq was also found to suppress NKTCL tumour growth via inhibition of the AKT and MAPK signalling pathways. Furthermore, the Gαq T96S mutant could act in a dominantly negative way to promote tumour growth in NKTCL.

Finally, they observed that patients with GNAQ p.Thr96Ser mutations had a shorter survival. The p.Thr96Ser confers loss of function to Gnaq protein, as demonstrated by increased binding to G beta-gamma protein in cell culture, high Erk and Akt phosphorylation in cultured cells and xenograft tumours, and increased tumour growth in mouse models compared to the wild-type Gnaq (**Li et al., 2019**). The same two genes (*RAC1* and *GNAQ*) were also found concomitantly mutated in another NR patient (#18). Interestingly, this patient revealed a well-known *KIT* mutation (p.Leu576Pro) responding to Imatinib. Finally, the #62 NR patient had a pathogenic p.Gln1313* stop mutation in *ARID2* gene, already described in melanoma (**Hartman et al., 2020**). Cancers with inactivating mutations in ARID2 are more sensitive to PD-1 blockade as well as other forms of immunotherapy (**Pan et al., 2018**). Moreover, a higher sensitivity to different DNA-damaging therapies in ARID2-deficient non-small cell lung cancer cells, likely due to the ARID2 involvement in DNA repair, was observed (**Moreno et al., 2020**).

Interestingly, all mutations found in common between two lesions (except p.Leu576Pro in *KIT* gene (#18), p.Val600Glu and p.Gln1313* in *BRAF and ARID2* genes (#62)) increased in AF over time.

Conversely, we identified 17 melanoma driver genes mutations in the second lesions only (**Table 3**).

Table 3. Melanoma driver gene mutations detected by WES acquired in the post-therapy melanoma lesions.

Patient ID	*BRAF* V600 status	R	Gene	Ref seq	aa change	codon change	AF %
#39	**+**	**Y**	*PREX2*	NM_024870.4	p.Lys621Asn	c.1863G>C	3.5
#42	**+**	**Y**	*KIT**	NM_000222.2	p.Met541Leu	c.1621A>C	22.7
			TP53	NM_000546.5	p.Ser99Tyr	c.296C>A	6.3
			*EZH2**	NM_004456.4	p.Tyr646Asn	c.1936T>A	16.7
			CNOT9	NM_001271634.2	p.Pro131Leu	c.392C>T	41.2
#1	**+**	**n**	*TP53*	NM_000546.5	p.Ser99Tyr	c.296C>A	1.9
			ARID2	NM_152641.4	p.Ala678Gly	c.2033C>G	8.8
			*GNAQ**	NM_002072.5	p.Tyr101*	c.303C>A	66.7
#62	+	n	*KIT**	NM_000222.2	p.Met541Leu	c.1621A>C	46.5
			*RB1**	NM_000321.2	p.Asn123Asp	c.367A>G	49.1
#34	**-**	**n**	*NF1*	NM_001042492.3	p.Ser1030Leu	c.3089C>T	10.3
			TP53	NM_000546.5	p.Ser99Tyr	c.296C>A	5.2
			ARID2	NM_152641.4	p.Pro1000Thr	c.2998C>A	5.9
			ARID2	NM_152641.4	p.His693Gln	c.2079C>A	16.7
			*GNAQ**	NM_002072.5	p.Tyr101*	c.303C>A	36.4
			*GNAQ**	NM_002072.5	p.Thr96Ser	c.286A>T	33.3
#18	**-**	**n**	*MTOR*	NM_004958.3	p.Ser1297Leu	c.3890C>T	19.6

*Abbreviations: R: Response; no: no; y: yes; *: Pathogenic Mutations; AF: Allele Frequency.*

Precisely, in 6 patients the second lesion showed the acquisition of mutations in PREX2, KIT, EZH2, CNOT9, TP53, ARID2, GNAQ, NF1, RB1, and MTOR genes. Among them, 5 are pathogenic mutations (NM_000222.2(KIT):c.1621A>C (p.Met541Leu); NM_004456.4 (EZH2): c.1936T>A (p.Tyr646Asn); NM_002072.5 (GNAQ): c.303C>A (p.Tyr101*); NM_002072.5 (GNAQ): c.286A>T (p.Thr96Ser); NM_000321.2 (RB1): c.367A>G (p.Asn123Asp)). However, we checked by IGV the presence of these muta-tions in the pre-therapy lesion finding only 9 mutations acquired (NM_024870.4 (PREX2): c.1863G>C (p.Lys621Asn) in #39; NM_004456.4 (EZH2): c.1936T>A (p.Tyr646Asn) in #42; NM_001271634.2 (CNOT9): c.392C>T (p.Pro131Leu) in #42; NM_152641.4 (ARID2): c.2033C>G (p.Ala678Gly) in #1; NM_152641.4 (ARID2): c.2998C>A (p.Pro1000Thr) in #34: NM_000321.2 (RB1): c.367A>G (p.Asn123Asp) in #62; NM_000222.2(KIT):c.1621A>C (p.Met541Leu) in #62;

NM_002072.5 (GNAQ): c.303C>A (p.Tyr101*) in #34; NM_002072.5 (GNAQ): c.286A>T (p.Thr96Ser) in #34) of which only 5 are pathogenic COSMIC mutations (**Table 3**). Notably, these 8 variants had been discarded by variant calling quality filters since at low allele frequency and poorly covered.

CNV analysis was evaluated in melanoma driver genes reporting in the 12 matched tumour samples 23 CNVs in common between the two melanoma lesions (**Supplementary Table 5**; **Supplementary Figure 5**) and 49 CNVs acquired in the second lesion (**Supplementary Table 6**; **Supplementary Figure 5**)**.** Interestingly, among the 4 *BRAF* V600+ patients, 2 (#39 and #1) showed acquired *BRAF* amplification and 1 of them (#39) also a *PTEN* deletion in common between the two lesions, as intrinsic resistance mechanism to TT (BRAF+MEKi). However, the *BRAF* amplification was confirmed by MLPA analysis in both lesions of the same patient (#1 and #39), supporting this finding as an intrinsic resistance mechanism.

GENOMIC LANDSCAPE OF DNA DAMAGE REPAIR DEFICIENCY (DDR)

We determined the prevalence of DDR alterations across our cohort considering only exonic somatic Loss Of Function (LOF) with an AF at least 10% (**Supplementary Table 7**). A total of 66 LOF variants, 41 of which are unique, were revealed. Interestingly, 66.7% (6/9) of *BRAF* V600- R patients showed at least one LOF variant *vs* 37.5% (3/8) of *BRAF* V600- NR patients. An opposite trend was found in *BRAF* V600+ patients. In the matched tumour samples, we found 50 DDR LOH in common between the two melanoma lesions (**Supplementary Table 8**). Interestingly, among the 12 matched tu-mour samples, only two patients (#39 and #63) revealed almost one LOH in common. Conversely, we identified 309 LOH in the second lesions only (**Supplementary Table 9**).

FUSION RNA EVENTS

Fusion events were found in all 20 tumours analysed with a total of 895 detected, including 24 recurrent (n ≥ 1); none of them was reported in TCGA Fusion Gene Database (**Hu et al., 2018**). There

was an overall average of 45 fusions per tumour, but further analyses should be performed to validate this result. **Table 4** includes fusions detected by WES in common between the melanoma lesions belonging to the same patient (#20 and #63). Interestingly, we found in the #39 sample a fusion event between two partners (BRAF-AGK) already found in the SKCM TCGA database and classified as Tier1 (variant of strong clinical significance). The biological effect and therapeutic implications of this structural variant have been described in several tumours, including melanoma (**Ross et al., 2016; Vojnicet et al., 2019; Bottonet et al., 2013; Ricarte-Filhoet et al., 2013**). However, in our sample, the BRAF fusion differs in the position of the breakpoints described in TCGA. Interestingly, the #39 sample, belonging to the responder cohort, in addition to the BRAF-AGK fusion, presents both *BRAF* V600E mutation and amplification.

Another interesting fusion event was reported in sample #47 in which a MITF-SNCA rearrangement was shown. This fusion is of particular interest since the protein expression of alpha-synuclein gene (SNCA) may be regulated by microphthalmia-associated transcription factor (MITF) in melanocytic cells (**Hoek et al., 2008**) and *MITF* is a master regulator gene of melanocyte development and differentiation associated with melanoma development and progression (**Yajima et al., 2011**).

Table 4. Fusion event in common between the melanoma lesions.

Sample ID	R	*BRAF* V600 status	Fusion	LeftGene	LeftBreakpoint	RightGene	RightBreakpoint
#20	y	-	AP5B1--FAM168A	AP5B1^ENSG00000254470.3	chr11:65780442:-	FAM168A^ENSG00000054965.10	chr11:73468492:-
			CAST--LINC02112	CAST^ENSG00000153113.23	chr5:96695907:+	LINC02112^ENSG00000249781.7	chr5:9902753:-
			FBXL8--AC138409.2	FBXL8^ENSG00000135722.9	chr16:67160056:+	AC138409.2^ENSG00000215158.9	chr5:34182867:-
			MAP3K1--SERINC5	MAP3K1^ENSG00000095015.6	chr5:56816055:+	SERINC5^ENSG00000164300.17	chr5:80203053:-
			PPFIA1--PPP6R3	PPFIA1^ENSG00000131626.18	chr11:70326818:+	PPP6R3^ENSG00000110075.14	chr11:68558566:+
			TBCA--IL6ST	TBCA^ENSG00000171530.14	chr5:77776205:-	IL6ST^ENSG00000134352.20	chr5:55982811:-
#63	n	-	NCOR1--ZFP3	NCOR1^ENSG00000141027.21	chr17:16079964:-	ZFP3^ENSG00000180787.6	chr17:5091497:+
			YAF2—RYBP	YAF2^ENSG00000015153.14	chr12:42238155:-	RYBP^ENSG00000163602.10	chr3:72446621:-

Abbreviations: R: Response; no: no; y: yes; +: positive; -: negative.

CFDNA MUTATION PROFILES AND DYNAMIC CHANGES DURING TREATMENT

ctDNA was extracted from 14 patients and sequenced by targeted NGS. Moreover, the cfDNA at two therapy consecutive points (t1 and t2 at the time of pre-first line therapy and at the time of disease progression, respectively) was evaluated for two patients (#8 and #62) (**Figure 2**). For one patient (#60 three consecutive points were analysed (t1 at the time at Progression Disease (PD) to adjuvant with BRAF+MEKi; t2 at 11 months after PD; t3 at 22 months after PD) (**Figure 2**). The genomic features of variants, CNVs and fusion, including in the NGS panel were evaluated in the 14 patients (**Supplementary Table 10**). An average of 82 million total reads was generated and mapped to the reference genome per library, and 95% of the mapped reads were on a target relative to the designed bed file. The mean depth of coverage ranged from 23,165× to 96,908× (average of 59,021x). The uniformity of each library, which is the percentage of amplicons (bases) covered greater than 20% of the mean amplicon (base) coverage, ranged from was 98.1 to 99.6%. A molecular coverage above 2000× was obtained only for one cfDNA sample (#8_T1) with an cfDNA input of 2ng was used. The hotspot mutations (*BRAF* p.Val600Glu and *KIT* p.Lys642Glu mutations) detected by WES in a TF were detected by NGS panel the on cfDNA, showing a 69.2% concordance. The discordant cfDNA samples were 4 (#26, #3, #8_T1, and #60). The cfDNA sample #8_T1 did not reveal the *BRAF* p.Val600Glu present in the corresponding tissue since the %LOD for this cfDNA sample range from 1% to 1.2% due to low molecular coverage obtained (443x). The absence of *BRAF* p.Val600Glu in the #26 cfDNA may be due to the response to the BRAF+MEKi therapy in this patient, whereas the lack in the #3 cfDNA may be ascribed to the presence of not-tumour cfDNA confirmed by the presence of the p.Pro61Ala in the *SMO* gene as evidenced by the WES on PBMC of this patient. Finally, #60 cfDNA did not reveal the *BRAF* p.Val600Glu, but this patient was a stage IIIB NED treated for a year and a half with BRAF+MEKi adjuvant with a local relapse. Finally, the dynamic mutation profiles during treatment in the 3 melanoma patients (#8, #62, and #60) are shown in **Figure 2**.

Figure 2. ctDNA dynamic changes in #8, #62, and #60.

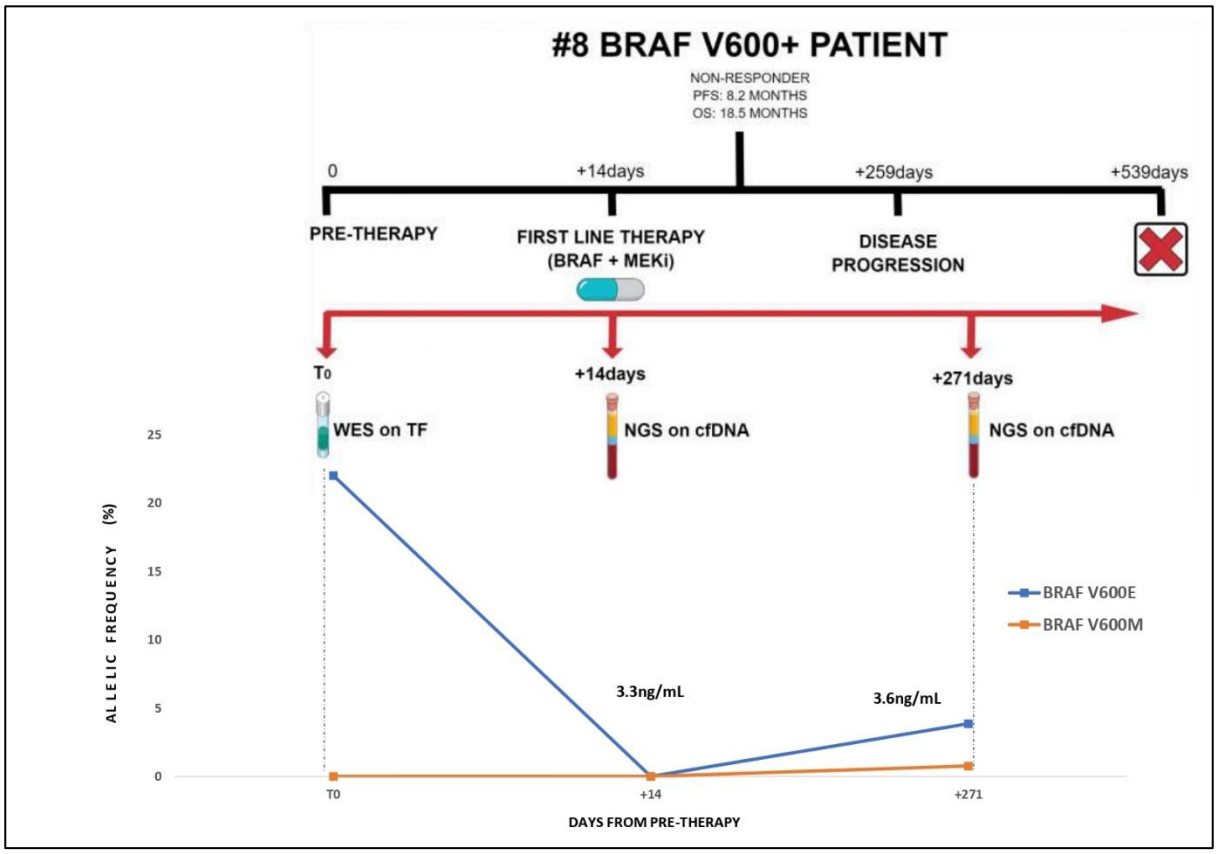

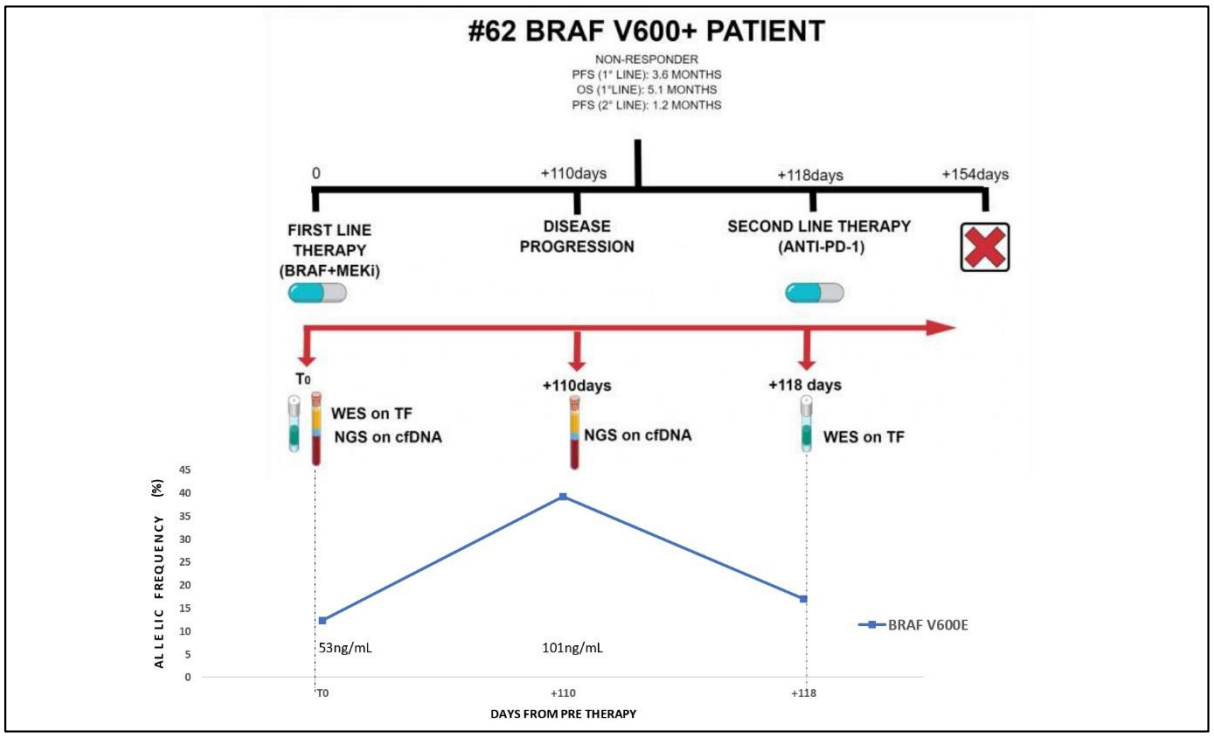

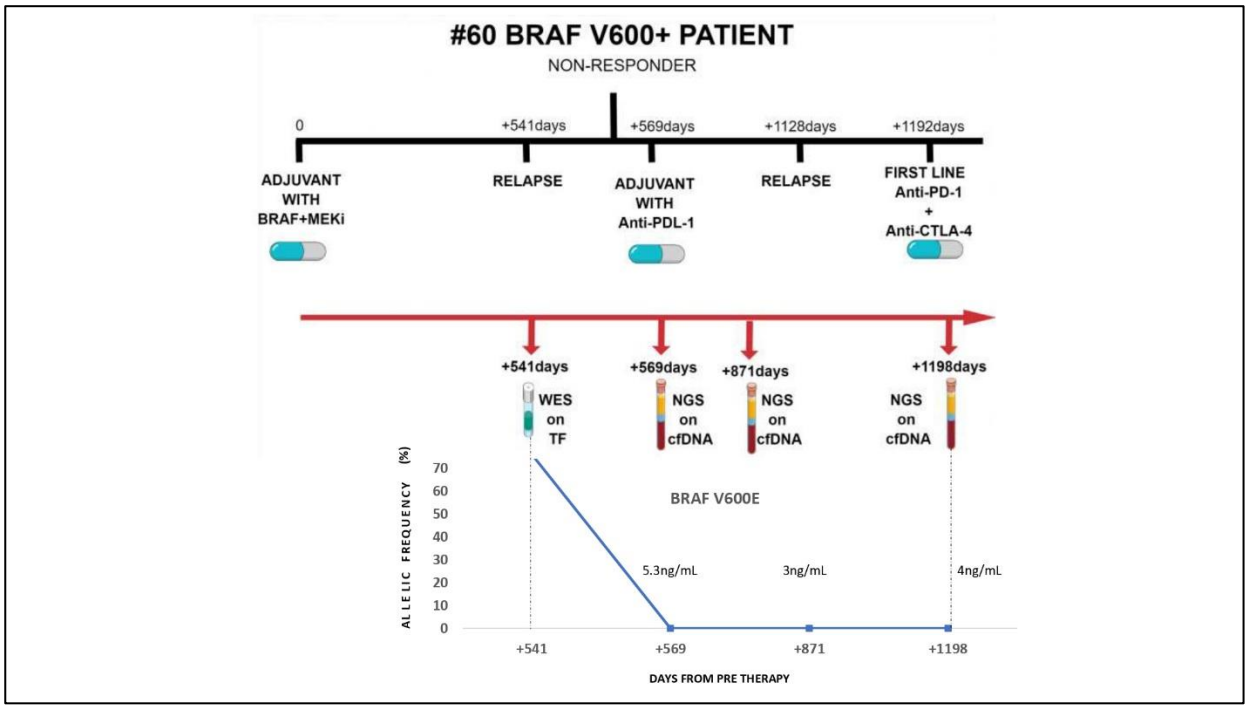

Abbreviations: AF: Allele Frequency; WES: Whole-exome Sequencing; PD: Disease Progression; ddPCR: Droplet digital PCR; cfDNA: circulating free DNA.

Interestingly, the median amount of total cfDNA was 13.5ng/1mL *vs* 45.1ng/1mL in responders *vs* non-responders patients.

CHARACTERIZATION OF GERMLINE MUTATIONS BY WES

WES was carried out on the 36 germline DNA in order to identify susceptibility and/or cancer predisposition genes. 166 cancer predisposition genes were investigated finding 83 exonic and non-synonymous variants (1 pathogenic, 1 Pathogenic/Likely pathogenic, 3 Pathogenic/other/risk factor, 50 conflicting interpretations of pathogenicity, 7 Variant of Uncertain Significance (VUS), 20 not provided, and 1 Benign by ClinVar) (**Aoude et al., 2020**).

Three Pathogenic Variants (PVs) in melanoma predisposition genes were found (*MITF* p.Glu318Lys and *CDKN2A* p.Gly101Trp in #56 and *MITF* p.Glu318Lys in #62). In addition, we found in #63 patient the p. Ser1993ArgfsTer23 PV in the *ATM* gene, which was recently associated with melanoma susceptibility (**Dalmasso et al., 2021**). Overall, three patients carried four melanoma predisposition PVs variants reporting a germline PV frequency of 8.3%. All 4 variants were confirmed in SS.

Interestingly, the p. Ser1993ArgfsTer23 variant in *ATM* was also present in the two tumour tissue lesions with an AF of 74% both at the time of PD with anti-PD-1 adjuvant therapy and before the first line with anti-PD-1. These data were also confirmed by RNA seq analysis reporting an AF of 94% and 82% in the two tumour tissue lesions. Immunohistochemistry (IHC) with anti-ATM Abcam antibody (ab32420) and Recombinant Anti-ATM (phospho S1981) antibody [EP1890Y] (ab81292) performed in FFPE tissue confirmed protein expression loss, in a collaborative study (Prof.ssa Daniela Massi). Western-Blotting (WB) also confirmed this finding carried out on the cell line established from TF showing a total loss of the ATM protein. In addition, in silico analysis of CNVs by WES in the two-tumour tissue lesions revealed a loss of one copy of the *ATM* gene and LOH (**Figure 3**).

Figure 3. Protein Expression and Loss Of Heterozygosity (LOH) induced by the *ATM* pathogenic germline variant (p. Ser1993ArgfsTer23) in the patient tissue and cell line.

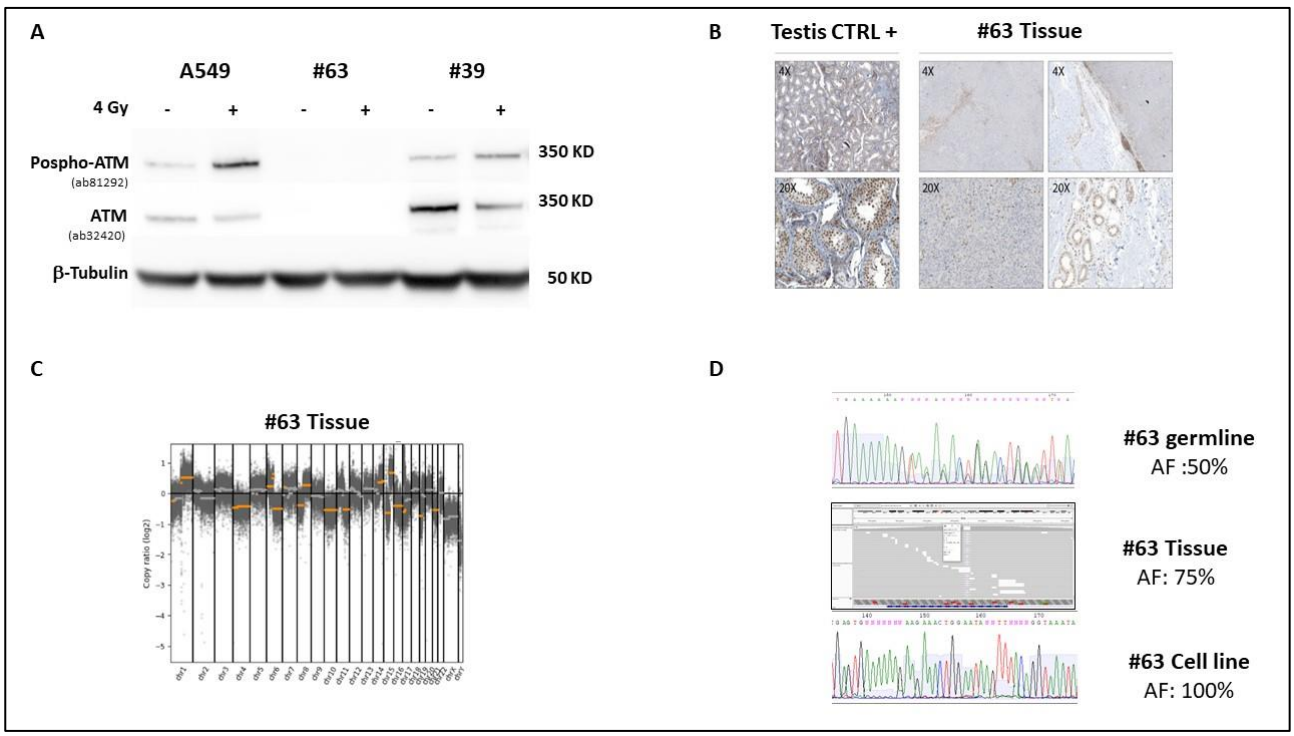

The figure shows (**A**) level of Anti Pospho-ATM and Anti-ATM in A549 (CTRL +) and in two patients' established melanoma cell lines (#63 and #39) at baseline (-) or under exposure to 4Gy radiation (+) by Western-Blotting (**B**) ATM protein expression by IHC in #63 tissue and in positive control (Testis) (**C**) *ATM* Allelic deletion in #63 tissue by WES (**D**) *ATM* variant frequency in germline, tissue and melanoma cell line DNA from #63 patient.

DISCUSSION

This study aimed to describe the genetic layout of advanced or metastatic melanoma in a real-world setting of 36 patients treated with TT (BRAF+MEKi) or ICB agents (nivolumab, pembrolizumab alone or in combination with ipilimumab), according to clinical practice, classifying them in responders or non-responders. Whole exome sequencing data were obtained from matched pre-therapy and post-therapy biopsies in 12 melanoma patients, focusing on acquired and intrinsic resistance mechanisms, to investigate tumor evolution and heterogeneity. In absence or in addition to temporarily available biopsy, cfDNA was used as a surrogate when available (**Supplemtary Table 10**). Melanoma driver gene mutations, TMB and CNVs were analysed in *BRAF* V600+ patients, while CNVs in the HLA-A, HLA-B, HLA-C, TAP2, PD-1 (PDCD1), PD-L1 (CD274) and PDL2 (PDCD1LG2) genes were additionally evaluated in *BRAF* V600- patients. Interestingly, we found an average of melanoma driver gene mutations in non-responders *BRAF* V600+ 1.7 times higher than in responders *BRAF* V600- (average of 2.0 and 3.3 in responder and in non-responder, respectively). This finding may suggest a genetic mechanism allowing tumour escape from response to TT. In contrast, no differences for both driver melanoma genes and interferon pathway genes were found in the cohort of *BRAF* V600- patients. In line with the four main melanoma genetic subtypes established by The Cancer Genome Atlas, we found 52.8% (19/36) *BRAF*mutant, 30.6% (11/36) NRASmutant, 8.3% NF1mutant and 13.9% (5/36) triple wild-type patients (**Cancer Genome Atlas Network, 2015)**.

Among the BRAF-mutant, we found a patient with concurrent *BRAF* V600 and *NRAS* Q61 mutation and another with *NF1* mutation. Finally, one patient, showed coexisting *NRAS* and *NF1* mutations. Since *NF1* mutations can be found in melanomas with concurrent *BRAF* or *NRAS* hotspot mutation, a three-group classification of melanoma (mutant BRAF, mutant RAS, non-BRAFmut/non-NRASmut) has been proposed (**Palmieri et al., 2018**), and our data are in agreement.

In addition to *BRAF*, *NRAS* and *NF1*, for which a high mutation frequency in melanoma is already known (**Cancer Genome Atlas Network, 2015; Vanni et al., 2020A**), the most frequently mutated driver genes detected in our cohort of 36 melanoma patients were *TP53* (N°10), *ARID2* (N°7), *KIT* (N°6), *PREX2* (N°5), *RAC1* (N°5), and *FBXW7* (n°4).

TP53 is the most frequently mutated gene in human cancer, with a significant prevalence of missense mutations, with a frequency of 36.8% in the TCGA database (**Hainaut et al., 2019**). In a recent review, we estimated a *TP53* gene mutation frequency of 14.9 in 992 skin melanoma samples (**Vanni et al., 2020A**). The frequency of *TP53* mutations in our study cohort is in line with the literature data (mutation rate of 27.8%).

Interestingly, among the 20 melanoma driver genes mutations (**Table 2**), we found a patient (#63) with a novel potentially pathogenetic variant in the *FBXW7* gene (p.Lys652*), confirmed by SS, in common between pre-therapy and post-therapy biopsy matched. *FBXW7* is a critical tumor suppressor gene and a member of the F-box protein family, ubiquitin ligase complex, that controls proteasome-mediated degradation of oncoproteins such as cyclin E, c-Myc, Mcl-1, mTOR, Jun, Notch, and AURKA, STAT2 (**Minella and Clurman, 2005; Yeh et al., 2018; Lee et al., 2020**). Inactivating mutations in *FBXW7* have been described in various human tumors and cancer cell lines (**Akhoondi et al., 2007**). LOF of FBXW7 in several human cancers has clinical implications and prognostic value: the use of rapamycin has proven to inhibit breast cancer cells with loss of FBXW7 by mTOR inhibition (**Mao et al., 2008; Yeh et al., 2018**). Moreover, another study revealed FBXW7α deficiency leading to HSF1 (Heat shock factor 1) accumulation and subsequent activation of the invasion-supportive transcriptional program and metastatic potential of human melanoma cells (**Kourtis et al., 2015**). The novel mutation found in our study, could have conferred resistance to immunotherapy in this patient, belonging to NR *BRAF* V600- cohort; its loss has been recently described to confer radiosensitivity to cancer cells through a mechanism that leads to the accumulation of TP53 (**Gstalder et al., 2020; Cui et al., 2020**). This gene has not been investigated

yet in this context. To gain a clearer picture of FBXW7 impact in melanoma, it will be necessary to confirm pathogenicity of this variant through functional assays.

Two other mutations (p.Pro29Ser in the *RAC1* and p.Thr96Ser in *GNAQ* gene), reported as pathogenic in COSMIC database, were concomitantly found in one *BRAF* V600+ NR patient (#1).

From a clinical point of view, #1 patient started a first-line therapy with BRAF+MEKi in August 2016. He had no clinical benefit from first line therapy, and, after a massive progression of the disease, he started a II-line anti-PD-1 therapy from which, equally, he had no clinical benefit (PFS 0.97 months). The death occurred one month after the start of anti-PD-1. The paradoxical activation of the MAPK/ERK pathway through p.Pro29Ser mutation in the *RAC1* gene is recognized mechanism responsible for primary/acquired resistance or secondary tumors occurrence in melanoma. Its role in conferring this resistance should be better defined, although RAC1 inhibitor drugs are not currently available and SRF / MRTF inhibitors in combination with BRAF inhibitors have recently been shown to be useful in the treatment of BRAF mutant and P29S RAC1 mutant melanoma (**Vanni et al., 2020A**). However, targeting *RAC1* is not currently being tested among available clinical trials (https://clinicaltrial.gov).

The p.Thr96Ser somatic mutation in the *GNAQ* gene was reported in patients with Natural killer / T cell lymphoma and recently in hepatocellular carcinoma increasing cell proliferation, anchorage-independent growth, and migration while also activating the MAPK signalling pathways. (**Li et al., 2019; Choi et al., 2021**).

The same two genes (*RAC1* and *GNAQ*) were also found concomitantly mutated in another NR patient (#18) with a well-known *KIT* mutation (p.Leu576Pro) that could be sensitive to Imatinib. Indeed, #18 patient started a I-line therapy with anti-PD-1 in July 2017. The disease progression occurred on December 2017 and the patient started a II-line chemotherapy. Imatinib was not considered as a possible therapeutic agent because the KIT specific analysis was not performed at the time of the therapy selection. Finally, the #62 NR patient had a pathogenic p.Gln1313* stop

mutation in *ARID2* gene, already described in melanoma (**Hartman et al., 2020**). Cancers with inactivating mutations in *ARID2* are more sensitive to PD-1 blockade as well as other forms of immunotherapy (**Pan et al., 2018**). Moreover, a higher sensitivity to different DNA-damaging therapies in ARID2-deficient non-small cell lung cancer cells, likely as a result of the ARID2 involvement in DNA repair, was observed (**Moreno et al., 2020**).

CNVs in melanoma driver genes reported an average of CNVs 1.2 times higher in *BRAF* V600+ NR than in *BRAF* V600+ R cohort. No difference was found in the cohort of *BRAF* V600- patients. The CNVs data confirmed the trend observed for driver genes mutations. Our WES data revealed no difference in TMB between R and NR patients, while *BRAF* V600- responders showed a doubled TMB compared to non-responders in keeping with other studies. *PTEN* deletion has been already identified as one of the best-known molecular mechanisms responsible for the intrinsic resistance to BRAF Inhibitors and in our cohort of *BRAF* V600+ patient we found a frequency of 42.1% (2 patient responder (#2 and #39) to BRAF+MEKi and 5 patient non-responder to BRAF+MEKi (#3,#14, #19, #56, and #10). The reactivation of the MAPK pathway at the level of BRAF could occur in several ways, including *BRAF* gene amplification, and 3 patients among the *BRAF* V600+ cohort revealed it (3/19 with a frequency of 15.8%), in accordance with melanoma WES data that showed acquisition of resistance to BRAF inhibitors due to *BRAF* gene amplification in around 20% of patients (**Shi et al.,2012**). Only one *BRAF* V600+ patient (#39), harboring *BRAF* amplification, responded to BRAF+MEKi, but in patients with concomitant *PTEN* deletion, revealed a *BRAF* fusion event that seems to lack the tyrosin kinase domain. This finding supports the idea that this patient could be respond despite the concomitant presence of V600E and amplification in *BRAF*. This hypothesis will be investigated *in vitro* study, being the melanoma cell line established from this patient.

LOH analysis showed an inverse correlation between TMB and the phenomena of whole-genome doubling (WGD) commonly in human cancers generating genetically unstable tetraploid cells that fuel tumour development. Indeed at the endstage disease loss of mutations was also

observed, often as a result of LOH. One potential role of LOH could be a mechanism of tumour biological advantage by eliminating multiple deleterious mutations and reducing immunogenicity through deletion of neoanti-gens in single mutational events. In our cohort, we observed in the most metastases The WGD that could protect sub-clones by providing adequate essential proteins permitting selective advantage from focal deletion events. We found that the majority of patients that showed WGD had a worse prognostic significance in mela-noma.

Finally, no associations with the response were found with the Cosmic signature, with the SBS7 as the most signature revealed, in line with data previously described for melanoma.

The further analysis of *TERT* promoter variants confirmed the data previously reported in literature regarding its association with response to TT therapy. Conversely, no difference was revealed in the 14 *BRAF* V600- patients.

Transcriptional profiles by total RNA sequencing performed on 20 TF from 16 melanoma patients of our cohort could integrate the mutational patterns identifying common altered signalling pathways and different gene expression patterns resulting from somatic changes in melanoma driver genes. Indeed, transcript alterations often result from somatic changes in cancer genomes, including overexpression, altered splicing and gene fusions. To date, I analysed the presence of fusion events, and mRNA expression analysis is ongoing.

Germline status of our cohort was established by searching for PVs in melanoma predisposition and DDR genes, finding 3 PVs in melanoma predisposition genes *(MITF* p.Glu318Lys and *CDKN2A* p.Gly101Trp in #56 and *MITF* p.Glu318Lys in #62). Inherited PVs in the *CDKN2A* tumor suppressor gene are among the strongest risk factors for cutaneous melanoma. Recent studies demonstrate that the clinical activity of BRAFi+MEKi in patients with germline *CDKN2A* PV was not inferior to that of clinical trials and real-world studies (**Spagnolo et al., 2021**), while the response rate in immunotherapy regimens was superior due to increased tumour mutational load (**Helgadottir et al., 2020**).

Our patient *BRAF* V600+ (#56) carrying germline *CDKN2A* PV concomitantly with germline *MITF* PV did not respond either to adjuvant therapy with BRAF+MEKi or with anti-PD-1. Finally, one patient (#63) *BRAF* V600- presented a novel PV in the *ATM* gene (p.Ser1993ArgfsTer23). In a recent multicentric international study on 2105 melanoma cases germline, *ATM* heterozygous variants have been associated with melanoma risk, therefore proposing *ATM*, which was previously established as a melanoma Genome-Wide Association Study (GWAS) hit (**Landi et al., 2020**), as a melanoma intermediate risk gene (**Dalmasso et al., 2020**). Since mutations of *ATM* rarely occur in melanoma, the status of its protein expression and its clinical significance have been rarely investigated. To the best of our knowledge, this is the first time that an *ATM* germline PV in a melanoma patient was fully investigated. Based on *ATM* IHC and WB analysis, we found that our PV implicates protein loss of expression supported by *ATM* LOH and loss of one copy. These results support *in silico* classification of this germline variant in *ATM* (p.Ser1993ArgfsTer23) as pathogenic with proof of concept functional data.

Despite being unselected for melanoma family history, our cohort revealed a high germline PVs rate (8.3%). None of these patients showed a personal history of multiple primary melanoma nor family melanoma history or associated cancers. Interestingly, this figure is comparable to 9.5% that we recently obtained in an overview of 5-years of multigene testing in melanoma patients selected for personal or family history of melanoma or associate cancers within the Italian Melanoma Intergroup (**Bruno et al., in press**), supporting the germline testing secondary to somatic WES.

Moreover, we test the utility of cfDNA analysis as a surrogate for tissue biopsy for non-invasive identification of hotspot mutations (*BRAF* p.Val600Glu and *KIT* p.Lys642Glu mutations) showing a concordance of 69.2% with tissue biopsy data (4 discordant cfDNA samples). We can formulate 2 main scenarios to explain this discrepancy. First, the presence of a low disease burden, as in #60 patient, could reflect in a low amount or even an absence of circulating DNA and alternatively, as in #26 patient, a response to TT probably resulted in absence of ctBRAF mutant DNA. Second, the

presence of exclusively encephalic metastases (#3, #8, and #60) ,effectively isolated by a functioning blood brain barrier, supports low levels of ctDNA (**Marczynski et al., 2020**).

Both these scenarios necessarily raise questions about the limits of ctDNA. In the first hypothesis, it is necessary to question the lower sensitivity limit of the method in relation to the burden of the disease. The second hypothesis should investigate whether ctDNA monitoring can be equally reliable in patients with extraencephalic or exclusively intraencephalic disease. In this regard, I plan to carry out a prospective study in patients with advanced melanoma with exclusively intra-brain disease in which ctDNA will be monitored at baseline, during therapy and at progression.

As ctDNA levels are thought to reflect tumor burden, a decrease in ctDNA while on therapy may suggest treatment efficacy. We assessed whether longitudinal changes in ctDNA of three patients could supplement or improve RECIST-based measures for decision making during drug therapy. Only in one case (#60), the level of BRAF mutant remain undetectable during the therapy both at the time of PD to the BRAF+MEKi adjuvant and during therapy with adjuvant and first line immunotherapy, which can be explained by the second hypothesis, also confirmed by total cfdna levels remaining low and constant over time (ranging from 3ng/ml to 5ng/mL) (**Figure 2**). Conversely, at the time of PD to first line therapy with BRAF+MEKi, patient #8 resurfaces the *BRAF* V600E in ctDNA together with another mutation in the same codon (p.Val600Met) that could explain the progression to TT (**Figure 2**). Finally, the *BRAF* V600E longitudinal changes in ctDNA of the #62 patient could predict TT treatment response (**Figure 2**). In fact, the *BRAF* V600E in ctDNA increased during the first-line therapy with BRAF+MEKi passing from an AF of 12% to 39% at the PD, as well as the total cfDNA (from 53ng/1mL to 101.3ng/mL).

CONCLUSIONS

Although our study presents the limitation of the small number of samples analyzed, to the best of our knowledge, it is rare to find studies assessing the genetic layout by WES from DNA extracted from TFs in a consecutive real-world setting of melanoma patients undergoing treatment, in order to pave the way to discriminate patients which could benefit from one treatment over another.

Indeed, the identification of mutations associated with primary resistance to BRAF+MEKi (i.e #1) remains one of the main objects of research, playing a progressively increasing role in clinical practice. In fact, the early recognition of these patients would allow to define with greater certainty the most suitable therapeutic path, allowing to exclude a therapy from which the patient could obtain exclusively toxicity without the possibility of clinical benefit. Moreover, the complete characterization of the molecular profile of the patient with advanced melanoma can allow access to specific therapies that, in clinical practice, could be under-used.

An example comes from #18 patient, who could have benefited from an c-kit inhibitor that was not used in the absence of the complete information.

In this study, we explore resistance-associated mutational profile pointing out known and novel potential melanoma driver and resistance gene mutations and encouraging functional *in vitro* and *in vivo* studies to confirm their role in melanoma.

The main limit of this study is represented by the low number of patients fully analyzed. Unfortunately, having consecutive biopsies of patients before systemic therapy and at the various times of progression of the disease, collides with the clinical context, the (sometimes inaccessible) sites of progression (i.e. brain), and the patient's will. However, this weakness can also be an opportunity, since this case series is entirely real-world, reflecting exactly the patient's characterization possibilities in terms of biopsy accessibility and available material. In this context,

liquid biopsy opens up considerable possibilities as a potential biomarker predictor of response or relapse.

This study is preliminary to the analysis of the complex interplay of the tumour cells with the tumour microenvironment and the immune system, including local and systemic factors, which are likely to modulate therapy efficacy. All of these factors are complex and change in time, and their integration in a real-world serie of melanoma patients longitudinally followed during therapy is going to yield major insight inthis interplay.

Supplementary Figures

Supplementary Figure 1: Melanoma driver genes, interferon-gamma pathway, DDR genes selected for mutation, CNV and LOH analysis

A

ARID2	EZH2	KRAS	PIK3CA	SNX31
BRAF	FBXW7	MAP2K1	PPP6C	STK19
CDK4	GNA11	MAP2K2	PREX2	TACC1
CDKN2A	GNAQ	MITF	PTEN	TERT
CNOT9	HRAS	MTOR	RAC1	TP53
CTNNB1	IDH1	NF1	RASA2	WT1
DDX3X	KIT	NRAS	RB1	/

B

CXCL10	IFR9	JAK1	PSME1	STAT3
IFGNR2	IL10RA	JAK2	SOCS1	STAT4
IFI30	IL10RB	PIAS1	SOCS3	/
IFNG	IL12RA	PIAS4	STAT1	/
IFNGR1	IRF1	PPKCD	STAT2	/

C

AEN	CDC25A	EME2	FANCL	LIG3	NEIL3	PMS1	PPP4R4	RECQL5	SETMAR	TDP2	XPA
ALKBH1	CDC25B	ENDOV	FANCM	LIG4	NFATC2IP	PMS2	PRKDC	REV1	SHFM1	TELO2	XPC
ALKBH2	CDC25C	ERCC1	FEN1	MAD2L2	NHEJ1	PNKP	PRPF19	REV3L	SHPRH	TOP3A	XRCC1
ALKBH3	CDC5L	ERCC2	GADD45A	MBD4	NSMCE1	POLA1	PTEN	RFC1	SLX1A	TOP3B	XRCC2
APEX1	CDK7	ERCC3	GADD45G	MDC1	NSMCE2	POLB	RAD1	RFC2	SLX1B	TOPBP1	XRCC3
APEX2	CETN2	ERCC4	GEN1	MGMT	NSMCE3	POLD1	RAD17	RFC3	SLX4	TP53	XRCC4
APITD1	CHAF1A	ERCC5	GTF2H1	MLH1	NSMCE4A	POLD2	RAD18	RFC4	SMARCA4	TP53BP1	XRCC5
APLF	CHEK1	ERCC6	GTF2H2	MLH3	NTHL1	POLD3	RAD23A	RFC5	SMARCAD1	TREX1	XRCC6
APTX	CHEK2	ERCC8	GTF2H3	MMS19	NUDT1	POLD4	RAD23B	RIF1	SMARCC1	TREX2	YWHAB
ASCC3	CLK2	EXO1	GTF2H4	MNAT1	NUDT15	POLE	RAD50	RMI1	SMC5	TTK	YWHAE
ATM	CUL3	EXO5	GTF2H5	MORF4L1	NUDT18	POLE2	RAD51	RMI2	SMC6	TYMS	YWHAG
ATR	CUL4A	FAAP100	H2AFX	MPG	OGG1	POLE3	RAD51B	RNF168	SMUG1	UBE2A	ZSWIM7
ATRIP	CUL5	FAAP20	HELQ	MPLKIP	PALB2	POLE4	RAD51C	RNF169	SOX4	UBE2B	/
ATRX	DCLRE1A	FAAP24	HERC2	MRE11A	PARG	POLG	RAD51D	RNF4	SPO11	UBE2N	/
BABAM1	DCLRE1B	FAM175A	HES1	MRPL40	PARP1	POLH	RAD52	RNF8	SPRTN	UBE2T	/
BARD1	DCLRE1C	FAN1	HFM1	MSH2	PARP2	POLI	RAD54B	RNMT	STRA13	UBE2V2	/
BCAS2	DDB1	FANCA	HLTF	MSH3	PARP3	POLK	RAD54L	RPA1	SWI5	UIMC1	/
BLM	DDB2	FANCB	HMGB1	MSH6	PARP4	POLL	RAD9A	RPA2	SWSAP1	UNG	/
BRCA1	DMC1	FANCC	HMGB2	MUS81	PARPBP	POLM	RAD9B	RPA3	TCEA1	USP1	/
BRCA2	DNA2	FANCD2	HUS1	MUTYH	PAXIP1	POLN	RBBP8	RPA4	TCEB1	UVSSA	/
BRCC3	DNTT	FANCE	IDH1	NABP2	PCNA	POLQ	RBX1	RRM1	TCEB2	WDR48	/
BRE	DUT	FANCF	INO80	NBN	PER1	PPP4C	RDM1	RRM2	TCEB3	WEE1	/
BRIP1	EID3	FANCG	KAT5	NEIL1	PLK3	PPP4R1	RECQL	RRM2B	TDG	WRN	/
CCNH	EME1	FANCI	LIG1	NEIL2	PLRG1	PPP4R2	RECQL4	RTEL1	TDP1	XAB2	/

Figure S1. Melanoma driver (**A**), interferon-gamma pathway (**B**), DNA Damage Repair Deficiency (DDR) genes (**C**) selected for mutation, Copy Number Variation (CNV) and Loss Of Heterozygosity (LOH) analysis.

Supplementary Figure 2. Melanoma driver and interferon-gamma pathway genes.

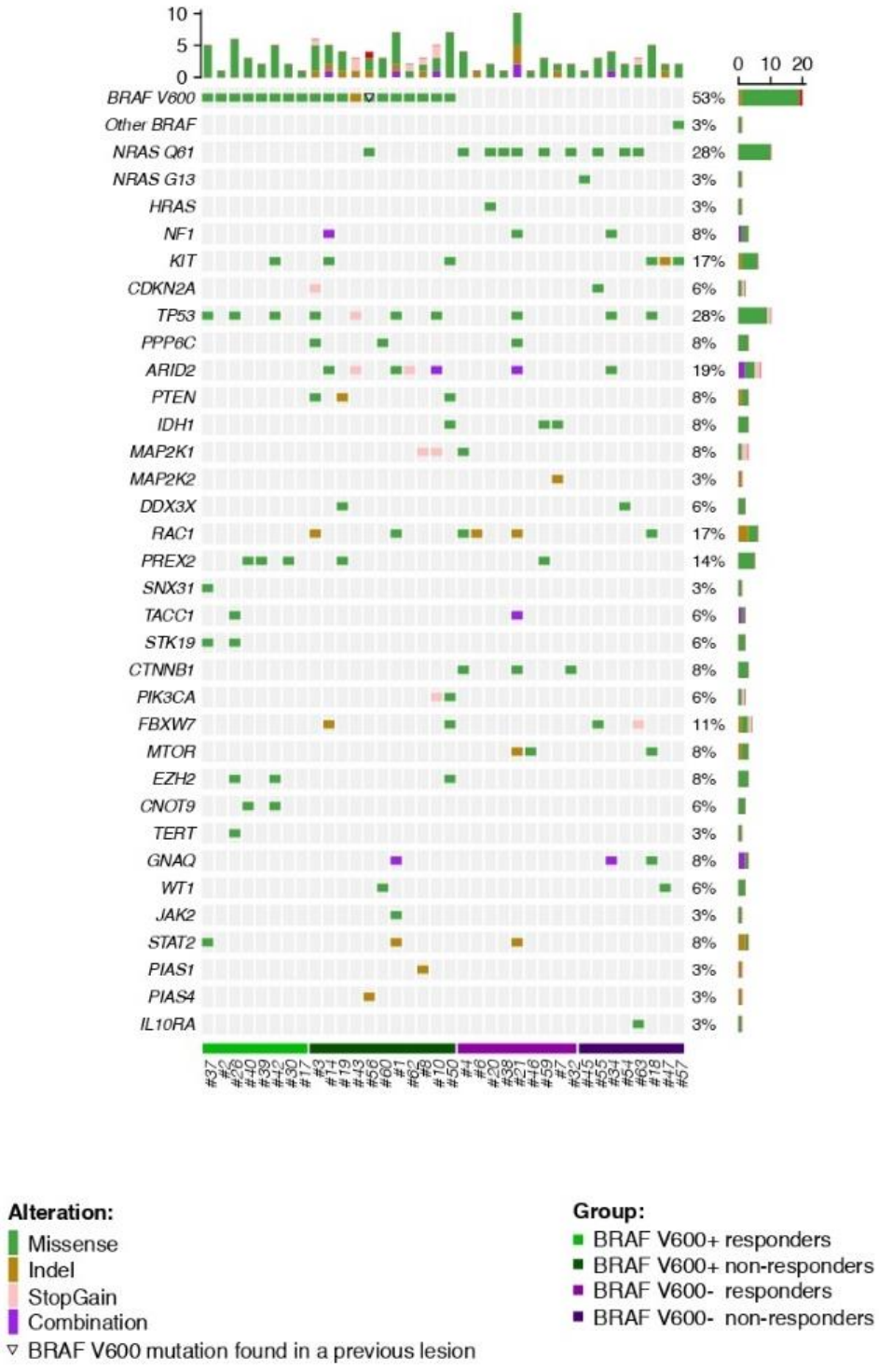

Figure S2. For each of 36 patients (columns), genomic profiles (rows) were characterized. Mutations in melanoma driver genes and interferon-gamma pathway genes was calculated using mutations with 'PASSING' filter (missense, indels and stopgain mutations). Missense variants (red), indel (ocher), stopgain (pink), and combination of different mutations type (violet) are shown for each sample. The cell with vertical black lines indicates a patient with BRAF V600 mutation found in a previous lesion. In each well are reported the variants with the allele frequency.

Supplementary Figure 3. Copy Number Variations (CNVs) and Loss Of Heterozygosity (LOH) in melanoma driver genes

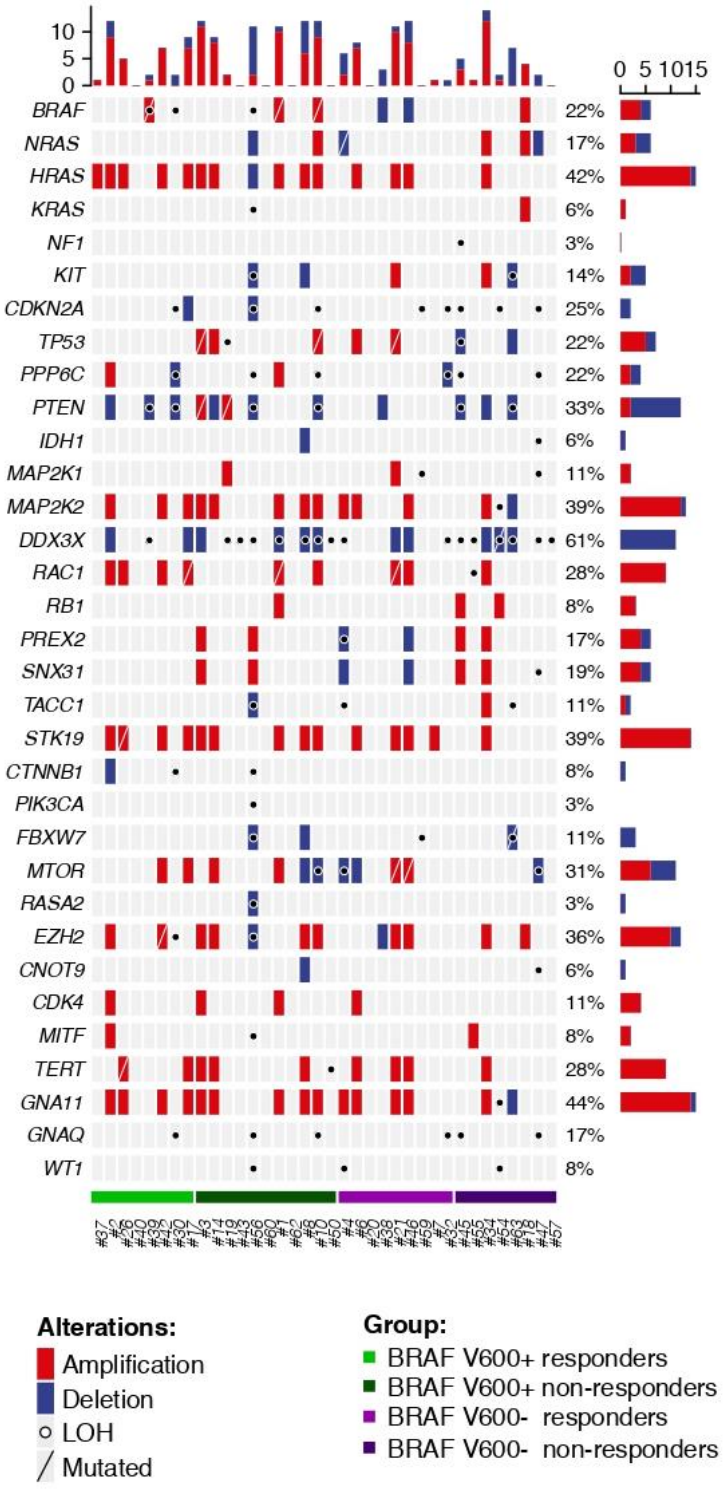

Figure S3. For each of 36 patients (columns), amplifications, deletions and LOH in driver genes (rows) were characterized. CNVs in melanoma driver genes was calculated using CNVkit 0.9.7, while LOH was performed using ASCAT. Bona fide LOH events were defined as region with number of copies of the minor allele equal to zero. Amplifications (red), deletions (blue), mutation plus amplification/deletion (transverse line), and LOH (circle) are shown for each sample.

Supplementary Figure 4. : Intrinsic resistance and/or acquired resistance to therapy in 12 melanoma patients.

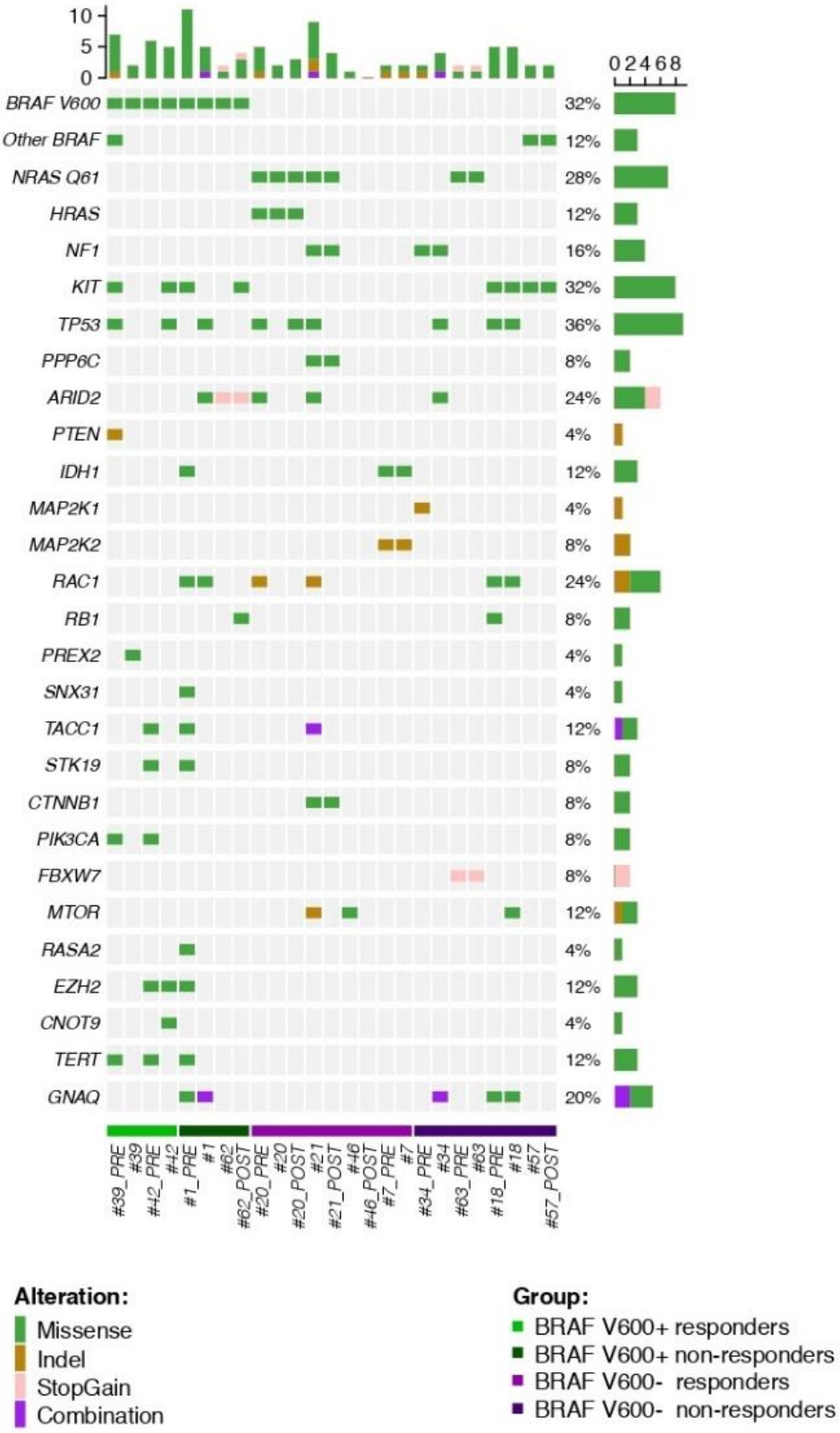

Figure S4. For each of 12 patients (25 tumour samples), genomic profiles in driver genes (rows) were characterized. Mutations in melanoma driver genes was calculated using mutations with 'PASSING' filter (missense, indels and stopgain mutations). Missense variants (red), indel (ocher), stopgain (pink), and combination of different mutations type (violet) are shown for each sample.

Supplementary Figure 5: Copy Number Variations (CNVs) and Loss Of Heterozygosity (LOH): Intrinsic resistance and/or acquired resistance to therapy in 12 melanoma patients

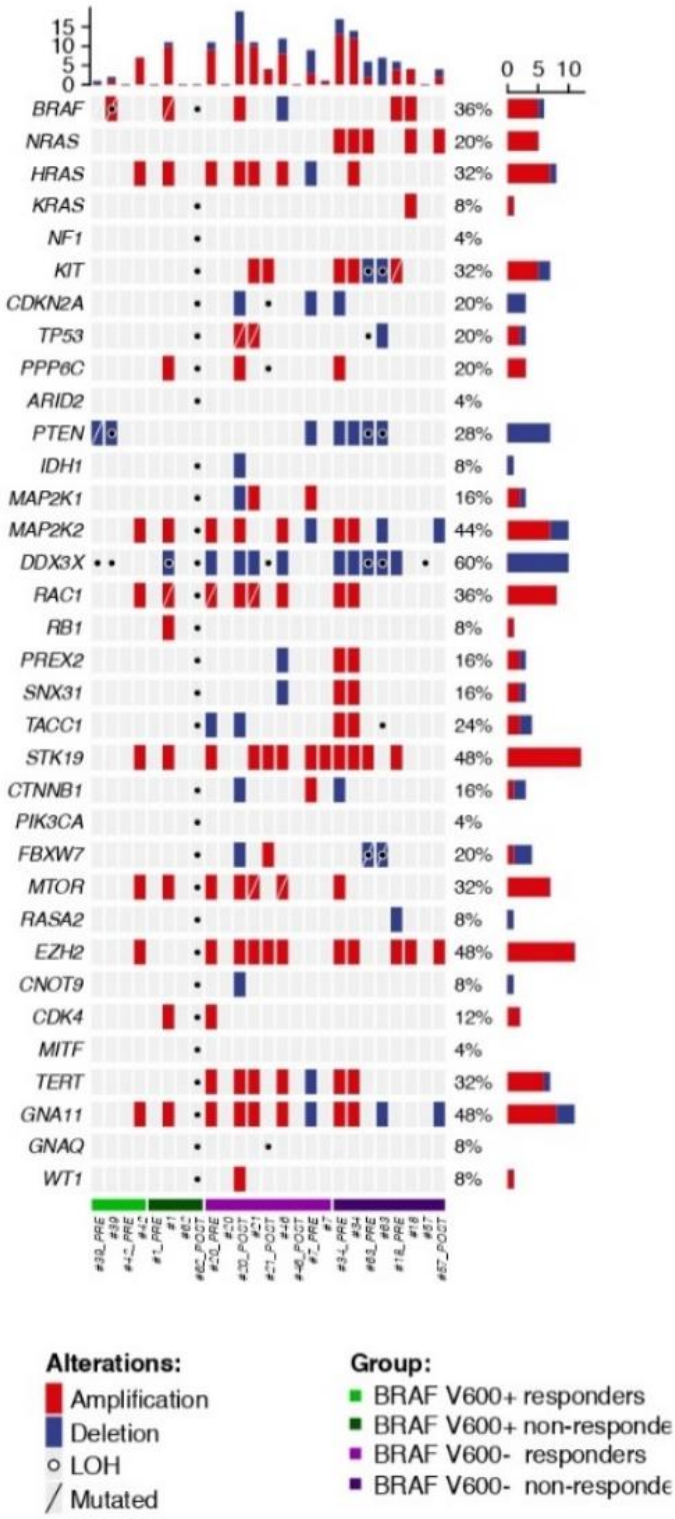

Figure S5. For each of 12 patients (25 tumour samples) (columns), amplifications, deletions and LOH in driver genes (rows) were characterized. CNVs in melanoma driver genes was calculated using CNVkit 0.9.7, while LOH was performed using ASCAT. Bona fide LOH events were defined as region with number of copies of the minor allele equal to zero. Amplifications (red), deletions (blue), mutation plus amplification/deletion (transverse line), and LOH (circle) are shown for each sample.

Supplementary Tables

Supplementary Table 1. Clinical characteristics of the enrolled patients.

Patient ID	*BRAF* V600 Status	Adjuvant therapy	1st line therapy	RECIST BOR 1st line therapy	PFS 1st line therapy	2nd line therapy	RECIST BOR 2nd line therapy	PFS 2nd line therapy	iAEs (G3-G5)	CLINICAL BENEFIT		
										Adjuvant	TT	ICI
#1	+	No	BRAF+MEKi	SD	7,53	Anti-PD-1	PD	0,93	No	NA	0	0
#2	+	No	BRAF+MEKi	SD	11,10	Anti-PD-1	PD	2,93	No	NA	1	0

#3	+	No	BRAF+MEKi	PD	3,07	No	NA	NA	No	NA	0	NA
#8	+	No	BRAF+MEKi	SD	8,17	No	NA	NA	No	NA	0	NA
#10	+	No	BRAF+MEKi	SD	5,73	Anti-PD-1	PR	9,07	No	NA	0	1

#14	+	No	Anti-CTLA-4 + Anti-PD-1	PD	1,37	BRAF+MEKi	PD	4,73	Colitis (G4)	NA	0	0
#17	+	No	Anti-PD-1	SD	11,20	No	NA	NA	Pneumonia (G1)	NA	NA	1
#19	+	No	BRAF+MEKi	SD	4,20	Anti-PD-1	PD	0,37	No	NA	0	0

#26	+	No	BRAF+MEKi	PR	13,07	BRAF+MEKi	PD	5,43	No	NA	1	NA
#30	+	No	Anti-PD-1	PR	7,93	No	NA	NA	Vitiligo	NA	NA	1
#37	+	No	BRAF+MEKi	PR	20,33	Anti-PD-1	PD	1,46	No	NA	1	0

									No				
#39	+	No	BRAF+MEKi	PR	24,97	Anti-PD-1	SD	7,33		NA	1	1	
									No				
#40	+	No	BRAF+MEKi	PR	19,63	Anti-PD-1	SD	12,2		NA	1	1	
									No				
#42	+	No	BRAF+MEKi	PR	20,10	No	NA	NA		NA	1	NA	

									No			
#43	+	Adjuvant with BRAF+MEKi	BRAF+MEKi	PR	4,90	No	NA	NA		0	0	NA
									No			
#50	+	No	Anti-PD-1	PD	1,00	BRAF+MEKi	PR	2,96		0	0	0
									No			
#56	+	Adjuvant with BRAF+MEKi	Anti-PD-1	PD	2,00	Chemotherapy	PD	1,93		0	NA	0

										No			
		Adjuvant with BRAF+MEKi									0		
#60	+		No	NA	NA	No	NA	NA				NA	NA
		Adjuvant with anti-PD-1									0		
#62	+	No	BRAF+MEKi	PR	3,60	Anti-PD-1	PD	1,2	No		NA	0	0

#4	-	No	Anti-CTLA-4	PD	5,27	Anti-PD-1	PR	13,1	Thyroiditis and hypophysitis	NA	NA	1
#6	-	No	Anti-PD-1	SD	10,30	Anti-CTLA-4	PR	6,76	No	NA	NA	1
#7	-	No	Anti-PD-1	PR	64,20	No	NA	NA	Bullous pemphigoid	NA	NA	1

#18	-	No	Anti-PD-1	PD	5,90	Chemotherapy	PD	0,77	No	NA	NA	0
#20	-	No	Anti-PD-1	SD	3,73	Anti-PD-1	CR	13,06	No	NA	NA	1
#21	-	Anti-PD-1 +/- anti-CTLA-4	No	NA	NA	No	NA	NA	Vitiligo	1	NA	NA

#32	-	No	Anti-PD-1	PD	9,33	Anti CTLA-4	PR	13,86	Vitiligo	NA	NA	1
#34	-	No	Anti-PD-1	PD	2,80	No	NA	NA	No	NA	NA	0
#38	-	No	Anti-PD-1	PD	4,57	Anti-CTLA-4	SD	10,86	Amylase and lipase	NA	NA	1

#45	-	No	Anti-PD-1	PD	1,53	No	NA	NA	No	NA	NA	0
#46	-	No	Anti-PD-1	PR	29,43	No	NONo	NA	Hypothyroidism and arthritis	NA	NA	1
#47	-	Adjuvant with anti-PD-1	c-Kit-i	PR	6,33	Anti-CTLA-4	PD	1,1	No	0	0	0

#54	-	Adjuvant with anti-PD-1	No	NA	NA	NA	NA	NA	Pancreatitis	0	NA	NA
#55	-	Adjuvant with anti-PD-1	Anti-CTLA-4	PD	3,80	NA	NA	NA	Diarrhea	0	NA	0
#57	-	Adjuvant with anti-PD-1	c-Kit-i	PR	8,03	Chemotherapy	PD	1,8	No	0	0	0

#59	-	Adjuvant with anti-PD-1	No	NA	NA	NA	NA	NA	No	1	NA	NA
#63	-	Adjuvant with anti-PD-1	Anti-PD-1	SD	4,47	NA	NA	NA	No	0	NA	1

Anti-PD-1: nivolumab, pembrolizumab; Anti-CTLA-4: ipilimumab; BRAF+MEKi: vemurafenib + cobimetinib, dabrafenib + trametinib, encorafenib + binimetinib; c-Kiti: imatinib.

Abbreviations: PD: NA: Not Available; SD: Stable Disease; PR: Partial Response; CR: Complete Response; PD: Disease Progression: ICB: Immunological Checkpoint Blocking; BOR: Best Overall Response; PFS: Progression Free Survival: iAEs. immuno-related Adverse Events; O: No clinical Benefit; 1: Clinical Benefit.

Supplementary Table 2. RNAs from 16 melanoma patients.

Sample ID	*BRAF* V600 status	R
#30	+	Y
#39	+	Y
#40	+	Y
#19	+	N
#50	+	N
#56	+	N
#62^	+	N
#20^	-	Y
#38	-	Y
#59	-	Y
#18	-	N
#45	-	N
#47	-	N
#54	-	N
#57^	-	N
#63^	-	N

Abbreviations: R: response; +: positive; -: negative; ^: two tumour lesions (pre and post-therapy); Y: yes; N: no

Supplementary Table 3. Loss of heterozygosity (LOH) in Dna Damage Repair Definciency (DDR) genes for our 36 melanomas patient's cohort

Gene	Sample ID	*BRAF* V600 status	R
AEN	#47	-	N
ALKBH1	#56	+	N
	#56	+	N
ALKBH3	#4	-	Y
	#54	-	N
APEX1	#56	+	N
	#39	+	Y
	#19	+	N
	#43	+	N
	#56	+	N
	#1	+	N
	#8	+	N
	#10	+	N
APEX2	#50	+	N
	#4	-	Y
	#59	-	Y
	#32	-	Y
	#45	-	N
	#55	-	N
	#63	-	N
	#47	-	N
	#57	-	N
APLF	#47	-	N
	#30	+	Y
APTX	#56	+	N
	#10	+	N
	#59	-	Y

	#32	-	y
	#45	-	n
	#54	-	n
	#47	-	n
	#39	+	y
ASCC3	#10	+	n
	#45	-	n
	#63	-	n
	#39	+	y
ATM	#56	+	n
	#4	-	y
	#54	-	n
ATR	#56	+	n
ATRIP	#56	+	n
	#39	+	y
	#19	+	n
	#43	+	n
	#56	+	n
	#1	+	n
	#8	+	n
	#10	+	n
ATRX	#50	+	n
	#4	-	y
	#59	-	y
	#32	-	y
	#45	-	n
	#55	-	n
	#63	-	n
	#47	-	n
	#57	-	n
BABAM1	#59	-	y

BARD1	#47	-	n
BCAS2	#56	+	n
	#47	-	n
BLM	#63	-	n
	#47	-	n
	#43	+	n
	#43	+	n
	#1	+	n
	#8	+	n
	#4	-	y
BRCA1	#4	-	y
	#4	-	y
	#4	-	y
	#4	-	y
	#45	-	n
	#54	-	n
	#43	+	n
	#43	+	n
BRCA2	#8	+	n
	#10	+	n
	#10	+	n
	#39	+	y
	#19	+	n
	#43	+	n
	#56	+	n
BRCC3	#1	+	n
	#8	+	n
	#10	+	n
	#50	+	n
	#4	-	y
	#59	-	y

	#32	-	y
	#45	-	n
	#55	-	n
	#54	-	n
	#63	-	n
	#47	-	n
	#57	-	n
CCNH	#56	+	n
	#47	-	n
CDC25A	#56	+	n
CDC25C	#47	-	n
	#39	+	y
	#19	+	n
	#43	+	n
	#56	+	n
	#1	+	n
	#8	+	n
	#10	+	n
	#50	+	n
CETN2	#4	-	y
	#59	-	y
	#32	-	y
	#45	-	n
	#55	-	n
	#54	-	n
	#63	-	n
	#47	-	n
	#57	-	n
CHAF1A	#59	-	y
	#54	-	n
CHEK1	#39	+	y

	#56	+	n
	#4	-	y
	#59	-	y
	#45	-	n
	#63	-	n
CHEK2	#47	-	n
CUL3	#59	-	y
	#47	-	n
CUL5	#39	+	y
	#56	+	n
	#4	-	y
	#54	-	n
DCLRE1A	#39	+	y
	#30	+	y
	#19	+	n
	#56	+	n
	#10	+	n
	#45	-	n
	#63	-	n
DCLRE1B	#56	+	n
	#47	-	n
	#30	+	y
	#19	+	n
DCLRE1C	#56	+	n
	#10	+	n
	#45	-	n
	#63	-	n
	#19	+	n
DDB1	#56	+	n
	#4	-	y
DDB2	#56	+	n

	#4	-	y
	#50	+	n
DMC1	#54	-	n
	#47	-	n
	#39	+	y
	#30	+	y
	#19	+	n
	#56	+	n
DNA2	#10	+	n
	#59	-	y
	#45	-	n
	#45	-	n
	#45	-	n
	#39	+	y
	#30	+	y
	#19	+	n
DNTT	#56	+	n
	#10	+	n
	#45	-	n
	#63	-	n
	#39	+	y
DUT	#63	-	n
	#47	-	n
EME1	#4	-	y
EME2	#47	-	n
ENDOV	#10	+	n
ERCC2	#59	-	y
ERCC3	#47	-	n
ERCC4	#59	-	y
	#47	-	n
ERCC6	#39	+	y

	#30	+	y
	#56	+	n
	#10	+	n
	#45	-	n
	#63	-	n
ERCC8	#57	-	n
EXO1	#39	+	y
EXO5	#47	-	n
	#10	+	n
FAAP20	#4	-	y
	#47	-	n
	#39	+	y
	#56	+	n
	#59	-	y
	#45	-	n
	#63	-	n
FANCA	#63	-	n
	#63	-	n
	#63	-	n
	#63	-	n
	#47	-	n
	#39	+	y
	#19	+	n
	#43	+	n
	#56	+	n
	#1	+	n
FANCB	#8	+	n
	#10	+	n
	#50	+	n
	#4	-	y
	#59	-	y

	#32	-	y
	#45	-	n
	#55	-	n
	#54	-	n
	#63	-	n
	#47	-	n
	#57	-	n
	#30	+	y
	#56	+	n
	#10	+	n
FANCC	#32	-	y
	#45	-	n
	#47	-	n
	#39	+	y
FANCD2	#56	+	n
FANCE	#56	+	n
	#56	+	n
	#4	-	y
FANCF	#54	-	n
	#63	-	n
	#30	+	y
	#56	+	n
	#10	+	n
FANCG	#32	-	y
	#45	-	n
	#54	-	n
	#47	-	n
FANCI	#47	-	n
	#56	+	n
FANCL	#4	-	y
	#47	-	n

FANCM	#56	+	n
	#59	-	y
FEN1	#56	+	n
	#4	-	y
GADD45A	#47	-	n
	#30	+	y
	#56	+	n
	#10	+	n
GADD45G	#59	-	y
	#32	-	y
	#45	-	n
	#47	-	n
GEN1	#47	-	n
	#56	+	n
GTF2H1	#4	-	y
	#54	-	n
GTF2H3	#4	-	y
	#45	-	n
	#39	+	y
	#56	+	n
GTF2H5	#59	-	y
	#32	-	y
	#45	-	n
	#63	-	n
	#39	+	y
	#56	+	n
H2AFX	#4	-	y
	#59	-	y
	#54	-	n
	#63	-	n
HELQ	#56	+	n

	#63	-	n
	#39	+	y
HERC2	#63	-	n
	#47	-	n
HES1	#56	+	n
HFM1	#47	-	n
HLTF	#56	+	n
	#56	+	n
HMGB2	#59	-	y
	#63	-	n
HUS1	#19	+	n
	#54	-	n
IDH1	#47	-	n
	#39	+	y
INO80	#19	+	n
	#63	-	n
	#47	-	n
	#56	+	n
KAT5	#4	-	y
	#54	-	n
	#30	+	y
LIG4	#56	+	n
	#57	-	n
	#10	+	n
MAD2L2	#4	-	y
	#47	-	n
MBD4	#56	+	n
	#39	+	y
MGMT	#30	+	y
	#19	+	n
	#56	+	n

	#10	+	n
	#45	-	n
	#63	-	n
MLH1	#56	+	n
MLH3	#56	+	n
	#39	+	y
	#30	+	y
MMS19	#19	+	n
	#56	+	n
	#10	+	n
	#63	-	n
MNAT1	#56	+	n
MORF4L1	#47	-	n
MPG	#47	-	n
MRPL40	#47	-	n
	#10	+	n
MSH2	#59	-	y
	#47	-	n
MSH6	#47	-	n
	#56	+	n
MUS81	#4	-	y
	#54	-	n
MUTYH	#47	-	n
NBN	#4	-	y
	#54	-	n
NEIL1	#59	-	y
	#47	-	n
NEIL2	#56	+	n
	#4	-	y
NEIL3	#56	+	n
	#50	+	n

	#59	-	y
	#63	-	n
NFATC2IP	#47	-	n
NHEJ1	#47	-	n
NSMCE1	#59	-	y
	#47	-	n
NSMCE2	#47	-	n
	#39	+	y
	#30	+	y
	#19	+	n
NSMCE4A	#56	+	n
	#10	+	n
	#45	-	n
	#63	-	n
NTHL1	#47	-	n
NUDT1	#59	-	y
NUDT18	#56	+	n
	#4	-	y
OGG1	#39	+	y
	#56	+	n
PALB2	#47	-	n
	#39	+	y
	#30	+	y
PARG	#56	+	n
	#10	+	n
	#63	-	n
PARP1	#39	+	y
PARP2	#56	+	n
PARP3	#56	+	n
	#54	-	n
PARP4	#10	+	n

PAXIP1	#30	+	y
	#56	+	n
PER1	#19	+	n
	#45	-	n
PLK3	#47	-	n
PLRG1	#56	+	n
	#59	-	y
	#63	-	n
PMS1	#47	-	n
PMS2	#45	-	n
	#45	-	n
PNKP	#43	+	n
	#59	-	y
POLA1	#39	+	y
	#19	+	n
	#43	+	n
	#56	+	n
	#1	+	n
	#8	+	n
	#10	+	n
	#50	+	n
	#4	-	y
	#59	-	y
	#32	-	y
	#45	-	n
	#55	-	n
	#54	-	n
	#63	-	n
	#47	-	n
	#57	-	n
POLB	#56	+	n

	#4	-	y
POLD3	#56	+	n
	#4	-	y
	#56	+	n
POLD4	#4	-	y
	#59	-	y
	#54	-	n
	#8	+	n
POLE	#4	-	y
	#59	-	y
POLE2	#56	+	n
	#59	-	y
	#30	+	y
	#56	+	n
POLE3	#10	+	n
	#32	-	y
	#45	-	n
	#47	-	n
POLE4	#47	-	n
POLG	#47	-	n
POLI	#54	-	n
	#39	+	y
	#30	+	y
	#19	+	n
POLL	#56	+	n
	#10	+	n
	#45	-	n
	#63	-	n
	#43	+	n
POLN	#56	+	n
	#59	-	y

	#45	-	n
	#63	-	n
POLQ	#56	+	n
	#50	+	n
PPP4C	#47	-	n
PPP4R1	#43	+	n
	#59	-	y
PPP4R2	#56	+	n
PRKDC	#4	-	y
	#63	-	n
PRPF19	#56	+	n
	#4	-	y
	#39	+	y
	#30	+	y
PTEN	#56	+	n
	#10	+	n
	#45	-	n
	#63	-	n
RAD18	#39	+	y
	#56	+	n
	#30	+	y
	#56	+	n
RAD23B	#10	+	n
	#32	-	y
	#45	-	n
	#47	-	n
RAD50	#47	-	n
	#39	+	y
RAD51	#19	+	n
	#63	-	n
	#47	-	n

	#56	+	n
RAD51B	#56	+	n
	#45	-	n
RAD52	#59	-	y
	#63	-	n
RAD54B	#4	-	y
RAD54L	#47	-	n
	#56	+	n
RAD9A	#4	-	y
	#59	-	y
	#54	-	n
RBBP8	#59	-	y
RBX1	#47	-	n
RECQL4	#55	-	n
	#47	-	n
RECQL5	#10	+	n
REV1	#47	-	n
	#39	+	y
	#10	+	n
REV3L	#59	-	y
	#45	-	n
	#63	-	n
RFC1	#56	+	n
	#63	-	n
RFC2	#30	+	y
	#56	+	n
RFC3	#56	+	n
RFC4	#56	+	n
	#39	+	y
RIF1	#55	-	n
	#54	-	n

	#47	-	n
	#30	+	y
	#56	+	n
RMI1	#10	+	n
	#32	-	y
	#45	-	n
	#47	-	n
RMI2	#47	-	n
RNF168	#56	+	n
RNF169	#56	+	n
	#4	-	y
	#56	+	n
RNF4	#1	+	n
	#63	-	n
RNMT	#43	+	n
	#59	-	y
RPA1	#19	+	n
	#45	-	n
RPA2	#10	+	n
	#47	-	n
	#39	+	y
	#19	+	n
	#43	+	n
	#56	+	n
	#1	+	n
RPA4	#8	+	n
	#10	+	n
	#50	+	n
	#4	-	y
	#59	-	y
	#32	-	y

	#45	-	n
	#55	-	n
	#63	-	n
	#47	-	n
	#57	-	n
	#56	+	n
RRM1	#4	-	y
	#45	-	n
RRM2	#47	-	n
RRM2B	#59	-	y
	#47	-	n
	#39	+	y
SETMAR	#30	+	y
	#56	+	n
	#39	+	y
	#56	+	n
SHPRH	#32	-	y
	#45	-	n
	#63	-	n
	#45	-	n
SLX1A	#45	-	n
	#47	-	n
SLX4	#47	-	n
SMARCA4	#54	-	n
	#56	+	n
SMARCAD1	#63	-	n
	#47	-	n
SMARCC1	#56	+	n
	#30	+	y
SMC5	#56	+	n
	#10	+	n

	#59	-	y
	#32	-	y
	#45	-	n
	#47	-	n
SMC6	#47	-	n
SOX4	#56	+	n
SPRTN	#39	+	y
	#30	+	y
	#56	+	n
SWI5	#10	+	n
	#32	-	y
	#45	-	n
	#47	-	n
SWSAP1	#54	-	n
TCEA1	#4	-	y
	#59	-	y
TDP1	#56	+	n
TDP2	#56	+	n
TELO2	#47	-	n
TOP3A	#19	+	n
TOP3B	#47	-	n
TOPBP1	#56	+	n
TP53	#19	+	n
	#45	-	n
	#39	+	y
TP53BP1	#63	-	n
	#63	-	n
	#47	-	n
TREX1	#56	+	n
TREX2	#39	+	y
	#19	+	n

	#43	+	n
	#56	+	n
	#1	+	n
	#8	+	n
	#10	+	n
	#50	+	n
	#4	-	y
	#59	-	y
	#32	-	y
	#45	-	n
	#55	-	n
	#54	-	n
	#63	-	n
	#47	-	n
	#57	-	n
	#39	+	y
TTK	#10	+	n
	#63	-	n
	#43	+	n
TYMS	#59	-	y
	#45	-	n
	#39	+	y
	#19	+	n
	#43	+	n
	#56	+	n
UBE2A	#1	+	n
	#8	+	n
	#10	+	n
	#50	+	n
	#4	-	y
	#59	-	y

	#32	-	y
	#45	-	n
	#55	-	n
	#63	-	n
	#47	-	n
	#57	-	n
UBE2B	#47	-	n
UBE2T	#39	+	y
UBE2V2	#4	-	y
	#63	-	n
UIMC1	#47	-	n
USP1	#47	-	n
	#43	+	n
UVSSA	#56	+	n
	#63	-	n
WDR48	#56	+	n
	#56	+	n
WEE1	#4	-	y
	#54	-	n
WRN	#56	+	n
	#4	-	y
XAB2	#54	-	n
	#30	+	y
	#56	+	n
XPA	#10	+	n
	#32	-	y
	#45	-	n
	#47	-	n
XPC	#56	+	n
XRCC2	#30	+	y
	#56	+	n

	#59	-	y
XRCC3	#56	+	n
XRCC5	#47	-	n
XRCC6	#47	-	n
YWHAG	#30	+	y
ZSWIM7	#19	+	n
	#45	-	n

Abbreviations: R: Response; y: yes; n: no

Supplementary Table 4. Mutational Signature.

Mutational Signature for our 36 melanomas patient's cohort and comparision between three different tools (DeconstructSigs, SigMa, and SigProfiler v3.2).

Sample ID	*BRAF* V600 Status	deconstructSig	SigMa	ssSigProfiler
#1	+	Signature_3	Signature_3_hc	SBS3
#2	+	Signature_3	Signature_3_hc	SBS3
#3	+	Signature_3	Signature_3_hc	SBS3
#8	+	Signature_3	Signature_3_hc	SBS3
#10	+	Signature_3	Signature_3_hc	SBS3
#14	+	Signature_3	Signature_3_hc	SBS3
#17	+	Signature_clock-like	Signature_clock	SBS5
#19	+	Signature_UV	Signature_UV	SBS7
#26	+	Signature_clock-like	Signature_clock	SBS5
#30	+	Signature_UV	Signature_UV	SBS7
#37	+	Signature_clock-like	Signature_clock	SBS5
#39	+	Signature_UV	Signature_UV	SBS7
#40	+	Signature_UV	Signature_UV	SBS7
#42	+	Signature_clock-like	Signature_3_hc	SBS3
#43	+	Signature_clock-like	Signature_msi	SBS1
#50	+	Signature_clock-like	Signature_clock	SBS5
#56	+	Signature_clock-like	Signature_clock	SBS5

#60	+	Signature_UV	Signature_UV	SBS7
#62	+	Signature_UV	Signature_UV	SBS7
#4	-	Signature_UV	Signature_UV	SBS7
#6	-	Signature_3	Signature_3_hc	SBS3
#7	-	Signature_UV	Signature_UV	SBS7
#18	-	Signature_UV	Signature_UV	SBS7
#20	-	Signature_UV	Signature_UV	SBS7
#21	-	Signature_3	Signature_3_hc	SBS3
#32	-	Signature_UV	Signature_UV	SBS7
#34	-	Signature_3	Signature_3_hc	SBS3
#38	-	Signature_UV	Signature_UV	SBS7
#45	-	Signature_UV	Signature_UV	SBS7
#46	-	Signature_3	Signature_3_hc	SBS3
#47	-	Signature_clock-like	Signature_clock	SBS5
#54	-	Signature_clock-like	Signature_clock	SBS5
#55	-	Signature_clock-like	Signature_UV	SBS7
#57	-	Signature_UV	Signature_UV	SBS7
#59	-	Signature_UV	Signature_UV	SBS7
#63	-	Signature_clock-like	Signature_clock	SBS5

Abbreviations: +: positive; -: negative

Supplementary Table 5. Copy Number variations (CNVs) in melanoma driver genes detected by Whole exome Sequencing (WES) in common between the pre-therapy and post-therapy melanoma lesions.

Gene	CNV	Sample ID	*BRAF* V600 status	R
		#39	+	y
PTEN	DELETION	#34	-	n
		#63	-	n
FBXW7	DELETION	#63	-	n
KIT	DELETION	#63	-	n

DDX3X	DELETION	#34	-	n
		#63	-	n
BRAF	AMPLIFICATION	#18	-	n
KIT	AMPLIFICATION	#21	-	y
		#34	-	n
STK19	AMPLIFICATION	#21	-	y
		#7	-	y
		#34	-	n

		#21	-	y
EZH2	AMPLIFICATION	#34	-	n
		#18	-	n
NRAS	AMPLIFICATION	#34	-	n
MAP2K2	AMPLIFICATION	#34	-	n
RAC1	AMPLIFICATION	#34	-	n
SNX31	AMPLIFICATION	#34	-	n
TACC1	AMPLIFICATION	#34	-	n

TERT	AMPLIFICATION	#34	-	n
GNA11	AMPLIFICATION	#34	-	n

Abbreviations: R: Response; n: no; y: yes: -: Negative; +: Positive; CNV: Copy Number Variation.

Supplementary Table 6. Copy Number variations (CNVs) in melanoma driver genes detected by Whole exome Sequencing (WES) acquired in the post-therapy melanoma lesions.

Gene	CNV	Sample ID	*BRAF* V600 status	R
		#39§	+	y
BRAF	AMPLIFICATION	#1§	+	n
		#20	-	y
		#1	+	n
HRAS	AMPLIFICATION	#20	-	y
		#34	-	n

CDK4	AMPLIFICATION	#1	+	n
KRAS	AMPLIFICATION	#18	-	n
MAP2K1	AMPLIFICATION	#20	-	y
MAP2K2	AMPLIFICATION	#42	+	y
		#1	+	n
GNA11	AMPLIFICATION	#1	+	n
		#42	+	y
		#20	-	y

		#42	+	y
EZH2	AMPLIFICATION	#20	-	y
		#57	-	n
FBXW7	AMPLIFICATION	#21	-	y
		#1	+	n
MTOR	AMPLIFICATION	#42	+	y
		#20	-	y
NRAS	AMPLIFICATION	#18	-	n

		#57	-	n
PPP6C	AMPLIFICATION	#1	+	n
		#20	-	y
RAC1	AMPLIFICATION	#1	+	n
		#42	+	y
		#20	-	y
RB1	AMPLIFICATION	#1	+	n
STK19	AMPLIFICATION	#1	+	n

		#42	+	y
TERT	AMPLIFICATION	#20	-	y
TP53	AMPLIFICATION	#20	-	y
WT1	AMPLIFICATION	#20	-	y
FBXW7	DELETION	#20	-	y
CDKN2A	DELETION	#20	-	y
CNOT9	DELETION	#20	-	y
CTNNB1	DELETION	#20	-	y

		#1	+	n
DDX3X	DELETION			
		#20	-	y
		#63	-	n
GNA11	DELETION			
		#57	-	n
HRAS	DELETION	#42	+	y
IDH1	DELETION	#20	-	y
MAP2K1	DELETION	#20	-	y
MAP2K2	DELETION	#63	-	n

		#57	-	n
TACC1	DELETION	#20	-	y
TP53	DELETION	#63	-	n

Abbreviations: R: Response; n: no; y: yes; -: Negative; +: Positive; CNV: Copy number variation; §: gain present in the pre-lesions and post lesion.

Supplementary Table 7. Loss Of Function (LOF) variants in DNA Damage Repair Deficiency (DDR) genes.

For each of 36 patients, exonic somatic LOF variants in DDR genes with an AF at least 10% are reported. In bold the variants found in common in the two lesions of the same patient.

Chr	*BRAF* V600 status	R	Gene	aa change	Ref seq	Coverage	AF
#2	+	Y	*TP53BP1*	p.Ser1359fs	*NM_001141980.3*	*58*	*63.6*
#2	+	Y	*DDB1*	p.Arg989fs	*NM_001923.5*	*45*	*42.9*
#17	+	Y	*RAD51B*	p.Gln371*	*NM_133509.4*	*76*	*20.0*
#39_PRE	+	Y	*TDG*	p.Ile98fs	*NM_003211.6*	*195*	*20.0*
#39_PRE	+	Y	*CUL4B*	p.Ser61fs	*NM_003588.3*	*63*	*12.8*
#39	+	Y	*CUL5*	p.Gln709*	*NM_003478.6*	*965*	*59.6*
#40	+	Y	*MSH6*	p.Asp1026fs	*NM_000179.2*	*585*	*10.1*
#42	+	Y	*ERCC6*	p.Ala298delinsGlyPheSerSerTerSerValProSer	*NM_000124.4*	*61*	*45.5*

#42	+	Y	*MLH3*	p.Asn629fs	*NM_001040108.1*	*182*	*11.4*
#10	+	N	*MDC1*	p.Arg944fs	*NM_014641.3.5*	*202*	*12.5*
#10	+	N	*TP53BP1*	p.Ser1359fs	*NM_001141980.3*	*88*	*50.0*
#10	+	N	*POLM*	p.Arg248*	*NM_001284330.2*	*1488*	*30.3*
#10	+	N	*ERCC6*	p.Ala298delinsGlyPheSerSerTerSerValProSer	*NM_000124.4*	*85*	*66.7*
#14	+	N	*HERC2*	p.Gln142fs	*NM_004667.5*	*67*	*17.6*
#14	+	N	*TP53BP1*	p.Ser1359fs	*NM_001141980.3*	*83*	*20.0*
#14	+	N	*ERCC6*	p.Ala298delinsGlyPheSerSerTerSerValProSer	*NM_000124.4*	*92*	*26.9*
#14	+	N	*LIG4*	p.Thr554fs	*NM_001352604.1*	*173*	*23.0*
#14	+	N	*SHPRH*	p.Asp944fs	*NM_001042683.3*	*38*	*21.4*

#19	+	N	*PTEN*	p.Arg303fs	*NM_001085384.3*	*410*	*64.8*
#3	+	N	*CHEK2*	p.Ser499fs	*NM_001005735.2*	*83*	*23.5*
#3	+	N	*FANCE*	p.Arg176fs	*NM_021922.3*	*81*	*14.6*
#3	+	N	*TP53BP1*	p.Ser1359fs	*NM_001141980.3*	*60*	*25.0*
#3	+	N	*ERCC6*	p.Ala298delinsGlyPheSerSerTerSerValProSer	*NM_000124.4*	*71*	*37.5*
#3	+	N	*APEX2*	p.Thr295fs	*NM_014481*	*88*	*23.8*
#3	+	N	*FANCA*	p.Ala1215fs	*NM_000135.4*	*81*	*18.9*
#3	+	N	*TDP1*	p.Asp346fs	*NM_001008744.2*	*59*	*53.8*
#3	+	N	*SHPRH*	p.Glu131*	*NM_001042683.3*	*117*	*15.2*
#62_POST	+	N	*GEN1*	p.Lys839fs	*NM_001130009.3*	*368*	*45.0*

#62_POST	+	N	*PMS1*	p.Leu164fs	*NM_001321049.2*	*269*	*44.1*
#6	-	Y	*RFC1*	p.Thr132fs	*NM_001204747.2*	*190*	*14.9*
#6	-	Y	*TP53BP1*	p.Ser980_Gly981insIleArgGly	*NM_001141980.3*	*36*	*33.3*
#6	-	Y	*ERCC6*	p.Ala298delinsGlyPheSerSerTerSerValProSer	*NM_000124.4*	*141*	*23.1*
#6	-	Y	*APEX2*	p.Thr295fs	*NM_014481*	*88*	*15.6*
#6	-	Y	*RBP1*	p.Ter158Glnext*?	*NM_001130992.2*	*45*	*18.2*
#20_PRE	-	Y	*APEX2*	p.Thr295fs	*NM_014481*	*51*	*50.0*
#20_PRE	-	Y	*ERCC6*	p.Ala298delinsGlyPheSerSerTerSerValProSer	*NM_000124.4*	*164*	*21.2*
#20_POST	-	Y	*ERCC6*	p.Ala298delinsGlyPheSerSerTerSerValProSer	*NM_000124.4*	*115*	*41.2*
#20_POST	-	Y	*LIG4*	p.Thr554fs	*NM_001352604.1*	*280*	*13.3*

#20_POST	-	Y	*REV3L*	p.Lys1044delinsAsnLeuTrpAspLeuCysPheSerGlnLysGluAsnLeuValTerThrTerHisHisTyrAsnSer	*NM_001372078.1*	*101*	*23.1*
#20_POST	-	Y	*DCLRE1B*	p.Lys290_Pro291insIleProValGlyProSerThrTerSerProSerPheGluThrHisArgLysAlaLeu	*NM_022836.4*	*115*	*20.0*
#20_POST	-	Y	TP53BP1	p.Thr514fs	NM_001141980.3	129	16.7
#21	-	Y	*GTF2H1*	p.Trp33*	*NM_001142307.1*	*109*	*12.0*
#21	-	Y	*TDP2*	p.Thr230fs	*NM_016614.3*	*103*	*33.3*
#21	-	Y	*BRCA1*	p.Ser377fs	*NM_007300.4*	*254*	*27.5*
#21	-	Y	*TP53BP1*	p.Ser1359fs	*NM_001141980.3*	*138*	*21.7*
#21	-	Y	*ATRX*	p.Ala1410fs	*NM_000489.5*	*89*	*23.5*
#21	-	Y	*RAD54B*	p.Lys132*	*NM_012415.3*	*279*	*18.8*
#38	-	Y	*BRCA2*	p.Glu954*	*NM_000059.3*	*376*	*34.5*

#46	-	Y	*ERCC6*	p.Ala298delinsGlyPheSerSerTerSerValProSer	*NM_000124.4*	*78*	*37.5*
#59	-	Y	*BLM*	p.Gln83*	*NM_000057.4*	*688*	*11.1*
#34_PRE	-	N	*TDP2*	p.Thr230fs	*NM_016614.3*	*43*	*29.4*
#34_PRE	-	N	*MDC1*	p.Val440_Leu441insAlaHisProGlyProProProHisGluLeuSerProAlaTerGluGlnLeuGlnProThrLeuProGlnHisPro	*NM_014641.3.5*	*59*	*23.5*
#34_PRE	-	N	*BRCA1*	p.Ser377fs	*NM_007300.4*	*172*	*30.3*
#34_PRE	-	N	*TP53BP1*	**p.Ser1359fs**	*NM_001141980.3*	*68*	*26.9*
#34	-	N	*TP53BP1*	**p.Ser1359fs**	*NM_001141980.3*	*66*	*15.4*
#34_PRE	-	N	*CDC5L*	p.Gly604fs	*NM_001253.4*	*159*	*10.3*
#34_PRE	-	N	*ERCC6*	**p.Ala298delinsGlyPheSerSerTerSerValProSer**	*NM_000124.4*	*79*	*80.0*
#34	-	N	*ERCC6*	**p.Ala298delinsGlyPheSerSerTerSerValProSer**	*NM_000124.4*	*100*	*25.9*

#34_PRE	-	N	*REV1*	p.Leu289fs	*NM_001321454.2*	*51*	*23.1*
#34_PRE	-	N	*LIG4*	**p.Thr554fs**	*NM_001352604.1*	*182*	*15.6*
#34	-	N	*LIG4*	**p.Thr554fs**	*NM_001352604.1*	*204*	*11.2*
#34	-	N	*FANCE*	p.Arg176fs	*NM_021922.3*	*95*	*17.2*
#34	-	N	*MLH3*	p.Asn629fs	*NM_001040108.1*	*218*	*11.8*
#34	-	N	*ATR*	p.Val2230fs	*NM_001184.4*	*68*	*21.9*
#63_PRE	-	N	*ERCC6*	**p.Arg1221***	*NM_000124.4*	*329*	*64.6*
#63	-	N	*ERCC6*	**p.Arg1221***	*NM_000124.4*	*340*	*65.4*

Abbreviations: Negative; Y: Yes; N: No; AF: Allele Frequency.

Supplementary Table 8. Loss of heterozygosity (LOH) in in Dna Damage Repair Definciency (DDR) genes detected by Whole exome Sequencing (WES) in common between the pre-therapy and post-therapy melanoma lesions.

Gene	Sample ID	*BRAF* V600 status	R
APEX2	#39	+	y
	#63	-	n
ATRX	#39	+	y
	#63	-	n
BRCC3	#39	+	y
	#63	-	n
CETN2	#39	+	y
	#63	-	n
FANCB	#39	+	y
	#63	-	n
POLA1	#39	+	y
	#63	-	n
RPA4	#39	+	y
	#63	-	n
TREX2	#39	+	y
	#63	-	n
UBE2A	#39	+	y
	#63	-	n
ASCC3	#63	-	n
ATM	#63	-	n
CHEK1	#63	-	n
DCLRE1A	#63	-	n
DCLRE1C	#63	-	n
DNTT	#63	-	n
DUT	#63	-	n

ERCC6	#63	-	n
FANCA	#63	-	n
GTF2H5	#63	-	n
H2AFX	#63	-	n
HELQ	#63	-	n
HERC2	#63	-	n
HMGB2	#63	-	n
INO80	#63	-	n
MGMT	#63	-	n
MMS19	#63	-	n
NEIL3	#63	-	n
NSMCE4A	#63	-	n
PARG	#63	-	n
PLRG1	#63	-	n
POLL	#63	-	n
POLN	#63	-	n
PTEN	#63	-	n
RAD51	#63	-	n
REV3L	#63	-	n
RFC1	#63	-	n
RNF4	#63	-	n
SHPRH	#63	-	n
SMARCAD1	#63	-	n
TP53BP1	#63	-	n
TTK	#63	-	n
UVSSA	#63	-	n

Abbreviations: R: Response; Y: yes; N: no

Supplementary Table 9. Loss of heterozygosity (LOH) in in Dna Damage Repair Definciency (DDR) genes detected by Whole exome Sequencing (WES) acquired in the post-therapy melanoma lesions.

Gene	Sample ID	*BRAF* V600 status	R
APEX2	#1	+	n
	#62	+	n
	#21	-	y
APTX	#62	+	n
	#21	-	y
ASCC3	#39	+	y
	#62	+	n
	#21	-	y
ATM	#39	+	y
	#62	+	n
ATRX	#1	+	n
	#62	+	n
	#21	-	y
BLM	#62	+	n
	#63	-	n
BRCA1	#1	+	n
	#62	+	n
	#21	-	y
BRCC3	#1	+	n
	#62	+	n
	#21	-	y
BRIP1	#62	+	n
	#21	-	y
CDC5L	#62	+	n
	#21	-	y
CETN2	#1	+	n

	#62	+	n
	#21	-	y
	#39	+	y
CHEK1	#62	+	n
	#62	+	n
CHEK2	#62	+	n
	#21	-	y
CUL5	#39	+	y
	#62	+	n
DCLRE1A	#39	+	y
	#62	+	n
DMC1	#62	+	n
	#21	-	y
DNA2	#39	+	y
	#62	+	n
DUT	#39	+	y
	#62	+	n
ENDOV	#62	+	n
	#21	-	y
ERCC6	#39	+	y
	#62	+	n
FAAP100	#62	+	n
	#21	-	y
	#1	+	n
FANCB	#62	+	n
	#21	-	y
FANCC	#62	+	n
	#21	-	y
FANCD2	#39	+	y
	#62	+	n
FANCE	#62	+	n

	#21	-	y
FANCF	#62	+	n
	#63	-	n
FANCG	#62	+	n
	#21	-	y
GADD45G	#62	+	n
	#21	-	y
	#39	+	y
GTF2H5	#62	+	n
	#21	-	y
H2AFX	#39	+	y
	#62	+	n
HERC2	#39	+	y
	#62	+	n
HUS1	#62	+	n
	#62	+	n
INO80	#39	+	y
	#62	+	n
MMS19	#39	+	y
	#62	+	n
NSMCE4A	#39	+	y
	#62	+	n
OGG1	#39	+	y
	#62	+	n
PARG	#39	+	y
	#62	+	n
PARP1	#39	+	y
	#62	+	n
	#1	+	n
POLA1	#62	+	n
	#21	-	y

POLE3	#62	+	n
	#21	-	y
POLH	#62	+	n
	#21	-	y
POLL	#39	+	y
	#62	+	n
PRKDC	#62	+	n
	#63	-	n
RAD18	#39	+	y
	#62	+	n
RAD23B	#62	+	n
	#21	-	y
RAD51C	#62	+	n
	#21	-	y
RAD52	#62	+	n
	#63	-	n
RBX1	#62	+	n
	#21	-	y
REV3L	#39	+	y
	#62	+	n
	#21	-	y
RMI1	#62	+	n
	#21	-	y
RNF4	#1	+	n
	#62	+	n
RNF8	#62	+	n
	#21	-	y
RPA4	#1	+	n
	#62	+	n
	#21	-	y
SETMAR	#39	+	y

	#62	+	n
	#39	+	y
SHPRH	#62	+	n
	#21	-	y
SMC5	#62	+	n
	#21	-	y
SOX4	#62	+	n
	#21	-	y
SPRTN	#39	+	y
	#62	+	n
SWI5	#62	+	n
	#21	-	y
TDP2	#62	+	n
	#21	-	y
TOP3B	#62	+	n
	#21	-	y
TP53BP1	#39	+	y
	#62	+	n
	#1	+	n
TREX2	#62	+	n
	#21	-	y
	#39	+	y
TTK	#62	+	n
	#21	-	y
	#1	+	n
UBE2A	#62	+	n
	#21	-	y
UBE2T	#39	+	y
	#62	+	n
UBE2V2	#62	+	n
	#63	-	n

XRCC6	#62	+	n
	#21	-	y
AEN	#62	+	n
ALKBH1	#62	+	n
ALKBH2	#62	+	n
ALKBH3	#62	+	n
APEX1	#62	+	n
APLF	#62	+	n
ATR	#62	+	n
BABAM1	#62	+	n
BARD1	#62	+	n
BCAS2	#62	+	n
BRCA2	#62	+	n
CCNH	#62	+	n
CDC25B	#62	+	n
CDC25C	#62	+	n
CHAF1A	#62	+	n
CUL3	#62	+	n
DCLRE1C	#62	+	n
DDB1	#62	+	n
DDB2	#62	+	n
DNTT	#39	+	y
EID3	#62	+	n
EME1	#21	-	y
EME2	#62	+	n
ERCC1	#62	+	n
ERCC2	#62	+	n
ERCC4	#62	+	n
ERCC5	#62	+	n
ERCC8	#62	+	n
EXO1	#39	+	y

EXO5	#62	+	n
FAAP20	#62	+	n
FAAP24	#62	+	n
FANCA	#39	+	y
FANCI	#62	+	n
FANCM	#62	+	n
FEN1	#62	+	n
GADD45A	#62	+	n
GEN1	#62	+	n
GTF2H3	#62	+	n
HELQ	#62	+	n
HES1	#62	+	n
HFM1	#62	+	n
HMGB1	#62	+	n
HMGB2	#62	+	n
IDH1	#62	+	n
LIG1	#62	+	n
LIG3	#62	+	n
LIG4	#62	+	n
MAD2L2	#62	+	n
MBD4	#62	+	n
MGMT	#39	+	y
MLH1	#62	+	n
MLH3	#62	+	n
MNAT1	#62	+	n
MORF4L1	#62	+	n
MPG	#62	+	n
MPLKIP	#62	+	n
MRPL40	#21	-	y
MSH2	#62	+	n
MSH3	#62	+	n

MSH6	#62	+	n
NABP2	#62	+	n
NBN	#62	+	n
NEIL2	#62	+	n
NEIL3	#62	+	n
NFATC2IP	#62	+	n
NHEJ1	#62	+	n
NSMCE1	#62	+	n
NTHL1	#62	+	n
NUDT15	#62	+	n
NUDT18	#62	+	n
PALB2	#62	+	n
PARP2	#62	+	n
PARP3	#62	+	n
PARP4	#62	+	n
PARPBP	#62	+	n
PAXIP1	#62	+	n
PER1	#62	+	n
PLK3	#62	+	n
PLRG1	#62	+	n
PMS1	#62	+	n
PMS2	#62	+	n
POLB	#62	+	n
POLD1	#62	+	n
POLD2	#62	+	n
POLD3	#62	+	n
POLD4	#62	+	n
POLE	#62	+	n
POLE2	#62	+	n
POLE4	#62	+	n
POLG	#62	+	n

POLI	#62	+	n
POLM	#62	+	n
POLQ	#62	+	n
PPP4C	#62	+	n
PPP4R1	#62	+	n
PPP4R2	#62	+	n
PRPF19	#62	+	n
PTEN	#39	+	y
RAD1	#62	+	n
RAD50	#62	+	n
RAD51	#39	+	y
RAD51B	#62	+	n
RAD51D	#62	+	n
RAD54B	#62	+	n
RAD9B	#62	+	n
RECQL4	#62	+	n
RECQL5	#21	-	y
REV1	#62	+	n
RFC1	#62	+	n
RFC2	#62	+	n
RFC3	#62	+	n
RFC4	#62	+	n
RFC5	#62	+	n
RIF1	#39	+	y
RMI2	#62	+	n
RNF168	#62	+	n
RNF169	#62	+	n
RNMT	#62	+	n
RPA1	#62	+	n
RPA2	#62	+	n
RPA3	#62	+	n

RRM1	#62	+	n
RRM2	#62	+	n
RRM2B	#62	+	n
RTEL1	#62	+	n
SLX1A	#62	+	n
SLX4	#62	+	n
SMARCAD1	#62	+	n
SMC6	#62	+	n
SMUG1	#62	+	n
SPO11	#62	+	n
TCEA1	#62	+	n
TDG	#62	+	n
TDP1	#62	+	n
TELO2	#62	+	n
TOP3A	#62	+	n
TOPBP1	#62	+	n
TP53	#62	+	n
TYMS	#62	+	n
UBE2B	#62	+	n
UBE2N	#62	+	n
UIMC1	#62	+	n
UNG	#62	+	n
USP1	#62	+	n
WDR48	#62	+	n
WRN	#62	+	n
XAB2	#62	+	n
XPA	#21	-	y
XPC	#62	+	n
XRCC1	#62	+	n
XRCC2	#62	+	n
XRCC3	#62	+	n

XRCC5	#62	+	n
YWHAB	#62	+	n
YWHAG	#62	+	n
ZSWIM7	#62	+	n

Abbreviations: R: Response; Y: yes; N: no

Supplementary Table 10. cfDNA mutation profile.

Sample ID	Sex	R	Stage	*BRAF* V600 status	Previous treatment	Treatment	cfDNA-NGS results	AF%	Tissue-WES results	AF%	Time variation from tissue to cfDNA (days)	Time variation from therapy to cfDNA (days)
							BRAF p.Val600Glu	4.8	BRAF V600E	52.4		
#2	M	Y	IV	+	Y	BRAF+MEKi	NRAS p.Gln61Lys	5.0	-	-	15	369
							CDK4 Amplification	1.3	CDK4 Amplification			
#17	F	Y	IV	+	Y	ICB	BRAF p.Val600Glu	0.3	BRAF V600E	42.0	610	946
#26	M	Y	IV	+	y	BRAF+MEKi	-	-	BRAF p.Val600Glu	8.0	39	482
#39	M	Y	IV	+	Y	BRAF+MEKi and ICB	BRAF p.Val600Glu	32.6	BRAF p.Val600Glu	97.0	137	1329
							BRAF p.Val600Glu	67.7	BRAF p.Val600Glu	77.0		
#1	M	N	IV	+	Y	BRAF+MEKi	NRAS p.Gln61Lys	3.5	-	-	19	245
							MAP2K2 p.Gln60Pro	0.9	-	-		
							MET Amplification	4.3	-	-		
#3	F	N	IV	+	N	-	-	-	BRAF p.Val600Glu	16.7	16	0
							SMO p.Pro641Ala	50	-	-		
#8_T1	M	N	IV	+	N	-	-	-	BRAF p.Val600Glu	22	14	0
#8_T2	M	N	IV	+	Y	BRAF+MEKi	BRAF p.Val600Glu	3.8	BRAF p.Val600Glu	22	271	257
							BRAF p.Val600Met	0.8	-	-		
#10	F	N	IV	+	Y	BRAF+MEKi and ICB	BRAF p.Val600Glu	8.8	BRAF p.Val600Glu	60.0	289	461
							GNA11 p.Gln209Leu	3.7	-	-		
#14	F	N	IV	+	Y	ICB	BRAF p.Val600Glu	2.4	BRAF p.Val600Glu	43.8	51	21
							PIK3CA p.Asn345Lys	1.2	-	-		

#19	M	N	IV	+	Y	BRAF+MEKi	BRAF p.Val600Glu	0.7	BRAF p.Val600Glu	36.4	83	56
							NRAS p.Gln61Arg	0.2	-	-		
#60_T1	F	N	IIIB	+	N	BRAF+MEKi adjuvant	-	-	BRAF p.Val600Glu	76.0	28	569
#60_T2	F	N	IIIB	+	N	BRAF+MEKi adjuvant	-	-	BRAF p.Val600Glu	76.0	329	871
#60_T3	F	N	IIIB	+	N	BRAF+MEKi adjuvant	-	-	BRAF p.Val600Glu	76.0	656	1198
#62_T1	M	N	IV	+	N	-	BRAF p.Val600Glu	12.3	BRAF p.Val600Glu	22.8	0	0
							PIK3CA p.Glu545Lys	0.4	-	-		
#62_T2	M	N	IV	+	N	BRAF+MEKi	BRAF p.Val600Glu	39.2	BRAF p.Val600Glu	17.0	-7	110
							GNA11 p.Gln209Leu	15.7	-	-		
							PIK3CA p.Glu545Lys	1.3	-	-		
#7	F	Y	IV	-	N	ICB	BRAF p.Val600Glu	0.8	-	-	825	1002
							KIT p. Lys642Glu	0.5	-	-		
							MET p.Arg988Cys 5	51.8	IDH1 p.Arg132Cys	23.0		
#57_Post	M	N	IV	-	Y	ICB adjuvant and Imatinib	BRAF p.Gly469Ala	46.7	BRAF p.Gly469Ala	58.7	-6	441
							KIT p.Lys642Glu	34.6	KIT p.Lys642Glu	47.0		
							EGFR Amplifications	1.32	EGFR Amplifications	-		
							CDK6 Amplifications	1.42	CDK6 Amplifications	-		
							MET Amplifications	1.31	-	-		

Abbreviations: R: Response; Y: yes; N: no; AF: Allele Frequency; ICB: Immunological Checkpoint Blocking; BRAF+MEKi: BRAF and MEK inhibitors.

REFERENCES

1. Akhoondi S, Sun D, von der Lehr N, Apostolidou S, Klotz K, Maljukova A, et al. FBXW7/hCDC4 is a general tumor suppressor in human cancer. Cancer Res. 2007 Oct 1;67(19):9006-12. doi: 10.1158/0008-5472.CAN-07-1320. Erratum in: Cancer Res. 2008 Feb 15;68(4):1245.
2. Alexandrov LB, Nik-Zainal S, Wedge DC, Aparicio SA, Behjati S, Biankin AV, et al. Signatures of mutational processes in human cancer. Nature. 2013 Aug 22;500(7463):415-21. doi: 10.1038/nature12477. Epub 2013 Aug 14. Erratum in: Nature. 2013 Oct 10;502(7470):258.
3. Aoude LG, Bonazzi VF, Brosda S, Patel K, Koufariotis LT, Oey H, et al. Pathogenic germline variants are associated with poor survival in stage III/IV melanoma patients. Sci Rep. 2020 Oct 19;10(1):17687. doi: 10.1038/s41598-020-74956-3.
4. Berger MF, Hodis E, Heffernan TP, Deribe YL, Lawrence MS, Protopopov A, et al. Melanoma genome sequencing reveals frequent PREX2 mutations. Nature. 2012 May 9;485(7399):502-6. doi: 10.1038/nature11071.
5. Botton T, Yeh I, Nelson T, Vemula SS, Sparatta A, Garrido MC, et al. Recurrent BRAF kinase fusions in melanocytic tumors offer an opportunity for targeted therapy. Pigment Cell Melanoma Res. 2013 Nov;26(6):845-51. doi: 10.1111/pcmr.12148.
6. Bray F, Ferlay J, Soerjomataram I, Siegel RL, Torre LA, Jemal A. Global cancer statistics 2018: GLOBOCAN estimates of incidence and mortality worldwide for 36 cancers in 185 countries. CA Cancer J Clin. 2018 Nov;68(6):394-424. doi: 10.3322/caac.21492. Epub 2018 Sep 12. Erratum in: CA Cancer J Clin. 2020 Jul;70(4):313. PMID: 30207593.
7. Carlino MS, Larkin J, Long GV. Immune checkpoint inhibitors in melanoma. Lancet. 2021 Sep 11;398(10304):1002-1014. doi: 10.1016/S0140-6736(21)01206-X.
8. Choi E, Park SJ, Lee G, Yoon SK, Lee M, Lee SK. The GNAQ T96S Mutation Affects Cell Signaling and Enhances the Oncogenic Properties of Hepatocellular Carcinoma. Int J Mol Sci. 2021 Mar 23;22(6):3284. doi: 10.3390/ijms22063284.

9. Cui D, Xiong X, Shu J, Dai X, Sun Y, Zhao Y. FBXW7 Confers Radiation Survival by Targeting p53 for Degradation. Cell Rep. 2020 Jan 14;30(2):497-509.e4. doi: 10.1016/j.celrep.2019.12.032.
10. Dalmasso B, Pastorino L, Nathan V, Shah NN, Palmer JM, Howlie M, et al. Germline ATM variants predispose to melanoma: a joint analysis across the GenoMEL and MelaNostrum consortia. Genet Med. 2021 Nov;23(11):2087-2095. doi: 10.1038/s41436-021-01240-8.
11. Davis EJ, Johnson DB, Sosman JA, Chandra S. Melanoma: What do all the mutations mean? Cancer. 2018 Sep 1;124(17):3490-3499. doi: 10.1002/cncr.31345.
12. Dobin A, Davis CA, Schlesinger F, Drenkow J, Zaleski C, Jha S, et al. STAR: ultrafast universal RNA-seq aligner. Bioinformatics. 2013 Jan 1;29(1):15-21. doi: 10.1093/bioinformatics/bts635.
13. Gershenwald JE, Scolyer RA, Hess KR, Sondak VK, Long GV, Ross MI, et al. Melanoma staging: Evidence-based changes in the American Joint Committee on Cancer eighth edition cancer staging manual. CA Cancer J Clin. 2017 Nov;67(6):472-492. doi: 10.3322/caac.21409.
14. Gstalder C, Liu D, Miao D, Lutterbach B, DeVine AL, Lin C, et al. Inactivation of Fbxw7 Impairs dsRNA Sensing and Confers Resistance to PD-1 Blockade. Cancer Discov. 2020 Sep;10(9):1296-1311. doi: 10.1158/2159-8290.CD-19-1416.
15. Gupta S, Vanderbilt CM, Cotzia P, Arias Stella JA 3rd, Chang JC, Chen Y, et al. JAK2, PD-L1, and PD-L2 (9p24.1) amplification in metastatic mucosal and cutaneous melanomas with durable response to immunotherapy. Hum Pathol. 2019 Jun;88:87-91. doi: 10.1016/j.humpath.2018.08.032.
16. Hainaut P, Pfeifer GP. Somatic TP53 Mutations in the Era of Genome Sequencing. Cold Spring Harb Perspect Med. 2016 Nov 1;6(11):a026179. doi: 10.1101/cshperspect.a026179
17. Hamid O, Robert C, Daud A, Hodi FS, Hwu WJ, Kefford R, et al. Five-year survival outcomes for patients with advanced melanoma treated with pembrolizumab in KEYNOTE-001. Ann Oncol. 2019 Apr 1;30(4):582-588. doi: 10.1093/annonc/mdz011.

18. Hartman ML, Sztiller-Sikorska M, Gajos-Michniewicz A, Czyz M. Dissecting Mechanisms of Melanoma Resistance to BRAF and MEK Inhibitors Revealed Genetic and Non-Genetic Patient- and Drug-Specific Alterations and Remarkable Phenotypic Plasticity. Cells. 2020 Jan 7;9(1):142. doi: 10.3390/cells9010142.

19. Hayward NK, Wilmott JS, Waddell N, Johansson PA, Field MA, Nones K, et al. Nature. 2017 May 11;545(7653):175-180. doi: 10.1038/nature22071.

20. Helgadottir H, Ghiorzo P, van Doorn R, Puig S, Levin M, Kefford R, et al. Efficacy of novel immunotherapy regimens in patients with metastatic melanoma with germline CDKN2A mutations. J Med Genet. 2020 May;57(5):316-321. doi: 10.1136/jmedgenet-2018-105610.

21. Hodi FS, O'Day SJ, McDermott DF, Weber RW, Sosman JA, Haanen JB, et al. N Engl J Med. 2010 Aug 19;363(8):711-23. doi: 10.1056/NEJMoa1003466. Epub 2010 Jun 5. Erratum in: N Engl J Med. 2010 Sep 23;363(13):1290.

22. Hodis E, Watson IR, Kryukov GV, Arold ST, Imielinski M, Theurillat JP, et al. A landscape of driver mutations in melanoma. Cell. 2012 Jul 20;150(2):251-63. doi: 10.1016/j.cell.2012.06.024.

23. Hoek KS, Schlegel NC, Eichhoff OM, Widmer DS, Praetorius C, Einarsson SO, et al. Novel MITF targets identified using a two-step DNA microarray strategy. Pigment Cell Melanoma Res. 2008 Dec;21(6):665-76. doi: 10.1111/j.1755-148X.2008.00505.x.

24. Hu X, Wang Q, Tang M, Barthel F, Amin S, Yoshihara K, et al. TumorFusions: an integrative resource for cancer-associated transcript fusions. Nucleic Acids Res. 2018 Jan 4;46(D1):D1144-D1149. doi: 10.1093/nar/gkx1018.

25. Kanemaru H, Mizukami Y, Kaneko A, Kajihara I, Fukushima S. Promising Blood-Based Biomarkers for Melanoma: Recent Progress of Liquid Biopsy and Its Future Perspectives. Curr Treat Options Oncol. 2022 Apr;23(4):562-577. doi: 10.1007/s11864-022-00948-2.

26. Korn EL, Liu PY, Lee SJ, Chapman JA, Niedzwiecki D, Suman VJ, et al. Meta-analysis of phase II cooperative group trials in metastatic stage IV melanoma to determine progression-free and

overall survival benchmarks for future phase II trials. J Clin Oncol. 2008 Feb 1;26(4):527-34. doi: 10.1200/JCO.2007.12.7837.

27. Kourtis N, Moubarak RS, Aranda-Orgilles B, Lui K, Aydin IT, Trimarchi T, et al. FBXW7 modulates cellular stress response and metastatic potential through HSF1 post-translational modification. Nat Cell Biol. 2015 Mar;17(3):322-332. doi: 10.1038/ncb3121.

28. Krauthammer M, Kong Y, Ha BH, Evans P, Bacchiocchi A, McCusker JP, et al. Exome sequencing identifies recurrent somatic RAC1 mutations in melanoma. Nat Genet. 2012 Sep;44(9):1006-14. doi: 10.1038/ng.2359.

29. Landi MT, Bishop DT, MacGregor S, Machiela MJ, Stratigos AJ, Ghiorzo P, et al. Genome-wide association meta-analyses combining multiple risk phenotypes provide insights into the genetic architecture of cutaneous melanoma susceptibility. Nat Genet. 2020 May;52(5):494-504. doi: 10.1038/s41588-020-0611-8.

30. Larkin J, Ascierto PA, Dréno B, Atkinson V, Liszkay G, Maio M, et al. Combined vemurafenib and cobimetinib in BRAF-mutated melanoma. N Engl J Med. 2014 Nov 13;371(20):1867-76. doi: 10.1056/NEJMoa1408868.

31. Lee CJ, An HJ, Kim SM, Yoo SM, Park J, Lee GE, et al. FBXW7-mediated stability regulation of signal transducer and activator of transcription 2 in melanoma formation. Proc Natl Acad Sci U S A. 2020 Jan 7;117(1):584-594. doi: 10.1073/pnas.1909879116.

32. Li Z, Zhang X, Xue W, Zhang Y, Li C, Song Y, et al. Recurrent GNAQ mutation encoding T96S in natural killer/T cell lymphoma. Nat Commun. 2019 Sep 16;10(1):4209. doi: 10.1038/s41467-019-12032-9.

33. Liu D, Schilling B, Liu D, Sucker A, Livingstone E, Jerby-Arnon L, et al. Integrative molecular and clinical modeling of clinical outcomes to PD1 blockade in patients with metastatic melanoma. Nat Med. 2019 Dec;25(12):1916-1927. doi: 10.1038/s41591-019-0654-5. Epub 2019 Dec 2. Erratum in: Nat Med. 2020 Jul;26(7):1147.

34. Long GV, Stroyakovskiy D, Gogas H, Levchenko E, de Braud F, Larkin J, et al. Combined BRAF and MEK inhibition versus BRAF inhibition alone in melanoma. N Engl J Med. 2014 Nov 13;371(20):1877-88. doi: 10.1056/NEJMoa1406037.

35. Mao JH, Kim IJ, Wu D, Climent J, Kang HC, DelRosario R, et al. FBXW7 targets mTOR for degradation and cooperates with PTEN in tumor suppression. Science. 2008 Sep 12;321(5895):1499-502. doi: 10.1126/science.1162981.

36. Marczynski GT, Laus AC, Dos Reis MB, Reis RM, Vazquez VL. Circulating tumor DNA (ctDNA) detection is associated with shorter progression-free survival in advanced melanoma patients. Sci Rep. 2020 Oct 29;10(1):18682. doi: 10.1038/s41598-020-75792-1.

37. Martin, M. Cutadapt removes adapter sequences from high-throughput sequencing reads. EMBnet.journal, [S.l.], 17 (1): 10-12 (2011). ISSN 2226-6089. Date accessed: 02 Apr. 2015. doi:http://dx.doi.org/10.14806/ej.17.1.200.

38. Minella AC, Clurman BE. Mechanisms of tumor suppression by the SCF(Fbw7). Cell Cycle. 2005 Oct;4(10):1356-9. doi: 10.4161/cc.4.10.2058.

39. Moreno T, Monterde B, González-Silva L, Betancor-Fernández I, Revilla C, Agraz-Doblas A, et al. ARID2 deficiency promotes tumor progression and is associated with higher sensitivity to chemotherapy in lung cancer. Oncogene. 2021 Apr;40(16):2923-2935. doi: 10.1038/s41388-021-01748-y.

40. Olbryt M, Rajczykowski M, Widłak W. Biological Factors behind Melanoma Response to Immune Checkpoint Inhibitors. Int J Mol Sci. 2020;21(11):4071. Published 2020 Jun 6. doi:10.3390/ijms21114071.

41. Palmieri G, Colombino M, Casula M, Manca A, Mandalà M, Cossu A; Italian Melanoma Intergroup (IMI). Molecular Pathways in Melanomagenesis: What We Learned from Next-Generation Sequencing Approaches. Curr Oncol Rep. 2018 Sep 14;20(11):86. doi: 10.1007/s11912-018-0733-7.

42. Pan D, Kobayashi A, Jiang P, Ferrari de Andrade L, Tay RE, Luoma AM, et al. A major chromatin regulator determines resistance of tumor cells to T cell-mediated killing. Science. 2018 Feb 16;359(6377):770-775. doi: 10.1126/science.aao1710.

43. Priestley P, Baber J, Lolkema MP, Steeghs N, de Bruijn E, Shale C, et al. Pan-cancer whole-genome analyses of metastatic solid tumours. Nature. 2019 Nov;575(7781):210-216. doi: 10.1038/s41586-019-1689-y.

44. Ricarte-Filho JC, Li S, Garcia-Rendueles ME, Montero-Conde C, Voza F, Knauf JA, et al. Identification of kinase fusion oncogenes in post-Chernobyl radiation-induced thyroid cancers. J Clin Invest. 2013 Nov;123(11):4935-44. doi: 10.1172/JCI69766.

45. Robert C, Grob JJ, Stroyakovskiy D, Karaszewska B, Hauschild A, Levchenko E, et al. Five-Year Outcomes with Dabrafenib plus Trametinib in Metastatic Melanoma. N Engl J Med. 2019 Aug 15;381(7):626-636. doi: 10.1056/NEJMoa1904059.

46. Robert C, Karaszewska B, Schachter J, Rutkowski P, Mackiewicz A, Stroyakovskiy D, et al. Three-year estimate of overall survival in COMBI-v, a randomized phase 3 study evaluating first-line dabrafenib (D) + trametinib (T) in patients (pts) with unresectable or metastatic BRAF V600E/K-mutant cutaneous melanoma. Ann. Oncol. 2016. 27:37 10.1093/annonc/mdw435.37.

47. Robert C, Long GV, Brady B, Dutriaux C, Maio M, Mortier L, et al. Nivolumab in previously untreated melanoma without BRAF mutation. N Engl J Med. 2015 Jan 22;372(4):320-30. doi: 10.1056/NEJMoa1412082.

48. Robinson JT, Thorvaldsdóttir H, Winckler W, Guttman M, Lander ES, Getz G, et al. Integrative genomics viewer. Nat Biotechnol. 2011;29(1):24–26. doi: 10.1038/nbt.1754.

49. Roh W, Chen PL, Reuben A, Spencer CN, Prieto PA, Miller JP, et al. Integrated molecular analysis of tumor biopsies on sequential CTLA-4 and PD-1 blockade reveals markers of response and resistance. Sci Transl Med. 2017 Mar 1;9(379):eaah3560. doi: 10.1126/scitranslmed.aah3560. Erratum in: Sci Transl Med. 2017 Apr 12;9(385).

50. Rosenthal R, McGranahan N, Herrero J, Taylor BS, Swanton C. DeconstructSigs: delineating mutational processes in single tumors distinguishes DNA repair deficiencies and patterns of carcinoma evolution. Genome Biol. 2016 Feb 22;17:31. doi: 10.1186/s13059-016-0893-4.

51. Ross JS, Wang K, Chmielecki J, Gay L, Johnson A, Chudnovsky J, et al. The distribution of BRAF gene fusions in solid tumors and response to targeted therapy. Int J Cancer. 2016 Feb 15;138(4):881-90. doi: 10.1002/ijc.29825.

52. Schachter J, Ribas A, Long GV, Arance A, Grob JJ, Mortier L, et al. Pembrolizumab versus ipilimumab for advanced melanoma: final overall survival results of a multicentre, randomised, open-label phase 3 study (KEYNOTE-006). Lancet. 2017 Oct 21;390(10105):1853-1862. doi: 10.1016/S0140-6736(17)31601-X.

53. Schadendorf D, van Akkooi ACJ, Berking C, Griewank KG, Gutzmer R, Hauschild A, et al. Melanoma. Lancet. 2018 Sep 15;392(10151):971-984. doi: 10.1016/S0140-6736(18)31559-9. Erratum in: Lancet. 2019 Feb 23;393(10173):746.

54. Seymour L, Bogaerts J, Perrone A, Ford R, Schwartz LH, Mandrekar S, et al. iRECIST: guidelines for response criteria for use in trials testing immunotherapeutics. Lancet Oncol. 2017 Mar;18(3):e143-e152. doi: 10.1016/S1470-2045(17)30074-8. Epub 2017 Mar 2. Erratum in: Lancet Oncol. 2019 May;20(5):e242.

55. Shi H, Moriceau G, Kong X, Lee MK, Lee H, Koya RC, et al. Melanoma whole-exome sequencing identifies (V600E)B-RAF amplification-mediated acquired B-RAF inhibitor resistance. Nat Commun. 2012 Mar 6;3:724. doi: 10.1038/ncomms1727.

56. Snyder A, Makarov V, Merghoub T, Yuan J, Zaretsky JM, Desrichard A, et al. Genetic basis for clinical response to CTLA-4 blockade in melanoma. N Engl J Med. 2014 Dec 4;371(23):2189-2199. doi: 10.1056/NEJMoa1406498. Epub 2014 Nov 19. Erratum in: N Engl J Med. 2018 Nov 29;379(22):2185.

57. Spagnolo F, Dalmasso B, Tanda E, Potrony M, Puig S, van Doorn R, et al. Efficacy of BRAF and MEK Inhibition in Patients with BRAF-Mutant Advanced Melanoma and Germline CDKN2A Pathogenic Variants. Cancers (Basel). 2021 May 18;13(10):2440. doi: 10.3390/cancers13102440.

58. Spagnolo F, Ghiorzo P, Orgiano L, Pastorino L, Picasso V, Tornari E, et al. BRAF-mutant melanoma: treatment approaches, resistance mechanisms, and diagnostic strategies. Onco Targets Ther. 2015 Jan 16;8:157-68. doi: 10.2147/OTT.S39096.

59. Talevich E, Shain AH, Botton T, Bastian BC. CNVkit: Genome-Wide Copy Number Detection and Visualization from Targeted DNA Sequencing. PLoS Comput Biol. 2016 Apr 21;12(4):e1004873. doi: 10.1371/journal.pcbi.1004873.

60. Tan J, Liu R, Zhu G, Umbricht CB, Xing M. TERT promoter mutation determines apoptotic and therapeutic responses of BRAF- mutant cancers to BRAF and MEK inhibitors: Achilles Heel. Proc Natl Acad Sci U S A. 2020 Jul 7;117(27):15846-15851. doi: 10.1073/pnas.2004707117.

61. Tanda ET, Vanni I, Boutros A, Andreotti V, Bruno W, Ghiorzo P, et al. Current State of Target Treatment in BRAF Mutated Melanoma. Front Mol Biosci. 2020 Jul 14;7:154. doi: 10.3389/fmolb.2020.00154.

62. Thielmann CM, Matull J, Zaremba A, Murali R, Chorti E, Lodde G, et al. TERT promoter mutations are associated with longer progression-free and overall survival in patients with BRAF-mutant melanoma receiving BRAF and MEK inhibitor therapy. Eur J Cancer. 2022 Jan;161:99-107. doi: 10.1016/j.ejca.2021.11.009.

63. Untergasser A, Nijveen H, Rao X, Bisseling T, Geurts R, Leunissen JA. Primer3Plus, an enhanced web interface to Primer3. Nucleic Acids Res. 2007 Jul;35(Web Server issue):W71-4. doi: 10.1093/nar/gkm306.

64. Van Allen EM, Miao D, Schilling B, Shukla SA, Blank C, Zimmer L, et al. Genomic correlates of response to CTLA-4 blockade in metastatic melanoma. Science. 2015 Oct 9;350(6257):207-211. doi: 10.1126/science.aad0095.

65. Van Loo P, Nordgard SH, Lingjærde OC, Russnes HG, Rye IH, Sun W, et al. Allele-specific copy number analysis of tumors. Proc Natl Acad Sci U S A. 2010 Sep 28;107(39):16910-5. doi: 10.1073/pnas.1009843107.

66. Vanni I, Tanda ET, Dalmasso B, Pastorino L, Andreotti V, Bruno W, et al. Non-BRAF Mutant Melanoma: Molecular Features and Therapeutical Implications. Front Mol Biosci. 2020 Jul 24;7:172. doi: 10.3389/fmolb.2020.00172. (**A**)

67. Vanni I, Tanda ET, Spagnolo F, Andreotti V, Bruno W, Ghiorzo P. The Current State of Molecular Testing in the BRAF-Mutated Melanoma Landscape. Front Mol Biosci. 2020 Jun 30;7:113. doi: 10.3389/fmolb.2020.00113. (**B**)

68. Vojnic M, Kubota D, Kurzatkowski C, Offin M, Suzawa K, Benayed R, et al. Acquired BRAF Rearrangements Induce Secondary Resistance to EGFR therapy in EGFR-Mutated Lung Cancers. J Thorac Oncol. 2019 May;14(5):802-815. doi: 10.1016/j.jtho.2018.12.038.

69. Wang K, Li M, Hakonarson H. ANNOVAR: functional annotation of genetic variants from high-throughput sequencing data. Nucleic Acids Res. 2010 Sep;38(16):e164. doi: 10.1093/nar/gkq603.

70. Yajima I, Kumasaka MY, Thang ND, Goto Y, Takeda K, Iida M, et al. Molecular Network Associated with MITF in Skin Melanoma Development and Progression. J Skin Cancer. 2011;2011:730170. doi: 10.1155/2011/730170.

71. Yeh CH, Bellon M, Nicot C. FBXW7: a critical tumor suppressor of human cancers. Mol Cancer. 2018 Aug 7;17(1):115. doi: 10.1186/s12943-018-0857-2.

PART II: QUALITY ASSESSMENT OF A CLINICAL NEXT-GENERATION SEQUENCING MELANOMA PANEL WITHIN THE ITALIAN MELANOMA INTERGROUP (IMI)

ABSTRACT

Identification of somatic mutations in key oncogenes in melanoma is important to lead the effective and efficient use of personalized anticancer treatment. Conventional methods focus on a few genes per run and, therefore, are unable to screen for multiple genes simultaneously. The use of Next-Generation Sequencing (NGS) technologies enables sequencing of multiple cancer-driving genes in a single assay, with reduced costs and DNA quantity needed and increased mutation detection sensitivity. We designed a customized IMI somatic gene panel for targeted sequencing of actionable melanoma mutations; this panel was tested on three different NGS platforms using 11 metastatic melanoma tissue samples in blinded manner between two EMQN quality certificated laboratory.

Our assay's detection limit was set to a Variant Allele Frequency (VAF) of 10% with a coverage of at least 200x. All somatic variants detected by all NGS platforms with a VAF ≥ 10%, were also validated by an independent method. The IMI panel achieved a very good concordance among the three NGS platforms.

This study demonstrated that, using the main sequencing platforms currently available in the diagnostic setting, the IMI panel can be adopted among different centers providing comparable results.

BACKGROUND AND RATIONALE

Malignant melanoma is one of the most aggressive, drug-resistant human cancers, and its incidence has risen persistently during the last few decades, particularly in the Caucasian population (**Siegel et al., 2017**). According to GLOBOCAN, more than 287,723 new cases of melanoma of the skin occurred worldwide in 2018 (1.6% of all cancers), with approximately 60,712 reported deaths (GLOBOCAN 2018) (**Bray et al., 2018**). In 2020, it was estimated that around 377,000 new cancer

cases was diagnosed in Italy and, among them, 14,863 cases are expected to be melanomas (AIOM, AIRTUM, I numeri del cancro in Italia 2020, available at: https://www.fondazioneaiom.it/wp-content/uploads/2020/10/2020_Numeri_Cancro-pazienti-web.pdf). Several tumor suppressor genes and/or oncogenes have been reported to be involved in melanomagenesis (**Hodis et al., 2012; Krauthammer et al., 2012; Canver Genome Atlas, 2015; Hayward et al., 2017**). The RAS-RAF-MEK-ERK, PI3K/PTEN and c-Kit pathways are of great interest since patients harboring activating mutations in *BRAF*, *NRAS* and *KIT* genes could be benefit from target treatment options or tailored combinations of target- and immuno-therapies. The identification of variants predictive of response or resistance to systemic treatments is already recommended today for proper management of advanced melanoma and molecular testing is a priority in determining the course of therapy. Indeed, molecular testing for actionable mutations is mandatory in patients with advanced disease (unresectable stage III or stage IV, and highly recommended in high-risk resected disease stage IIc, stage IIIb–IIIc). In case of a *BRAF*-wild type tumor, *NRAS* and *c-KIT* (mucosal and acrolentigenous primaries) testing should be performed (Italian Association of Medical Oncology/AIOM Guidelines Melanoma - 2019, available at: https://www.aiom.it/linee-guida-aiom-melanoma-2019/; National Comprehensive Cancer Network/NCCN clinical practice guidelines in oncology: melanoma - 2019, available at: https://www.nccn.org/professionals/physician_gls/pdf/cutaneous_melanoma.pdf) (**Coit et al., 2019**).

Recent evidence provided by the use of Whole Exome and Whole Genome Sequencing (WES and WGS) pointed out the involvement of other genes in melanoma pathogenesis, suggesting the importance of screening multiple genes at the same time to better classify the three main molecular melanoma subtypes (BRAFmut, RASmut, and non-BRAFmut /non-RASmut) (**Hodis et al., 2012; Krauthammer et al., 2012; Cancer Genome Atlas, 2015; Hayward et al., 2017; Berger et al., 2011; Furney et al., 2013; Johansson et al., 2016; Hintzche et al., 2017; Lyu et al., 2018; Palmieri et al., 2018; Wilmott et al., 2019; Zhou et al., 2019)**.

To date, various molecular strategies are available for mutational analysis of the *BRAF* gene, such as Sanger Sequencing (SS), real-time PCR, high-resolution melting analysis, Peptide Nucleic Acid (PNA)-mediated real-time PCR clamping, digital PCR, pyosequencing, and immunohistochemistry. Each technique is able to detect mutations on single genes per run with a specific sensitivity, specificity, and limit of detection (**Lamy et al., 2015; Harlé et al., 2016; Bruno et al., 2017; Franczak et al., 2017; Sener et al., 2017; Cheng et al., 2018; Malicherova et al., 2018; McEvoy et al., 2018**). At the beginning, Cobas 4800 BRAF V600 Mutation Test (Roche Molecular Systems) and THxID™-BRAF kit (BioMerieux, Inc.) were the only FDA-approved assays for *BRAF* V600E mutation and for *BRAF* V600E/V600K mutations in DNA samples extracted from Formalin-Fixed Paraffin-Embedded (FFPE) human melanoma tissue, respectively (http://www.fda.gov/companiondiagnostics) (**Marchant et al., 2014; Spagnolo et al., 2015; Martinuzzi et al., 2016**). The advent of high throughput Next-Generation Sequencing (NGS) technology has revolutionized the understanding of cancer biology and improved personalized treatment strategies in a large variety of human cancers, including melanoma. Development and use of NGS targeted gene sequencing panels may represent an attractive method in hospitals and clinics, since they can simultaneously screen disease-related mutations in multiple several genes per run, thus reducing both reagents cost and DNA quantity necessary, with enough sensitivity and specificity to detect somatic variants with frequencies higher than 5%. In the clinical setting, the application of NGS targeted gene panels requires analytical validation to ensure the detection of somatic variants and high quality of sequencing results (**Jennings et al., 2017**). NGS methods for cancer -related genes testing have been rapidly adopted by clinical laboratories (**Akkari et al., 2019**), but no consensus on the use of NGS tests and validation of a customize panel in clinical practice for melanoma are established in Italy, yet. A consensus was reported by the AIOM 2019 guidelines, but only for *BRAF* mutations (AIOM Guidelines for Melanoma - version 2019, available at: https://www.aiom.it/linee-guida-aiom-melanoma-2019/).

Here, we present the design and the mutational concordance between three different NGS platforms of a customized panel that analyzes target regions of 25 genes frequently mutated in melanoma, based on literature evidences (**Cancer Genome Atlas Network, 2015**). By using three NGS platforms often available in the research and clinical centers, this multicenter study aims to develop quality controls to be adopted by IMI centers.

AIM

To assess a clinical next-generation sequencing melanoma panel in order to develop quality controls to be adopted within the Italian Melanoma Intergroup (IMI).

PATIENTS AND METHODS

SAMPLES' COLLECTION

We selected a total of 11 metastatic melanoma cancer cases, 5 treated at the IRCCS Ospedale Policlinico San Martino (Genoa, Italy) and 6 treated at the Unit of Cancer Genetics, National Research Council (CNR) (Sassari, Italy). Both centers have passed previous External Quality Assessment (EQA) tests conducted by both the Italian Association of Medical Oncology (AIOM) and The European Molecular Genetics Quality Network (EMQN). These procedures of quality assurance are actually widely recognized systems to assess the performance of a laboratory, allowing laboratories to demonstrate consensus with their peers and providing information on inter-method comparability.

All samples were FFPE tissues, except for two fresh frozen tumor samples. All tumor samples were evaluated by pathologists for the presence of adequate tumor cell content (≥70%). The clinical characteristics of the metastatic melanoma patients are reported in **Table 1**. All specimens had already been screened for the presence of *BRAF* codon 15 mutations by SS approach and Real Time

PCR assay (PNAClamp™ BRAF Mutation Detection Kit; Panagene, Daejeon, Korea) or Therascreen™ BRAF Pyro assay (Qiagen, Valencia, CA) for molecular diagnostic purposes.

All patients were informed about the use of their tumour tissues samples for mutation analyses, gave the permission to collect tissue specimens for such purposes and signed a written consent. The study was approved by local Ethics Committees of the institution involved in this study (National Research Council and Ospedale Policlinico San Martino). Medical records were used for collecting clinical and pathological data (clinical presentation, tumour size and characteristics; **Table 1**).

Table 1. Clinical characteristics of the metastatic melanoma patients

Sample ID	Sex	I	LN MTS cell tumor content (%)	Melanoma site	Primary tumor syze	Regional lymph node status	B	M	U	P	BRAF Exon 15 mutation by SS	BRAF Exon 15 mutation by additional method	NRAS Exon 1-2 mutations by SS
#1	M	G	~70	left lower leg	pT3b	pN3	3.55	9	Y	n.a.	WT	PNAClamp™ BRAF Mutation Detection Kit: WT	NM_002524: c.182A>G p.Gln61Arg
#2	F	G	>90	left upper leg	pT4b	pN3	5.53	11	Y	Y	NM_004333: c.1799T>A p.Val600Glu	PNAClamp™ BRAF Mutation Detection Kit: Mutated	n.d.
#3	M	G	>80	right lower leg	n.a	pN3	2.92	3	n.a	N	NM_004333: c.1799T>A p.Val600Glu	PNAClamp™ BRAF Mutation Detection Kit: Mutated	n.d.
#4	F	G	80-85	right arm	pT4a	pN3	12.5	14	Y	Y	WT	PNAClamp™ BRAF Mutation Detection Kit: WT	NM_002524: c.181C>A p.Gln61Lys
#5	F	G	~80	left upper leg	pT3a	pN3	3.5	5-9	N	Y	NM_004333: c.1799_1800delTGinsAC p.Val600Asp	PNAClamp™ BRAF Mutation Detection Kit: Mutated	WT
#6	M	S	~80	upper back	pT3a	pN2b	2.75	4	N	N	NM_004333: c.1799T>A p.Val600Glu	Therascreen™ BRAF Pyro Kit: Mutated	WT
#7	M	S	>80	left upper leg	pT3b	pN3b	3.53	5	Y	Y	NM_004333: c.1798_1799delGTinsAA p.Val600Lys	Therascreen™ BRAF Pyro Kit: Mutated	WT
#8	F	S	~80	left forearm	pT3a	pN2b	2.26	3	N	N	NM_004333: c.1799T>A p.Val600Glu	Therascreen™ BRAF Pyro Kit: Mutated	WT
#9	M	S	>80	right lower leg	pT4b	pN3b	7.45	8	Y	N	WT	Therascreen™ BRAF Pyro Kit: WT	WT
#10	F	S	~90	left foot	pT3b	pN2b	2.15	2	Y	Y	NM_004333: c.1790T>G p.Leu597Arg	Therascreen™ BRAF Pyro Kit: Not Detected	WT
#11	M	S	~80	upper back	pT3a	pN2b	2.84	2	N	N	NM_004333: c.1799T>A p.Val600Glu	Therascreen™ BRAF Pyro Kit: Mutated	WT

Abbreviations: M: Male; F: female; I: institute; G: IRCCS Ospedale Policlinico San Martino, Genoa; S: Unit of Cancer Genetics at the National Research Council/CNR, Sassari; LN MTS: lymph node metastases; B: Breslow; M: mitosis/mm2; U: ulceration; P: pigmentation; SS: sanger sequencing; Y: yes; N: no; n.a.: not available, n.d.: not done, WT: wild type.

DNA EXTRACTION AND QUALITY CONTROL

Five genomic DNA (gDNA) samples from IRCCS Ospedale Policlinico San Martino were extracted from the tumor sections using the Genomic DNA FFPE One-Step Kit for Diatech MagCore® HF16Plus extractor (RBC Bioscience, New Taipei City, Taiwan) according to the manufacturer's instructions. Quantity and purity of the gDNA was examined by SPECTROstar Nano (BMG Labtech, Offenburg, Germany) to measure the whole absorption spectrum (220–750 nm) and calculating absorbance ratios at both 260/280 and 260/230. Six gDNAs from Institute of Biomolecular Chemistry (ICB), National Research Council (CNR) were extracted from FFPE tissue sections with QIAamp DNA Mini purification kit and QIAamp DNA FFPE Tissue kit (Qiagen, Valencia, CA). DNA purity and concentration were assessed with both Nanodrop 2000 spectrophotometer (Thermo Scientific, Wilmington, DE, USA) and Qubit® 2.0 Fluorometer (Invitrogen, Carlsbad, CA, USA). Moreover, all samples were quantified by Qubit® 2.0 Fluorometer (Invitrogen, Carlsbad, CA, USA) and Agilent 2200 TapeStation system using the Genomic DNA ScreenTape assay (Agilent Technologies, Santa Clara, CA, USA). gDNA fragmentation status was evaluated by the Agilent 2200 TapeStation system using the Genomic DNA ScreenTape assay (Agilent Technologies, Santa Clara, CA, USA) able to produce a DNA Integrity Number (DIN). gDNA quality showed a DIN ranging from 2.9 to 8.6.

All DNA samples belonging to each laboratory were distributed in a blind-coded manner to the other.

MELANOMA PANEL DESIGN

The "IMI Somatic Panel" - IAD79062 - was created to facilitate the identification of the genetic regions most significantly associated with melanoma using the Ion AmpliSeq™ Designer™ tool [at https://ampliseq.com/login/login.action]; the chosen targets of 35.13 kb were entered into the online tool and the resulting 343 amplicons (ranging from 125 to 175 bp) were divided by the online designer into three primer pools to maximize target specificity (**Manca et al., 2019**).

TARGETED NEXT GENERATION SEQUENCING (NGS)

All gDNA samples were blindly analyzed by both laboratories (IRCCS Ospedale Policlinico San Martino and Unit of Cancer Genetics at the National Research Council/CNR), using three different NGS platforms. The IRCCS Ospedale Policlinico San Martino center performed NGS analysis with the MiSeq™ Illumina and PGM™ Ion Torrent platforms, whereas the CNR center used the Proton™ Ion Torrent platforms. The DNA was amplified using the designed "IMI Somatic Panel" (3 primers pool), which analyzes 343 amplicons in target regions of 25 genes: *ARID2* (all coding sequences), *BAP1* (all coding sequences), *BRAF* (exons 1 and 15), *CCND1* (all coding sequences), *CDK4* (exons 1, 3 and 4), *CDKN2A* (all coding sequences), *DDX3X* (exons 2–3, 6–7, 10–15 and 17), *ERBB4* (exons 2–3, 8–12, 14, 21, 23, and 27), *GNA11* (exon 5), *GNAQ* (exon 5), *HRAS* (all coding sequences), *KDR* (Q472H), *KIT* (exons 2, 9–11, 13–15, and 17–18), *KRAS* (all coding sequences), *MAP2K1* (all coding sequences), *MET* (exons 1, 10, 13, 15 and 18), *MITF* (E318K), *NF1* (exons 28–30, 33–34, 36–37, 39, 41–43, 45, 48–53, and 55–58), *NOTCH1* (exons 26–27, and 34), *NRAS* (all coding sequences), *PIK3CA* (exons 1, 4, 6–7, 9, 13, 18, and 20), *PPP6C* (exons 2 and 4–7), *PTEN* (exons 1, 3, 5, and 8), *RB1* (exons 4, 6, 10–11, 14, 17–18, and 20– 22), and *TP53* (exons 1, 3–7, and 9).

ILLUMINA

Overall, 30 ng of gDNA for each sample was used for library construction using IMI Somatic Panel (3 primers pool) and Ampliseq Library PLUS for Illumina (Illumina Inc., San Diego, CA, USA) following the manufacturer's instructions. Cycling conditions were performed according to the DNA type and primer pairs per pool: 23 cycles with an extension time of 4 min in the first multiplex PCR, whereas in the second, optional PCR, the gDNA were subjected to seven cycles. Sample libraries was combined and diluted to 2 nM, denatured with 0.2 N fresh NaOH, diluted to 8.4 pM by addition of Illumina HT1 buffer. Then, the libraries, spiked with 1% PhiX (8.4 pM), were sequenced on an

Illumina MiSeq™ instrument by using the 300-cycle (2 × 150 paired ends) MiSeq v2 Reagent Kit v2 (Illumina).

PGM™ ION TORRENT

gDNA from the 11 tumor samples were amplified using the Ion AmpliSeq™ Library Kit 2.0 (ThermoFisher Scientific) starting from 30 ng of gDNA, barcoding each sample following the manufacturer's instructions. Cycling conditions were performed according to the DNA type and primer pairs per pool: 23 cycles with an extension time of 4 min in the first multiplex PCR, whereas in the second, optional PCR, the gDNA were subjected to five cycles. The library size was checked using the Agilent High Sensitivity DNA Kit by the Bioanalyzer 2100 instrument (Agilent Technologies), and library concentration was evaluated with a Qubit® 2.0 Fluorometer using the Agilent High Sensitivity DNA Kit (Life Technologies). Each diluted library (100 pM) was amplified through emulsion PCR using the OneTouch™ Instrument (ThermoFisher Scientific) and enriched by the OneTouch™ ES Instrument (ThermoFisher Scientific) using the Ion PGM™ Hi-Q™ View OT2 Kit, following the manufacturer's instructions. Finally, sequencing was performed on the Ion PGM™ (ThermoFisher Scientific) with the Ion PGM™ Hi-Q™ View Sequencing Kit (ThermoFisher Scientific), loading barcoded samples into a 316v.2 chip.

PROTON™ ION TORRENT

The eleven libraries were generated starting from 30 ng of input DNA with the Ion AmpliSeq Library Kit 2.0, according with the manufacturer instructions, barcoded with Ion Xpress Barcode Adapters, diluted at a final concentration of 50 pM, and pooled together. Template preparation and chip loading were performed on the Ion Chef; PI™ v2 BC chips were subsequently sequenced on the Ion Proton™ instrument using the Ion PI™ IC 200 Kit.

BIOINFORMATICS ANALYSIS

The Variant Caller (VC) analysis for each sample was carried out using the Ion and Illumina informatics solution integrated by each specific NGS platform.

For Ion Torrent platforms, initial variant calling from the Ion AmpliSeq™ sequencing data was generated using Torrent Suite v.5.10.1 (ThermoFisher Scientific) with a plug-in VC program (VC v.5.10.1.20) with Generic - PGM (3xx) - Somatic - Low Stringency parameters. Moreover, Ion Reporter™ Software were used for variant annotation.

Illumina data was analyzed using BaseSpace (Illumina) to convert *.bcl files into FASTQ files, which contain base call and quality information for all reads passing filtering. DNA Amplicon App v.2.1.0 was used for alignment in the targeted regions (specified in a manifest file), or the Burrows Wheeler Aligner across the entire genome. We selected the option “Somatic Variant Caller” with a Variant Allele Frequency (VAF) threshold of 0.01 (Percentage) and a depth threshold of 10. The tertiary analysis was carried out using BaseSpace Variant Interpreter.

All identified variants were confirmed by the Integrative Genomics viewer (IGV) by visually examining mutations using Integrative Genomics Viewer software (http://www.broadinstitute.org/igv) (**Robinson et al., 2011**).

SANGER SEQUENCING (SS) VALIDATION

All NGS variants with frequency higher than 10% were validated by SS using primer sets, designed by Primer3Plus tool (http://www.bioinformatics.nl/cgi-bin/primer3plus/primer3plus.cgi). All primer sequences are reported in **Table 2**. The PCR reactions were performed by amplifying 40 ng of gDNA in a final volume of 15.5 µL containing 200 mol/L dNTPs, 10× Taq buffer, 0.322 µM of each PCR primer, 1.5 U of Taq Hot Start (Qiagen). The PCR program consists of 10 min at 95 °C and 35 cycles with 30 s at 95 °C, 30 s at specific annealing temperature of primer, and 30 s at 72 °C, followed by 5 min at 72 °C. Purified products were sequenced, using the same primers of the PCR amplification,

with the BigDye Terminator v1.1 cycle sequencing kit (Applied Biosystems) under the following conditions: 1 µl BigDye Terminator v1.1, 2 µl sequencing buffer 5X, 3.2 pmol forward or reverse primer, 1.5 µl PCR purified product and 4 µl sterile water to a final reaction volume of 10.5 µl. Cycle sequencing was performed using initial denaturation step at 96 °C for 10 s followed by 25 cycles at 96 °C for 10 s, 60 °C for 3 min on GeneAmp® PCR System 9700 (Applied Biosystems). The sequencing products were separated by capillary electrophoresis in an automated sequencer (ABI 3130XL Genetic Analizer, Applied Biosystems) with a 36 cm length capillary and POP-7™ polymer, according to the manufacturer's instructions. Data were analyzed with Sequencing Analysis Software version 5.3.1 (Applied Biosystems).

Table 2. Primer sequences and PCR amplification conditions for Sanger Sequencing (SS) validation

Gene	Chromosome Position	RefSeq	Coding DNA	Protein	PCR primers	Ta (°C)	Length amplicon (bp)
CDKN2A	chr9:21974792	NM_001195132	c.35delC	p.(Ser12TrpfsTer14)	F:ACTTCAGGGGTGCCACATTC R:GCGCTACCTGATTCCAATTC	60	493
TP53	chr17:7579472	NM_000546.5	c.215C>G	p.Pro72Arg	F:TGAAGCTCCCAGAATGCCAG R:GCTGCCCTGGTAGGTTTTCT	60	136
TP53	chr17:7577543	NM_000546.5	c.738G>A	p.Met246Ile	F:TGGCTCTGACTGTACCACCA R:CAAGTGGCTCCTGACCTGG	60	123
ERBB4	chr2:212812278	NM_005235	c.298G>A	p.Glu100Ly	F:ACAGGCTACGTGTTAGTGGC R:GCCAAGGCATATCGATCCTCA	60	104
ERBB4	chr2:212578373	NM_005235	c.884A>T	p.His295Leu	F:TGTTTTGAGCTTGTTTGCTGA R:GGGCAAATGTCAGTGCAAGG	60	176
ARID2	chr12:46244997	NM_152641	c.3091C>T	p.Gln1031Ter	F:CGTCGTCCTCTACCCCTCAA R:CACCAGAGGCAGGCTGAC	60	201
KDR	chr4:55972974	NM_002253	c.1416A>T	p.Gln472His	F:TACCATGGTAGGCTGCGTTG R:GGAAGTCCTCCACACTTCTCC	60	191
MET	chr7:116340262	NM_001127500	c.1124A>G	p.Asn375Ser	F:ATTCTTTTCGGGGTGTTCGC R:TGGGGAACTGATGTGACTTACC	60	201
PIK3CA	chr3:178927410	NM_006218	c.1173A>G	p.Ile391Met	F:AGGTGGAATGAATGGCTGAATTA R:ACCTCTTTAGCACCCTTTCGG	60	110
PPP6C	chr9:127912080	NM_001123355	c.790C>T	p.Arg264Cys	F:GGTGACAGTATGGTCTGCTCC R:CGTTGTCGTTCTGGGAGGAA	60	148
BRAF	chr7:140453136	NM_004333	c.1799T>A	p.Val600Glu	F:GCTTGCTCTGATAGGAAAATGAGAT R:CATCCACAAAATGGATCCAGACAAC	60	175
BRAF	chr7:140453136	NM_004333	c.1798_1799delGTinsAA	p.Val600Lys	F:GCTTGCTCTGATAGGAAAATGAGAT R:CATCCACAAAATGGATCCAGACAAC	60	175
BRAF	chr7:140453135	NM_004333	c.1799_1800delTGinsAC	p.Val600Asp	F:GCTTGCTCTGATAGGAAAATGAGAT R:CATCCACAAAATGGATCCAGACAAC	60	175
BRAF	chr7:140453145	NM_004333	c.1790T>G	p.Leu597Arg	F:GCTTGCTCTGATAGGAAAATGAGAT R:CATCCACAAAATGGATCCAGACAAC	60	175
KIT	chr4:55593464	NM_000222	c.1621A>C	p.Met541Leu	F:AGTGGCTGTGGTAGAGATCC R:CAAAAAGGTGACATGGAAAGC	60	427
NRAS	chr1:115256529	NM_002524	c.182A>G	p.Gln61Arg	F:CACCCCCAGGATTCTTACAG R:TCCGCAAATGACTTGCTATT	60	173
NRAS	chr1:115256530	NM_002524	c.181C>A	p.Gln61Lys	F:CACCCCCAGGATTCTTACAG R:TCCGCAAATGACTTGCTATT	60	173
PTEN	chr10:89720709	NM_000314	c.860C>G	p.Ser287Ter	F:GCAACAGATAACTCAGATTGC R:TTCTTCATCAGCTGTACTCC	60	505
CDKN2A	chr9:21971089	NM_001195132	c.256_268delGCCCGGGAGGGCT	p.Ala86fs	F:AGCTTCCTTTCCGTCATGC R:GGAAGCTCTCAGGGTACAAAT	60	0

Abbreviations: F: primer Forward; R: primer reverse; Ta: annealing temperature.

NGS CONCORDANCE

The concordance of variant calls across the 3 different NGS approaches, was measured on with the Intra-class Correlation Coefficient (ICC) (**Bartko et al., 1966**), using the IRR package within the R computational environment (**Gamer et al., 2019; Core Team R, 2019**). The ICC analysis was

calculated considering cut-off of 200 depth of coverage and VAF of 10.0%, and then repeated using only the VAF criterion.

RESULTS

The NGS analysis was performed using a specific multiple-gene panel constructed by the Italian Melanoma Intergroup, the IMI Somatic Panel, arranged in three primer pools, and designed using the Ion AmpliSeq Designer to explore the mutational status of selected regions (343 amplicons; amplicon range: 125–175 bp; coverage 100%) within the 25 genes reported as the most frequently mutated in melanomas by The Cancer Genome Atlas (TGCA) and successive NGS-based studies (**Cancer Genome Atlas Network, 2015; Palmieri et al., 2018**).

PGM™ ION TORRENT PLATFORM

Eleven tumor samples were sequenced by IRCCS Ospedale Policlinico San Martino in Genoa on PGM™ Ion Torrent platform. The total number of reads was 12,475,778 (median average of 1,134,162 reads) with an average number of reads per amplicon and uniformity of 3023.7x and 87.6%, respectively. In these settings, more than 89.5% (ranging: 65.3–96.2%) of the targeted regions were covered at least 500x and 90.5% (ranging: 69.7–98.3%) of the targeted regions were covered 200x, and less than 4.0% (ranging: 1.5–26.5%) of targeted regions had coverage below 100x (**Table 3a**). Notably, the tumor sample with the highest number of amplicons not covered more than 200x was ID #9. More specifically, the sample ID #9 with a DIN 3.2 showed a 30.3% of mplicons <200x suggesting that low quality of gDNA could affect sequencing results. Low-covered regions (uncovered or with coverage <200x) in almost 2 tumor samples were constantly observed in 21/343 genes (≥18.2%; **Figure 1**). In particular, 3 amplicons (AMPLP226642480, CDKN2A: chr9: 21974448–21,974,570; AMPLP273979995, ARID2: chr12: 46285681–46,285,772; AMPLP222165518, BAP1: chr3: 52443880–52,443,996) were never covered ≥200x.

The VC plugin reported a total of 60 exonic genetic variants (51 Single Nucleotide Variants (SNVs), 2 Multi Nucleotide Variants (MNVs), and 7 frameshift deletions), irrespective of coverage and VAF. Notably, all the *BRAF* mutations, previously detected by SS /Real Time PCR assay/Therascreen™ BRAF Pyro Kit, were confirmed in all tumor samples. In particular, eight tumor samples reported a *BRAF* mutation of which 5 was p.Val600Glu, 1 p.Leu597Arg, 1 p.Val600Lys, and 1 p.Val600Asp all sufficiently covered (>200x) with an VAF > 19.0%. Among melanoma pharmacologically targetable genes, in addition to *BRAF* gene mutations, Ion Torrent called 2 *NRAS* mutations in different samples as follows: LRG_92/NM_002524.3: c.182A > G p.Gln61Arg and LRG_92/NM_002524.3: c.181C > A p.Gln61Lys with an VAF of 49.9% (6687x) and 64.6% (5642x), respectively. Notably, the two samples harboring *NRAS* mutation did not display mutations in *BRAF* gene supporting the idea that *BRAF* and *NRAS* mutations are commonly mutually exclusive.

Figure 1.

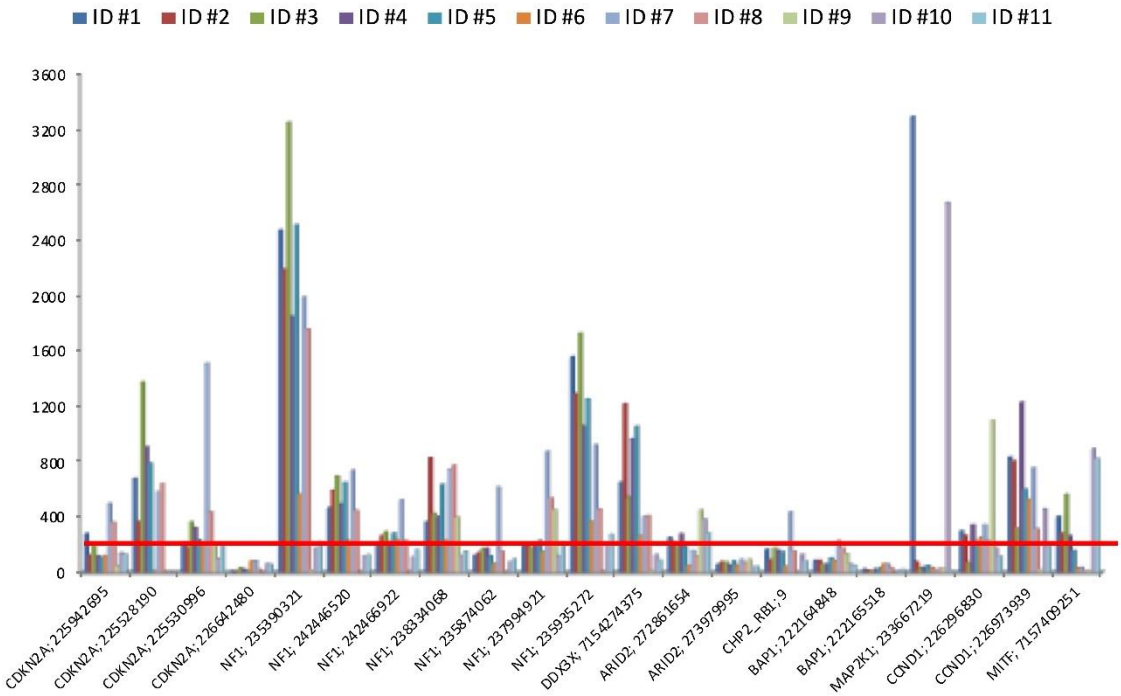

Amplicon name	ID #1	ID #2	ID #3	ID #4	ID #5	ID #6	ID #7	ID #8	ID #9	ID #10	ID #11
CDKN2A; 225942695	284	127	195	118	112	124	498	363	51	143	133
CDKN2A; 225528190	680	368	1374	906	790	8	584	641	2	9	4
CDKN2A; 225530996	220	182	366	325	240	206	1509	437	197	105	209
CDKN2A; 226642480	15	8	36	26	16	86	87	25	0	66	59
NF1; 235390321	2470	2186	3245	1849	2505	565	1988	1756	17	178	224
NF1; 242446520	470	595	696	497	649	231	738	449	1	118	129
NF1; 242466922	219	267	296	225	287	242	524	233	0	112	168
NF1; 238334068	368	829	427	405	638	235	746	776	399	125	155
NF1; 235874062	126	145	176	178	122	69	619	153	0	80	101
NF1; 237994921	200	205	183	202	233	150	874	536	454	124	219
NF1; 235935272	1557	1290	1727	1056	1253	370	921	460	1	198	277
DDX3X; 7154274375	651	1218	546	966	1054	266	406	412	16	131	91
ARID2; 272861654	255	225	198	282	189	52	160	120	452	386	285
ARID2; 273979995	63	78	77	55	86	57	96	74	96	44	46
CHP2_RB1; 9	169	94	179	162	151	48	440	153	2	132	84
BAP1; 222164848	89	89	62	67	106	86	230	179	139	63	56
BAP1; 222165518	26	21	10	28	35	64	62	40	0	15	24
MAP2K1; 233667219	3287	79	36	44	54	34	24	32	33	2667	18
CCND1; 226296830	302	268	75	345	227	256	345	230	1094	181	120
CCND1; 226973939	833	805	322	1228	602	528	755	314	25	460	192
MITF; 7157409251	406	285	565	267	160	36	38	14	12	894	822

PGM™ platform low-covered regions. The figure shows for amplicons with a coverage lower than 200x in at least two tumor samples. The histograms report on the x axis the amplicons name not covered 200x in at least two sample for all case and in y axis the amplicon coverage.

Table 3. NGS data quality.

		ID #1	ID #2	ID #3	ID #4	ID #5	ID #6	ID #7	ID #8	ID #9	ID #10	ID #11
A	N°Amplicons ≥500x	322	318	320	317	324	313	331	318	225	302	295
	% Amplicons ≥500x	93.9	92.7	93.3	92.4	94.5	91.3	96.5	92.7	65.6	88.0	86.0
	N°Amplicons ≥200x	337	334	332	336	334	331	338	335	240	327	328
	% Amplicons ≥200x	98.3	97.4	96.8	98.0	97.4	96.5	98.5	97.7	70.0	95.3	95.6
	N°Amplicons <100x	4	6	6	5	4	10	5	5	91	6	8
	% Amplicons <100X	1.2	1,7	1,7	1,5	1,2	2,9	1,5	1,5	26,5	1,7	2,3
	Average amplicon coverage	3,93	4,002	3,375	3,26	3,522	3,126	4,083	3,302	3,714	2,146	1,737
	Uniformity (%)	90.1	89.8	88.2	91.15	91.44	82.3	92.5	90.7	65.1	91.1	91.8
B	N°Amplicons ≥500x	337	340	340	338	341	290	289	294	338	302	254
	% Amplicons ≥500x	98.3	99.1	99.1	98.5	99.4	84.5	84.3	85.7	98.5	88.0	74.1
	N°Amplicons ≥200x	342	342	342	342	343	330	332	338	339	331	324
	% Amplicons ≥200x	99.7	99.7	99.7	99.7	100.0	96.2	96.8	98.5	98.8	97.1	94.5
	N°Amplicons <100x	0	0	0	0	0	6	3	4	3	5	7
	% Amplicons <100x	0.0	0.0	0.0	0.0	0.0	1.7	0.9	1.2	0.9	1.5	2.0
	Average amplicon coverage	9,75	15,009	12,239	11,254	14,842	967	1,137	1,102	1,647	1,308	1,083
	Uniformity (%)	94.7	92.7	93.9	96.2	93.9	95.6	96.0	97.1	92.0	95.7	93.8
C	N°Amplicons ≥500x	307	277	307	306	321	240	310	310	209	310	339
	% Amplicons ≥500x	89.5	80.8	89.5	89.2	93.6	70.0	90.4	90.4	60.9	90.4	98.8
	N°Amplicons ≥200x	336	326	336	335	337	300	336	334	286	334	340
	% Amplicons ≥200x	98.0	95.0	98.0	97.7	98.3	87.5	98.0	97.4	83.4	97.4	99.1
	N°Amplicons <100x	3	11	4	4	4	23	4	6	26	2	2
	% Amplicons <100x	0.9	3.2	1.2	1.2	1.2	6,7	1,2	1,7	7,6	0,6	0,6
	Average amplicon coverage	1,91	1,267	1,825	1,617	2,016	1,531	2,085	2,292	1,217	1,387	3,73
	Uniformity (%)	93.9	93.3	93.0	94.2	95.6	81.2	92.7	91.3	80.5	94.2	96.2

The table shows for each NGS platforms ((**A**) PGM™ platform, (**B**) Proton™ platform, and (**C**) MiSeq™ Illumina platform) data quality for the eleven tumor samples in terms of uniformity (the percentage of bases in all target regions covered by at least 20% of the average base coverage depth reads), average amplicon coverage depth and number (%) of amplicons at different coverage.

PROTON™ ION TORRENT PLATFORM

The same eleven tumor samples were sequenced by the Unit of Cancer Genetics at the National Research Council (CNR) in Sassari on Proton™ Ion Torrent platform. The total number of reads was 25,637,162 (median average of 1,573,735 reads) with an average number of reads per amplicon and uniformity of 6748x and 94.7%, respectively. In these settings, more than 91.8% (ranging: 74.1–99.4%) of the targeted regions were covered at least 500x and 98.3% (ranging: 94.5–100.0%) of the targeted regions were covered 200x, and less than 0.74% (ranging: 0.0–2.0%) of targeted regions

had coverage below 100x (**Table 3b**). The tumor sample with the highest number of amplicons not covered more than 200x was ID #11 with a 5.5% of amplicons <200x. However, the DIN of ID #11 sample was 6.6 which is a DNA good quality value. Low-covered regions (uncovered or with coverage <200x) in almost 2 tumor samples were constantly observed in 18/343 genes (≥5.2%; **Figure 2**). Notably, 3 amplicons (AMPL-P233667219, MAP2K1: chr15:66735563–66,735,643; AMPL-P272861654, ARID2: chr12: chr12:46215132–46,215,226; AMPL-P226642480, CDKN2A: chr9:21994132–21,994,263; AMPL-P222165518) were not covered ≥200x in the half of samples. The NGS analysis reported a total of 78 exonic genetic variants (67 SNVs, 2 MNVs, and 9 Insertions/deletions (indels), irrespective of coverage and VAF. All the 8 *BRAF* mutations disclosed by SS/Real Time PCR assay/Therascreen™ BRAF Pyro Kit were called in all tumor samples with a coverage >200x and an VAF > 18.8%. In addition to *BRAF* gene mutations, Proton™ called 3 *NRAS* mutations in different samples: LRG_92/NM_002524.3: c.182A > G p.Gln61Arg, LRG_92/NM_002524.3: c.181C > A p.Gln61Lys, and LRG_92/NM_002524.3: c.35G > A p.Gly12Asp with an VAF of 47.8% (1987x), 64.6% (5642x), 5.3% (1958x), respectively. As above, the samples harboring NRAS mutations did not display mutations in *BRAF* gene.

Figure 2.

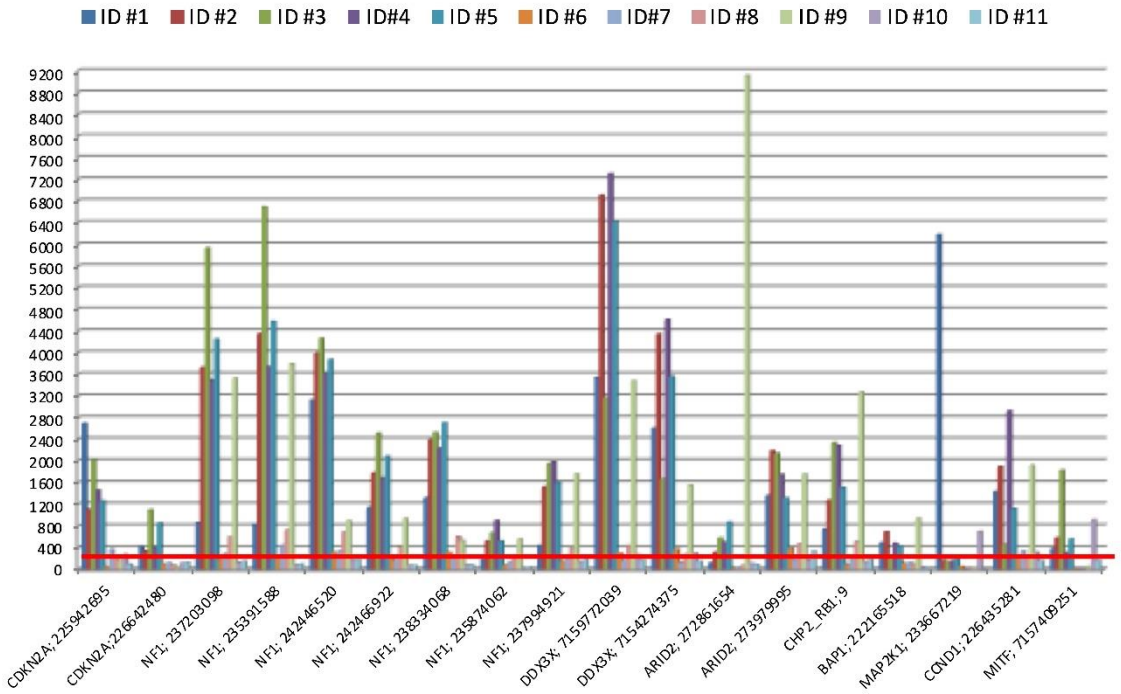

Amplicon name	ID #1	ID #2	ID #3	ID #4	ID 5	ID #6	ID #7	ID #8	ID #9	ID #10	ID #11
CDKN2A; 225942695	2695	1102	2025	1465	1267	53	372	205	162	276	95
CDKN2A;226642480	407	351	1095	406	861	100	124	80	46	120	131
NF1; 237203098	868	3724	5927	3500	4250	191	295	599	3526	131	156
NF1; 235391588	834	4350	6690	3735	4576	215	443	728	3797	83	100
NF1; 242446520	3125	3984	4264	3612	3870	320	342	689	899	169	190
NF1; 242466922	1140	1780	2512	1695	2088	229	166	412	939	75	66
NF1; 238334068	1323	2390	2524	2241	2709	317	217	608	535	83	80
NF1; 235874062	200	528	670	903	526	80	146	233	557	19	41
NF1; 237994921	440	1525	1956	1988	1603	152	223	388	1761	143	223
DDX3X; 7159772039	3545	6902	3170	7296	6412	303	166	439	3477	275	173
DDX3X; 7154274375	2604	4345	1671	4615	3559	375	133	279	1556	300	149
ARID2; 272861654	122	319	580	499	876	19	40	72	9110	107	90
ARID2; 273979995	1365	2193	2141	1756	1317	389	186	473	1762	176	338
CHP2_RB1; 9	743	1273	2340	2289	1514	96	194	516	3273	146	204
BAP1; 222165518	495	694	200	484	431	112	130	100	947	46	38
MAP2K1; 233667219	6178	166	148	160	209	55	7	30	36	699	6
CCND1; 226435281	1438	1898	463	2930	1122	196	340	244	1919	316	158
MITF; 7157409251	379	582	1828	318	559	16	7	8	51	918	113

Proton™ platform low-covered regions. The figure shows amplicons with a coverage lower than 200x in at least two tumor samples. The histograms report on the x axis the amplicons name not covered 200x in at least two sample for all case and in y axis the amplicon coverage
Illumina platform.

ILLUMINA PLATFORM

The same series of tumor samples were sequenced by IRCCS Ospedale Policlinico San Martino in Genoa on Illumina MiSeq™ platform. The total number of reads was 7,562,830 (median average of 687,530 reads) with an average number of reads per amplicon and uniformity of 1897.6x and 89.3%, respectively. More than 85.8% (ranging: 60.9–98.8%) of the targeted regions were covered at least

500x and 95.4% (ranging: 83.4–99.1%) of the targeted regions were covered 200x, and less than 8.1% (ranging: 2–26%) of targeted regions had coverage below 100x (**Table 3c**). The ID #9 was the sample with the highest number of amplicons not covered more than 200x (16.6% of amplicons with coverage <200x). A total of 40 amplicon regions (11.6%; **Figure 3**) in almost 2 tumor samples were present with a coverage <200x. Seven amplicons (AMPL-P225530996, CDKN2A: chr9: 21974673–21,974,792; AMPL-P226642480, CDKN2A: chr9: 21974448–21,974,570; AMPL-7159772013, DDX3X: chrX:41206085–41,206,199; AMPL-P273705807, ARID2: chr12:46285693–46,285,805; AMPL-P222164848, BAP1: chr3:52443752–52,443,884; AMPL-P233667219, MAP2K1: chr15:66735563–66,735,643; AMPL-7157409251, MITF: chr3:70013925–70,014,246) were observed not covered ≥200x in the half of samples. The DNA Amplicon App on BaseSpace displayed a total of 83 exonic genetic variants (64 SNVs, 2 MNVs, and 17 indels). The exon 15 of *BRAF* gene was sufficiently covered (>200x) reporting the 8 *BRAF* mutations previously disclosed by SS/Real Time PCR assay/Therascreen™ BRAF Pyro Kit and 2 *NRAS* mutations in 2 different samples confirmed by SS (LRG_92/NM_002524.3: c.182A > G p.Gln61Arg with an VAF of 51.7% and coverage of 1657x; LRG_92/NM_002524.3: c.181C > A p.Gln61Lys with an VAF 62.2% and coverage of 623x).

Figure 3.

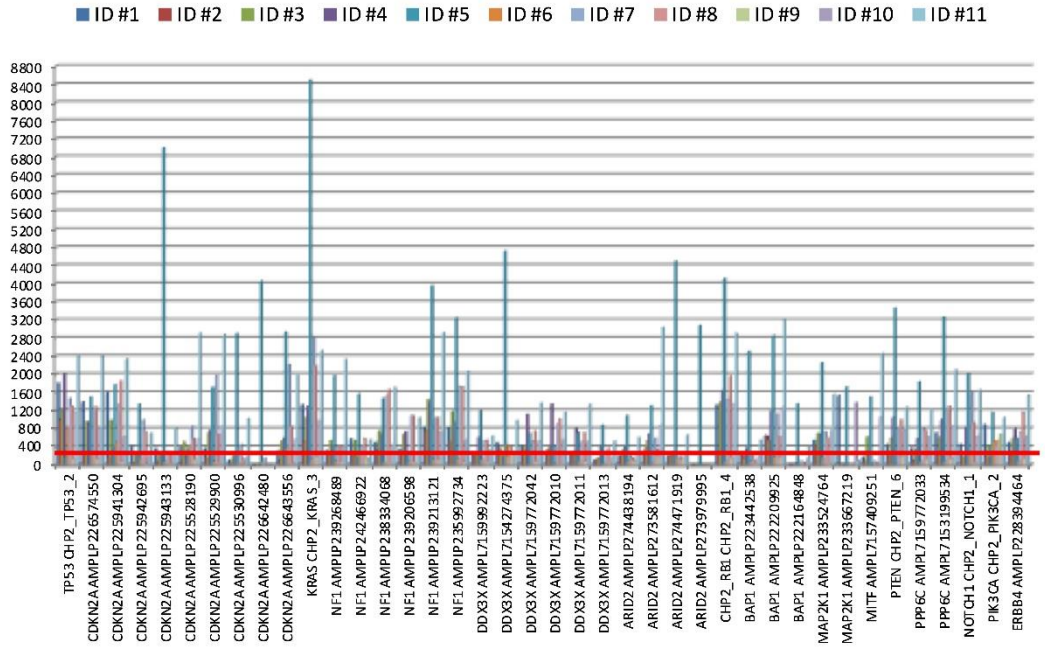

Amplicon name	ID #1	ID #2	ID #3	ID #4	ID #5	ID #6	ID #7	ID #8	ID #9	ID #10	ID #11
TP53; _2	1814	997	1212	2015	182	830	1472	1300	127	1169	2422
CDKN2A; 226574550	1394	241	961	935	1506	291	1277	1282	146	818	2408
CDKN2A; 225941304	1596	177	982	386	1777	497	1337	1867	84	632	2342
CDKN2A; 225942695	424	62	241	248	1350	161	995	742	33	214	703
CDKN2A; 225943133	367	66	235	256	7003	75	301	274	27	250	834
CDKN2A; 225528190	398	94	514	203	380	430	859	582	121	571	2912
CDKN2A; 225529900	367	160	715	776	1718	86	1976	676	48	860	2881
CDKN2A; 225530996	109	36	188	269	2899	49	455	132	16	179	1028
CDKN2A; 226642480	21	4	25	4	4064	82	156	12	9	9	21
CDKN2A; 226643556	312	92	526	594	2939	367	2217	852	26	567	1975
KRAS;_3	1334	546	1052	1304	8502	120	2810	2197	198	988	2526
NF1; 239268489	318	271	543	434	1967	103	416	429	70	401	2331
NF1; 242466922	579	278	541	172	1563	310	421	589	149	111	556
NF1; 238334068	506	339	758	654	1478	64	1540	1669	59	460	1711
NF1; 239206598	358	258	670	741	269	73	1091	1083	62	244	1043
NF1; 239213121	838	755	1451	1393	3960	113	1043	1042	120	742	2921
NF1; 235992734	821	523	1176	942	3255	133	1739	1728	62	556	2071
DDX3X; 7159992223	257	211	250	609	1194	124	536	545	56	320	643
DDX3X; 7154274375	500	375	300	174	4725	449	197	407	299	228	983
DDX3X; 7159772042	423	366	420	1122	695	38	530	751	82	528	1369

Amplicon name	ID #1	ID #2	ID #3	ID #4	ID #5	ID #6	ID #7	ID #8	ID #9	ID #10	ID #11
DDX3X; 7159772010	249	349	393	1350	441	36	894	1023	48	569	1165
DDX3X; 7159772011	257	265	306	800	720	111	525	718	77	527	1341
DDX3X; 7159772013	122	126	149	408	882	32	277	371	46	184	528
ARID2; 274438194	208	175	328	392	1100	94	212	152	98	231	606
ARID2; 273581612	252	375	540	698	1313	59	595	345	197	889	3041
ARID2; 274471919	208	228	257	296	4503	146	193	145	170	278	666
ARID2; 273979995	4	14	14	13	3079	0	6	12	4	6	26
CHP2_RB1;_4	1330	295	1392	1646	4120	82	1458	1960	148	1368	2909
BAP1; 223442538	253	209	156	377	2513	64	258	97	34	199	549
BAP1; 222209925	651	640	544	1198	2863	177	1133	624	168	1271	3211
BAP1; 222164848	27	25	11	54	1359	2	88	48	4	128	409
MAP2K1; 233524764	550	428	698	669	2262	160	735	597	37	756	1562
MAP2K1; 233667219	1537	25	27	18	1729	12	32	40	9	1377	105
MITF; 7157409251	175	83	619	307	1505	0	78	61	0	1054	2464
PTEN;_6	458	214	593	1044	3465	24	833	1002	198	772	1285
PPP6C; 7159772033	383	93	353	580	1840	67	799	758	119	632	1240
PPP6C; 7153199534	715	236	624	1008	3268	76	1284	1299	135	872	2107
NOTCH1;_1	460	144	224	826	2004	246	1598	934	57	642	1658
PIK3CA;_2	892	179	428	186	1166	537	441	550	674	248	1048
ERBB4; 228394464	503	274	597	791	589	85	737	1169	148	637	1539

MiSeq™ Illumina platform low-covered regions. The figure shows amplicons with a coverage lower than 200x in at least two tumor samples. The histograms report on the x axis the amplicons name not covered 200x in at least two sample for all case and in y axis the amplicon coverage

ANALYTICAL PERFORMANCE

We evaluated the performance of somatic variants detection by three NGS platforms using the 11 tumor samples that had been blindly sequenced in the two centers. The combination of variant calls between the three platforms identified a total of 126 exonic genetic variants among the different systems irrespective of coverage and VAF (**Figure 4a**). By setting a coverage ≥200x and VAF ≥10%, a total of 36 variants were called by the three systems (PGM™, Proton™, and Miseq™) (**Table 4**).

Therefore, concordance was calculated based on our assay detection limit (coverage ≥200x and VAF ≥10%) on these 36 variants. Despite different coverage depending on the platform used and pipeline of analysis, considering a minimum coverage of 200x and a VAF greater than 10%, the concordance on the absolute number of exonic variants found by each of the three NGS assays was 100%. Moreover, all variants with frequency higher than 10% were confirmed and validated by SS. In general, similar VAF were reported across the three platform for the 36 genetic variants, with an ICC of 0.901 (95%CI: 0.837–0.945, $p < 0.01$). The allele frequencies between the two Ion Torrent platforms displayed an ICC of 0.868 whereas ICC between PGM versus Illumina was 0.979 and ICC between Proton versus Illumina was 0.842. Only for three variants Proton called very dissimilar allele frequency compared to the other two NGS systems (±25.5). Noteworthy, Illumina called two additional unique *CDKN2A* variants (NM_001195132: c.35C > T (p.Ser12Leu) and c.35delC (p.Ser12TrpfsTer14)) in one tumor sample (ID #10), but both variants had a coverage of 108x and were thus excluded by our detection limit. Variants called by the three NGS systems with a coverage of at least 200x and a VAF ≥10%

Interestingly, the two *CDKN2A* genetic variants started in the same chromosome position with a considerably different VAF. Since one of the two had been called by Illumina with a VAF of 48.1%, we decided to validate it by SS. The SS confirmed the presence in this chromosome position (NM_001195132: chr9:21974792) of p.(Ser12TrpfsTer14) with a VAF ~ 50% instead of p.Ser12Leu. A possible explanation of the incorrect call could be the position of the variant (GRCh37.p13; chr9:21974792) located in the last base of the designed amplicon. The region in which Illumina called the CDKN2A variant was covered at a similar (105X) and higher (250X) depth by PGM™ and Proton™, and therefore we considered this variant as called at a frequency of 0% by these two platforms. In light of this findings, we re-assessed the concordance between the three platforms dropping the coverage cut-off and including all the 37 variants with VAF higher than 10% (**Figure 4b**), and obtained an ICC of 0.863 between the three platforms (95%CI = 0.779–0.922, $p < 0.01$).

Figure 4.

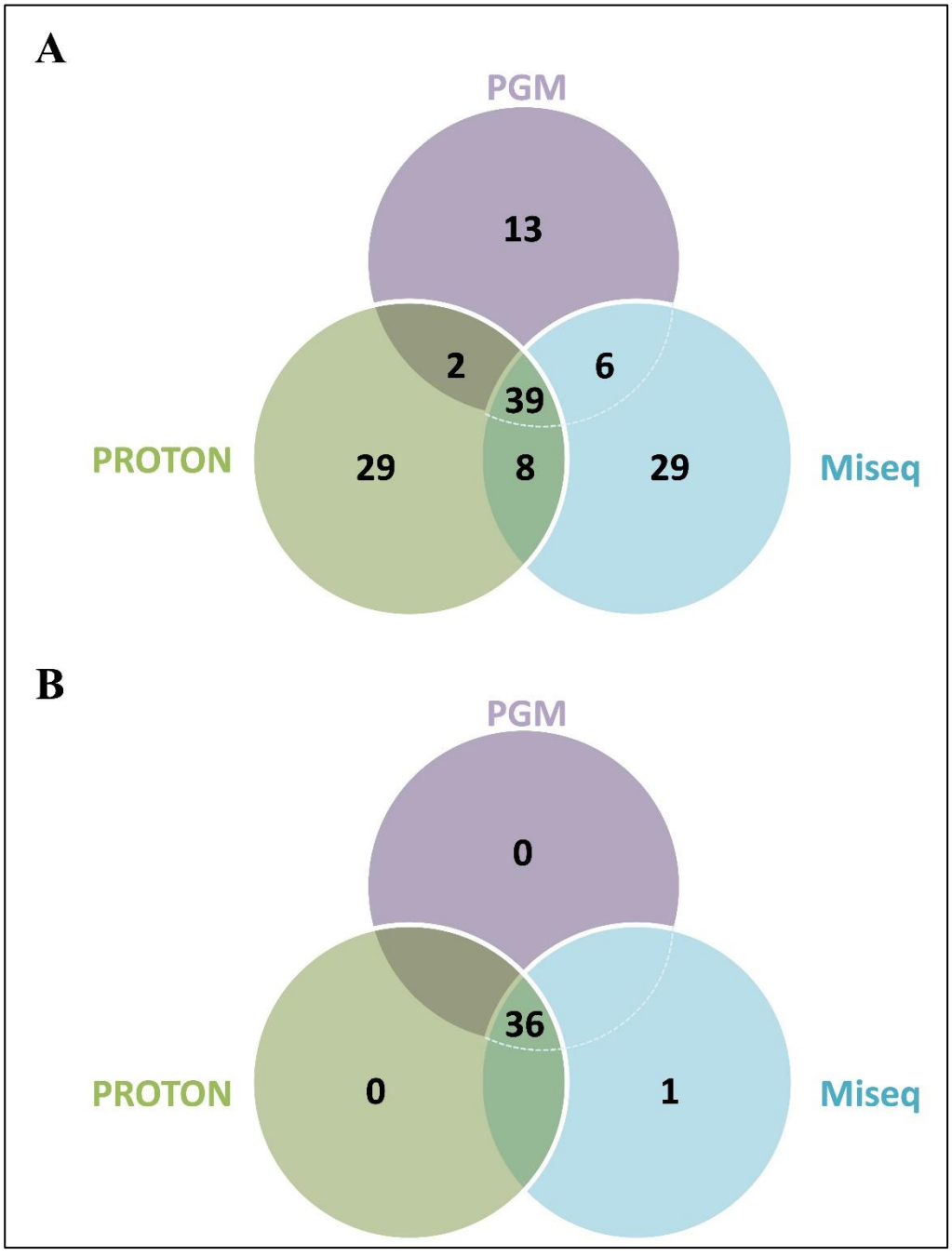

Venn Diagram of 126 exonic genetic variants called using the three different NGS platforms regardless of coverage and allele frequency (A) and of 37 exonic genetic variants called using the three different NGS platforms with an VAF > 10% (**B**).

Table 4. Variants called by the three NGS systems with a coverage of at least 200x and a variant allele frequency (VAF) ≥10%.

Gene	RefSeq	Protein	DNA change	N°
ARID2	NM_152641	p.Gln1031Ter	c.3091C>T	1
BRAF	NM_004333	p.Leu597Arg	c.1790T>G	1
BRAF	NM_004333	p.Val600Glu	c.1799T>A	5
BRAF	NM_004333	p.Val600Lys	c.1798_1799delGTinsAA	1
BRAF	NM_004333	p.Val600Asp	c.1799_1800delTGinsAC	1
CDKN2A	NM_001195132	p.Ala86fs	c.256_268delGCCCGGGAGGGCT	1
ERBB4	NM_005235	p.Glu100Lys	c.298G>A	1
ERBB4	NM_005235	p.His295Leu	c.884A>T	1
KDR	NM_002253	p.Gln472His	c.1416A>T	4
KIT	NM_000222	p.Met541Leu	c.1621A>C	2
MET	NM_001127500	p.Asn375Ser	c.1124A>G	1
NRAS	NM_002524	p.Gln61Arg	c.182A>G	1
NRAS	NM_002524	p.Gln61Lys	c.181C>A	1
PIK3CA	NM_006218	p.Ile391Met	c.1173A>G	2
PPP6C	NM_001123355	p.Arg264Cys	c.790C>T	1
PTEN	NM_000314	p.Ser287Ter	c.860C>G	1
TP53	NM_000546	p.Pro72Arg	c.215C>G	10
TP53	NM_000546	p.Met246Ile	c.738G>A	1

DISCUSSION

As the number of actionable genes in melanoma tumors is steadily growing there is an increasing need to perform multi-gene mutation testing in molecular diagnostics. Several NGS panels are commercially available, but these panels often contain genes or hotspots that are not of particular interest for molecular diagnostics due to their uncertain clinical significance, or to the lack of genes or hotspots specific for tumor types studied. Today, only two commercial NGS panels are specifically

designed to test somatic melanoma. However, these panels, namely Sentosa® SQ Melanoma Panel (Vela Diagnostics) and MELP Panel (MAYO Clinic Laboratories), contain only 10 (16 exons) and 5 (17 exons) genes, respectively, thus leaving out several genes of interest in the cutaneous melanoma research area. To overcome this issue, we have developed a custom panel to screen hotspots in 25 genes for clinically relevant mutations in melanoma based on the available literature at the time of panel design, including information retrieved from TGCA and available literature data on melanoma. The relevant factors taken into consideration when selecting the regions of interest to be included in the panel were the presence of variants with clinical significance in terms of prognostic, therapeutic and diagnostic value and the estimated cost per sample with an optimal depth of coverage. In particular, our custom panel covers all regions of MELP Panel (MAYO Clinic Laboratories), while it does not include *AKT3* (exon 5 and 6) and *FGFR3* (exon 7, 9, and 14) genes included in the Sentosa® SQ Melanoma Panel (Vela Diagnostics). However, *FGFR3* activating mutations play a key role in the pathogenesis of bladder cancer and have been found in benign conditions such as seborrheic keratosis and epidermal nevi. Moreover, TCGA cutaneous melanoma project has revealed low-frequency pathogenetic mutations in AKT3 (0.3%) and FGF3 (2.5%) (Cancer Genome Atlas Network, 2015). However, it should be observed that currently only *BRAF* exon 15 testing, and partially, *NRAS* exons 2 and 3, and *KIT* exons 11 and 13, in *BRAF* negative cases is recommended in clinical routine for the selection of target therapy and/or inclusion in clinical trials, and all these exons are included in the three panels here discussed. The application of the panel described here is for research purposes. The panel has already been used in research studies performed within the Italian Melanoma Intergroup with the analyses performed in a single center (**Manca et al., 2019**). We therefore obtained a panel with a total size of 35.13 kb, made up of three primers pools and with limited amount of DNA required (30 ng), offering sufficiently extensive and clinically relevant mutational profiling in a cost-efficient way. We then evaluated the concordance of this custom NGS panel in the identification of somatic genetic variants clinically relevant in

melanoma patients using three different benchtop sequencers by a bicentric-study. To do this, we tested the panel using the most used NGS platform available in the laboratories: Ion Torrent PGM™ and Ion Proton™ for the ThermoFisher and MiSeq™ benchtop sequencers for the Illumina. Notably, at the time of the "IMI somatic panel" design the Ion Torrent S5 XL sequencer (ThermoFisher Scientific) was not present in the two centers, for the evaluation on this additional NGS platform, so due to the limited availability of the DNA of the eleven samples of the study, another patients setting was subsequently tested on S5 XL. In any case, the S5 XL sequencer employs the same chemistry as the Ion Torrent PGM™ and the Ion Torrent Proton™, so it would not be relevant to our analysis. In fact, although several platforms available for routine diagnostic applications can perform high-throughput analysis within few days, with considerably reduced costs compared to SS (**Williams et al., 2013**), two of these are mainly used in clinical laboratories: Ion Torrent and Illumina systems.

We also estimated the total cost for the analysis of a single patient with the "IMI somatic panel" using the three different sequencing platforms. The cost for testing 25 genes using the "IMI somatic panel" was €270 (loading 3 samples on chip 316v2), €337 (loading all samples on Miseq Reagent Nano kit v2), and €398 (loading all samples on Ion PI Chip Kit V2) per sample for PGM™, Illumina, and Proton™, respectively, not taking into account panel primers, DNA extraction and quantity/quality control, labor time and bioinformatics analysis costs.

All platforms used in this study demonstrated comparable performance in the detection of somatic variants from the DNA samples tested, reaching an amplicon mean coverage higher than 1897x and an uniformity average greater than 87.6%. The Proton™ platform has revealed to have higher NGS quality metrics compared to the other 2 platforms. This data could be due to a load of fewer samples, which allowed to obtain a superior coverage than that of the other platforms.

Our analysis revealed that some amplicons are consistently not covered >200x across all samples and NGS platforms. Of note, two amplicons (CDKN2A-226,642,480 and MAP2K1–233,667,219) have been constantly covered less than 200x in half of the samples analyzed, proving that some amplicons

in the “IMI somatic panel” design have an intrinsic impairment in their coverage ability. Published scientific data have shown how uneven coverage of amplicons is associated with GC bias introduced during PCR amplification of library, cluster amplification, or sequencing. In fact, the GC content of the amplified region is also critical for NGS sequencing performance on both Illumina and Ion Torrent platforms (**Liu et al., 2012; Quail et al., 2012; Ross et al., 2013; Damiati et al., 2016; Sato et al., 2019**). However, only the CDKN2A-226,642,480 amplicon displayed % GC content higher than 90, explaining a lower coverage, while the MAP2K1–233,667,219 amplicon showed a % GC of 33 (**Damiati et al., 2016**). Moreover, not even the amplicons length can explain this lack of coverage, since the “IMI somatic panel” designed has an amplicon range of 125-175 bp. Finally, gDNA degradation status also did not influence the NGS quality data since the three different NGS platforms showed a different coverage for the same sample analyzed, irrespective of DIN, although unsurprisingly, the DIN values were lower in FFPE compared to fresh frozen samples. On the contrary, some amplicons show consistently a coverage <200x across all samples and NGS platforms, regardless of sample DIN.

Regardless the NGS quality metrics, the three NGS platforms achieved a very good concordance (ICC of 0.901; 95%CI: 0.837–0.945, $p < 0.01$) considering a 200 depth of coverage and a VAF of 10.0%. It is known that Ion torrent NGS platforms present a higher per base error rate and a quality of base calling accuracy lower than that of Illumina sequencing platforms. Moreover, the Ion torrent platforms have a tendency of misreading the length of homopolymers compared to other platforms (e.g. Illumina) (**Liu et al., 2012; Quail et al., 2012; Bragg et al., 2013**). Unlike the two Ion Torrent platforms, in one tumor sample the Illumina platform called two different genetic variants [NM_001195132: c.35C > T (p.Ser12Leu) and c.35delC (p.Ser12TrpfsTer14)] in the same position of a CDKN2A amplicon (AMPL- 225530996). Although the coverage of the aforementioned CDKN2A amplicon was similar across the three different platforms (105x, 230x and 108x for the PGM™, Proton™ and Illumina sequencer, respectively), the two variants were only called by the Illumina

platform. Interestingly, the p.(Ser12TrpfsTer14) CDKN2A variant was confirmed by SS at a VAF of around 50.0%.

Considering this *CDKN2A* additional variant called by Illumina, the ICC between the three platforms remains good (ICC of 0.863; 95%CI = 0.779–0.922, $p < 0.01$).

A possible explanation of this phenomenon could be due to the well documented characteristic of the Ion Torrent's current semiconductor sequencing platforms to call a higher number of indel error rate, particularly after long homopolomeric stretches, compared to Illumina platforms (**Bragg et al., 2013; Laehnemann et al., 2016**). In fact, Illumina's overall indel error rate is the lowest of all NGS technologies. Moreover, paired-end reads sequencing is more sensitive and accurate than single-end reads sequencing, because it greatly facilitates alignment operations, allowing among other things, to detect any deletion, duplication or insertion in the patient's DNA. The reason why Illumina miscalled the variant and identified it as SNV at a frequency of around 50% could be clarified by the fact that the genetic variants were both located at the end of the amplicon AMPL-225530996. The risk of false negative variants, as well as the allele drop-out phenomenon could be reduced by a tiling primer design that results in multiple overlapping amplicons for each target, to ensure the correct identification of all variants present in the target regions of the panel design. Moreover, this bias could be solved decreasing the number of samples sequenced in the same NGS run, which will increase coverage per sample while deliver a raised cost per sample for sequencing. Specific regions refractory to NGS, such as AMPL-225530996, need to be sequenced by SS and/or validated by alternative assays, in order to cover the gap and to validate the NGS data (**Aziz et al., 2015**).

All these observations justify the need to improve analytical solutions to detect somatic mutations with high confidence, to avoid false positives or inaccurate call measurements. Nevertheless, both the detection of some variants located at the end of the amplicons mistakenly called and the insufficiently coverage highlighted the importance of validating variants by an independent test before clinical application. Moreover, NGS results should not be transferred to clinical reports and

practice without acceptable validation. It is fundamental to confirm the genetic variation on a newly extracted DNA from the same sample using another NGS platform, SS, or another proper technique, in order to exclude false positive results. Indeed, in our study, all variants called at VAF higher than 10% were further confirmed by SS (**Table 2**). Moreover, all samples were previously screened for the presence of mutations in *BRAF* codon 15 by Real Time PCR assay (PNAClamp™ BRAF Mutation Detection Kit; Panagene, Daejeon, Korea) and Therascreen™ BRAF Pyro assay (Qiagen, Valencia, CA) **(Table 1**). In fact, PNAClamp™ and Therascreen™ tests were performed as part of the routine diagnostic approach and the outcome of these tests was documented in the patient report file and communicated with the medical oncologists. The technique used to validate the results should be included in the NGS report. Finally, all variants should be annotated and reported according to the HGVS (**den Dunnen et al., 2016**) and, for diagnostic purposes, only those genes with an established (i.e. published and confirmed) relationship between the aberrant genotype and melanoma should be included in the analysis. The information provided in the NGS report should be limited to the disease status, its targets, the names of the genes tested, their reportable ranges, as well as the analytical sensitivity and specificity of the technique (**Matthijs et al., 2015; Hume et al., 2019**). On the contrary, variants not linked with melanoma or gene variants not requested by medical oncologist should be not reported. It should also be emphasized that the interpretation of pathogenicity of a variant must be circumscribed to the evidence of its role in melanoma tumorigenesis at the time of the report, and that it could change over time as new information becomes available.

Massive efforts should be made to unify the interpretation and reporting of NGS molecular results among laboratories. In this context, a joint consensus recommendation for the interpretation and reporting of sequence variants in cancer was published (**den Dunnen et al., 2016**).

The IMI somatic panel represent a relevant, highly scalable, and robust tool that is easy to implement and that can be fully adapted to daily clinical practice in determining melanoma

actionable gene mutations, with a very good concordance - to detect somatic variants with frequencies higher than 10% with a coverage of 200x among the three NGS platforms. However, further validation studies on a greater number of samples from metastatic melanoma patients are required. Currently, the screening of clinically-actionable mutations is performed on FFPE tumor biopsies, but the amount of tumor tissue is often limited, and DNA quality may not be always optimal. We showed that this panel can be applied in the analysis of tumor FFPE tissue with varying status of DNA degradation. In fact, for all the samples, gDNA obtained from routine molecular testing of *BRAF* in metastatic melanoma and extracted with different methods in the two laboratories proved to be good reference material for the evaluation of this panel.

CONCLUSIONS

Since the advent of targeted therapy, treatment decisions are increasingly based on the molecular features of the tumor. Hence, laboratories need comprehensive molecular testing covering all actionable melanoma mutations using only limited amount of tumor tissue, mostly FFPE tissues, in a time-and cost-effective manner and with good performance. We show that the IMI panel, which include all established and several candidate melanoma driver genes, has optimal concordance- in the detection of actionable melanoma mutations using the main three NGS platforms available in research and clinical centers. We also achieve a good sequencing performance based upon amplicon and hotspot variants within the 25 genes of our designed NGS custom panel, obtaining an average amplicon coverage above 1800x with all three platforms.

Although our study is limited by the small number of samples analyzed, our study showed a high level of concordance in mutational patterns of the panel between two centers, using different extraction methods and NGS platforms to identify challenges and opportunities of center-specific platforms/protocols to analyze the same samples with the same panel. To the best of our knowledge, this is the first study in which concordance obtained using an NGS melanoma custom

panel was evaluated by a bi-centric study with three different NGS platforms. This study may lay the ground for developing collaborations and share positive controls here analyzed to other centers working together within the Italian Melanoma Intergroup.

REFERENCES

1. Akkari Y, Smith T, Westfall J, Lupo S. Implementation of cancer next-generation sequencing testing in a community hospital. Cold Spring Harb Mol Case Stud. 2019;5(3):a003707. doi: 10.1101/mcs.a003707.
2. Aziz N, Zhao Q, Bry L, Driscoll DK, Funke B, Gibson JS, et al. College of American Pathologists' laboratory standards for next-generation sequencing clinical tests. Arch Pathol Lab Med. 2015;139:481–493. doi: 10.5858/arpa.2014-0250-CP.
3. Bartko JJ. The intraclass correlation coefficient as a measure of reliability. Psychol Rep. 1966;19(1):3–11. doi: 10.2466/pr0.1966.19.1.3.
4. Berger AH, Knudson AG, Pandolfi PP. A continuum model for tumour suppression. Nature. 2011;476(7359):163–169. doi: 10.1038/nature10275.
5. Bragg LM, Stone G, Butler MK, Hugenholtz P, Tyson GW. Shining a light on dark sequencing: characterising errors in ion torrent PGM data. PLoS Comput Biol. 2013;9(4):e1003031. doi: 10.1371/journal.pcbi.1003031.
6. Bray F, Ferlay J, Soerjomataram I, Siegel RL, Torre LA, Jemal A. Global cancer statistics 2018: GLOBOCAN estimates of incidence and mortality worldwide for 36 cancers in 185 countries. CA Cancer J Clin. 2018;68(6):394–424. doi: 10.3322/caac.21492.
7. Bruno W, Martinuzzi C, Andreotti V, Pastorino L, Spagnolo F, Dalmasso B, et al. Heterogeneity and frequency of BRAF mutations in primary melanoma: Comparison between molecular methods and immunohistochemistry. Oncotarget. 2017;8(5):8069–8082. doi: 10.18632/oncotarget.14094.
8. Cancer Genome Atlas Network Genomic classification of cutaneous melanoma. Cell. 2015;161(7):1681–1696. doi: 10.1016/j.cell.2015.05.044.

9. Cheng L, Lopez-Beltran A, Massari F, MacLennan GT, Montironi R. Molecular testing for BRAF mutations to inform melanoma treatment decisions: a move toward precision medicine. Mod Pathol. 2018;31(1):24–38. doi: 10.1038/modpathol.2017.104.
10. Coit DG, Thompson JA, Albertini MR, Barker C, Carson WE, Contreras C, et al. Cutaneous melanoma, version 2.2019, NCCN clinical practice guidelines in oncology. J Natl Compr Cancer Netw. 2019;17(4):367–402. doi: 10.6004/jnccn.2019.0018.
11. Core Team R. R Foundation for statistical computing. Vienna: Austria. URL; 2019. R: a language and environment for statistical computing.
12. Damiati E, Borsani G, Giacopuzzi E. Amplicon-based semiconductor sequencing of human exomes: performance evaluation and optimization strategies. Hum Genet. 2016;135(5):499–511. doi: 10.1007/s00439-016- 1656-8.
13. den Dunnen JT, Dalgleish R, Maglott DR, Hart RK, Greenblatt MS, McGowan-Jordan J, et al. HGVS recommendations for the description of sequence variants: 2016 update. Hum Mutat. 2016;37(6):564–569. doi: 10.1002/humu.22981.
14. Franczak C, Salleron J, Dubois C, Filhine-Trésarrieu P, Leroux A, Merlin JL, et al. Comparison of five different assays for the detection of BRAF mutations in formalin-fixed paraffin embedded tissues of patients with metastatic melanoma. Mol Diagn Ther. 2017;21(2):209–216. doi: 10.1007/s40291-017-0258-z.
15. Furney SJ, Turajlic S, Stamp G, Nohadani M, Carlisle A, Thomas JM, et al. Genome sequencing of mucosal melanomas reveals that they are driven by distinct mechanisms from cutaneous melanoma. J Pathol. 2013;230(3):261–269. doi: 10.1002/path.4204.
16. Furney SJ, Turajlic S, Stamp G, Thomas JM, Hayes A, Strauss D, et al. The mutational burden of acral melanoma revealed by whole-genome sequencing and comparative analysis. Pigment Cell Melanoma Res. 2014;27(5):835–838. doi: 10.1111/pcmr.12279.

17. Gamer M. Lemon J. Fellows I. Singh P. Irr: various coefficients of interrater reliability and agreement. R Package Version 0.84.1. 2019. Available at: https://CRAN.R-project.org/package=irr.

18. Harlé A, Salleron J, Franczak C, Dubois C, Filhine-Tressarieu P, Leroux A, et al. Detection of BRAF mutations using a fully automated platform and comparison with high resolution melting, real-time allele specific amplification, immunohistochemistry and next generation sequencing assays, for patients with metastatic melanoma. PLoS One. 2016;11(4):e0153576. doi: 10.1371/journal.pone.0153576.

19. Hayward NK, Wilmott JS, Waddell N, Johansson PA, Field MA, Nones K, et al. Whole-genome landscapes of major melanoma subtypes. Nature. 2017;545(7653):175–180. doi: 10.1038/nature22071.

20. Hintzsche JD, Gorden NT, Amato CM, Kim J, Wuensch KE, Robinson SE, et al. Whole-exome sequencing identifies recurrent SF3B1 R625 mutation and comutation of NF1 and KIT in mucosal melanoma. Version 2. Melanoma Res. 2017;27(3):189–199. doi: 10.1097/CMR.0000000000000345.

21. Hodis E, Watson IR, Kryukov GV, Arold ST, Imielinski M, Theurillat J-P, et al. A landscape of driver mutations in melanoma. Cell. 2012;150:251–263. doi: 10.1016/j.cell.2012.06.024.

22. Hume S, Nelson TN, Speevak M, McCready E, Agatep R, Feilotter H, et al. CCMG practice guideline: laboratory guidelines for next-generation sequencing. J Med Genet. 2019;56(12):792–800. https://doi.org/10.1136/jmedgenet-2019-106152

23. Jennings LJ, Arcila ME, Corless C, Kamel-Reid S, Lubin IM, Pfeifer J, et al. Guidelines for validation of next-generation sequencing-based oncology panels: a joint consensus recommendation of the Association for Molecular Pathology and College of American pathologists. J Mol Diagn. 2017;19(3):341–365. doi: 10.1016/j.jmoldx.2017.01.011.

24. Johansson P, Aoude LG, Wadt K, Glasson WJ, Warrier SK, Hewitt AW, et al. Deep sequencing of uveal melanoma identifies a recurrent mutation in PLCB4. Oncotarget. 2016;7(4):4624–4631. doi: 10.18632/oncotarget.6614.

25. Krauthammer M, Kong Y, Ha BH, Evans P, Bacchiocchi A, McCusker JP, et al. Exome sequencing identifies recurrent somatic RAC1 mutations in melanoma. Nat Genet. 2012;44:1006–1014. doi: 10.1038/ng.2359.

26. Laehnemann D, Borkhardt A, McHardy AC. Denoising DNA deep sequencing data-high-throughput sequencing errors and their correction. Brief Bioinform. 2016;17(1):154–179. doi: 10.1093/bib/bbv029.

27. Lamy PJ, Castan F, Lozano N, Montélion C, Audran P, Bibeau F, et al. Next-generation genotyping by digital PCR to detect and quantify the BRAF V600E mutation in melanoma biopsies. J Mol Diagn. 2015;17(4):366–373. doi: 10.1016/j.jmoldx.2015.02.004.

28. Liu L, Li Y, Li S, Hu N, He Y, Pong R, et al. Comparison of next-generation sequencing systems. J Biomed Biotechnol. 2012;2012:251364. doi: 10.1155/2012/251364.

29. Lyu J, Song Z, Chen J, Shepard MJ, Song H, Ren G, et al. Whole-exome sequencing of oral mucosal melanoma reveals mutational profile and therapeutic targets. J Pathol. 2018;244(3):358–366. doi: 10.1002/path.5017.

30. Malicherova B, Burjanivova T, Grendar M, Minarikova E, Bobrovska M, Vanova B, et al. Droplet digital PCR for detection of BRAF V600E mutation in formalin-fixed, paraffin-embedded melanoma tissues: a comparison with Cobas® 4800, sanger sequencing, and allele-specific PCR. Am J Transl Res. 2018;10(11):3773–3781.

31. Manca A, Paliogiannis P, Colombino M, Casula M, Lissia A, Botti G, et al. Mutational concordance between primary and metastatic melanoma: a next-generation sequencing approach. J Transl Med. 2019;17(1):289. doi: 10.1186/s12967-019-2039-4.

32. Marchant J, Mange A, Larrieux M, Costes V, Solassol J. Comparative evaluation of the new FDA approved THxID™-BRAF test with high resolution melting and sanger sequencing. BMC Cancer. 2014;14:519. doi: 10.1186/1471-2407-14-519.

33. Martinuzzi C, Pastorino L, Andreotti V, Garuti A, Minuto M, Fiocca R, et al. A combination of immunohistochemistry and molecular approaches improves highly sensitive detection of BRAF mutations in papillary thyroid cancer. Endocrine. 2016;53(3):672–680. doi: 10.1007/s12020-015-0720-9.

34. Matthijs G, Souche E, Alders M, Corveleyn A, Eck S, Feenstra I, et al. Guidelines for diagnostic next-generation sequencing. Eur J Hum Genet. 2016;24(1):2–5. doi: 10.1038/ejhg.2015.226.

35. McEvoy AC, Wood BA, Ardakani NM, Pereira MR, Pearce R, Cowell L, et al. Droplet digital PCR for mutation detection in formalin-fixed, paraffin-embedded melanoma tissues: a comparison with sanger sequencing and pyrosequencing. J Mol Diagn. 2018;20(2):240–252. doi: 10.1016/j.jmoldx.2017.11.009.

36. Palmieri G, Colombino M, Casula M, Manca A, Mandalà M, Cossu A. Italian Melanoma Intergroup (IMI). Molecular Pathways in Melanomagenesis: What We Learned from Next-Generation Sequencing Approaches. Curr Oncol Rep. 2018;20(11):86. doi: 10.1007/s11912-018-0733-7.

37. Quail MA, Smith M, Coupland P, Otto TD, Harris SR, Connor TR, et al. A tale of three next generation sequencing platforms: comparison of ion torrent, Pacific Biosciences and Illumina MiSeq sequencers. BMC Genomics. 2012;13:341. doi: 10.1186/1471-2164-13-341.

38. Robinson JT, Thorvaldsdóttir H, Winckler W, Guttman M, Lander ES, Getz G, et al. Integrative genomics viewer. Nat Biotechnol. 2011;29(1):24–26. doi: 10.1038/nbt.1754.

39. Ross MG, Russ C, Costello M, Hollinger A, Lennon NJ, Hegarty R, et al. Characterizing and measuring bias in sequence data. Genome Biol. 2013;14(5):R51. doi: 10.1186/gb-2013-14-5-r51.

40. Sato MP, Ogura Y, Nakamura K, Nishida R, Gotoh Y, Hayashi M, et al. Comparison of the sequencing bias of currently available library preparation kits for Illumina sequencing of bacterial genomes and metagenomes. DNA Res. 2019;26(5):391–398. doi: 10.1093/dnares/dsz017.
41. Sener E, Yildirim P, Tan A, Gokoz O, Tezel GG. Investigation of BRAF mutation analysis with different technical platforms in metastatic melanoma. Pathol Res Pract. 2017;213(5):522–530. doi: 10.1016/j.prp.2017.01.010.
42. Siegel RL, Miller KD, Jemal A. Cancer statistics, 2017. CA Cancer J Clin. 2017;67(1):7–30. doi: 10.3322/caac.21387.
43. Spagnolo F, Ghiorzo P, Orgiano L, Pastorino L, Picasso V, Tornari E, et al. BRAF-mutant melanoma: treatment approaches, resistance mechanisms, and diagnostic strategies. Onco Targets Ther. 2015;8:157–168. doi: 10.2147/OTT.S39096.
44. Williams ES, Hegde M. Implementing genomic medicine in pathology. Adv Anat Pathol. 2013;20(4):238– 244. doi: 10.1097/PAP.0b013e3182977199.
45. Wilmott JS, Johansson PA, Newell F, Waddell N, Ferguson P, Quek C, et al. Whole genome sequencing of melanomas in adolescent and young adults reveals distinct mutation landscapes and the potential role of germline variants in disease susceptibility. Int J Cancer. 2019;144(5):1049–1060. doi: 10.1002/ijc.31791.
46. Zhou R, Shi C, Tao W, Li J, Wu J, Han Y, et al. Analysis of mucosal melanoma whole-genome landscapes reveals clinically relevant genomic aberrations. Clin Cancer Res. 2019;25(12):3548–3560. doi: 10.1158/1078-0432.CCR-18-3442.